Title
Regulatory Interactions between Myeloid Cells and Skeletal Muscle during Aging

Author
Wang, Ying

Publication Date
2018

Peer reviewed|Thesis/dissertation

UNIVERSITY OF CALIFORNIA

Los Angeles

Regulatory Interactions between Myeloid Cells and Skeletal Muscle during Aging

A dissertation submitted in partial satisfaction of the requirements for the degree Doctor of Philosophy in Molecular, Cellular and Integrative Physiology

by

Ying Wang

2018

ABSTRACT OF THE DISSERTATION

Regulatory Interactions

between Myeloid Cells and Skeletal Muscle

during Aging

by

Ying Wang

Doctor of Philosophy in Molecular, Cellular and Integrative Physiology

University of California, Los Angeles, 2018

Professor James G. Tidball, Chair

Skeletal muscle undergoes progressive mass loss, termed sarcopenia, and increased accumulation of fibrotic tissue during aging, which reduce the life quality of the elderly and cause significant economic burden on healthcare services of society. The importance of the immune system, especially myeloid cells, in modulating muscle growth and regeneration following injury suggests that myeloid cells may also have significant influences on sarcopenia and muscle fibrosis during aging. In this investigation, we studied the regulatory interactions between myeloid cells and skeletal muscle during aging. We found that muscle aging is associated with

increased number of anti-inflammatory M2a macrophages that can increase muscle fibrosis. Expression of a muscle-specific transgene of *nNOS* prevented the age-related increases in M2a macrophage and reduced fibrosis in aging muscle. We then tested whether aging of myeloid cells contributes to the age-related increases in M2a macrophages and the associated increases in fibrosis. Transplantation of young bone marrow cells into old mice resulted in fewer M2a macrophages and less accumulation of collagen compared to age-matched, non-transplant mice. We also found that transplantation of young bone marrow cells into old mice prevented sarcopenia. On the other hand, muscles of young mice receiving old bone marrow cells showed decreased numbers of muscle stem cells, called satellite cells, and increased numbers of fibrogenic-converted satellite cells. *In vitro*, media conditioned by young, but not old, bone marrow-derived macrophages increased muscle cell proliferation. These data suggest that aging of myeloid cells promotes the shift of satellites cell from a myogenic lineage to a more fibrogenic lineage during aging, and contributes to sarcopenia and muscle fibrosis. However, both the *nNOS* transgene and the heterochronic bone marrow transplantation can also affect muscle aging through unknown mechanisms other than changes in myeloid cells. To specifically manipulate the myeloid cell population, we designed a mouse line with a myeloid-cell-specific mutation of transcription factor *Sfpi1* which specifically reduced the number of M2 macrophages in muscle. Myeloid-cell-specific mutation of *Sfpi1* prevented sarcopenia and age-related muscle fibrosis, strongly suggesting that muscle aging is at least partly attributable to myeloid cells. Previous studies in our lab and by other groups suggested that tumor necrotic factor-alpha

(TNFα) is a macrophage-derived factor that may contribute significantly to muscle aging. We found that systemic *TNFα* knockout increased satellite cell fusion into muscle fibers in old muscle and prevented sarcopenia. Furthermore, we observed that transplantation of wild-type bone marrow cells into *TNFα* knockout mice induced sarcopenia and reduced muscle cell fusion, indicating that *TNFα* secreted by myeloid cells contributes significantly to the reduction of satellite cell myogenic capacity during aging and causes sarcopenia. Overall, our findings provide insight into mechanisms of muscle aging and the regulatory interactions between myeloid cells and skeletal muscle during aging.

This dissertation of Ying Wang is approved.

Kenneth A Dorshkind

Victor R Edgerton

David William Walker

James G. Tidball, Committee Chair

University of California, Los Angeles

2018

DEDICATION

I would like to dedicate this dissertation to my loving family: my father Xiushan, my mother Yuying, and my younger sister Haisu. It is their love and encouragement that supported me through good and bad times throughout life.

TABLE OF CONTENTS

LIST OF FIGURES

LIST OF TABLES

ACKNOWLEDGEMENTS

I would like to thank my supervisor and committee chair, Dr. James Tidball for his guidance and support throughout my graduate career at UCLA. His inspiring mentorship made my past several years a remarkable and rewarding time of my life and also nourished my passion in research which I hope to carry on in the future. I would also like to sincerely thank my other committee members, Dr. Kenneth Dorshkind, Dr. Reggie Edgerton, and Dr. David Walker for their valuable insights into my work.

Thanks to all members, previous and present, of the Tidball lab for their contributions to this dissertation. Working with you was such a wonderful experience. I have learned many valuable things from each of you both in science and in life. I also would like to thank members of the Dorshkind lab, especially Ying Kong and Enca Montecino-Rodriguez, for their contribution to this dissertation.

I also would like to express my gratitude to the Cross-disciplinary Scholars in Science and Technology (CSST) program which started my adventure in UCLA, and the Molecular, Cellular and Integrative Physiology program which perfectly completed it.

Chapter 2 is a version of the following article: Wang Y, Wehling-Henricks M, Samengo G, Tidball JG (2015). Increases of M2a macrophages and fibrosis in aging muscle are influenced by bone marrow aging and negatively regulated by muscle-derived nitric oxide. *Aging cell.* **14**, 678-688. I would like to thank the co-authors for their contributions.

VITA

2007—2011	Bachelor of Science, Biological Science Nankai University. Tianjin, China P.R.
2010	Cross-disciplinary Scholars in Science and Technology (CSST) program, summer University of California, Los Angeles
2011	Outstanding graduate of Nankai University
2011—present	Ph.D. in Molecular, Cellular and Integrative Physiology (expected) University of California, Los Angeles
2011—2015	China Scholarship Council Scholarship, China P.R.
2016—2017	Edith I. Hyde Fellowship University of California, Los Angeles
2016—2017	Dissertation Year Fellowship University of California, Los Angeles

PUBLICATIONS AND PRESENTATIONS

Wehling-Henricks M, Welc SS, Samengo G, Rinaldi C, Lindsey C, **Wang Y**, Lee J, Kuro-o M, Tidball JG (2018). Macrophages escape Klotho gene silencing in the mdx mouse model of Duchenne muscular dystrophy and promote muscle growth and increase satellite cell numbers through a Klotho-mediated pathway. *Human Molecular Genetics*. **27**, 14-29.

Wehling-Henricks M, Li Z, Lindsey C, **Wang Y**, Welc SS, Ramos JN, Khanlou N, Kuro-o M, Tidball JG (2016). Klotho gene silencing promotes pathology in the mdx mouse model of Duchenne muscular dystrophy. *Human Molecular Genetics*. **25**, 2465-2482.

Wang Y, Wehling-Henricks M, Samengo G, Tidball JG (2015). Increases of M2a macrophages and fibrosis in aging muscle are influenced by bone marrow aging and negatively regulated by muscle‐derived nitric oxide. *Aging Cell.* **14**, 678-688.

Deng B, Wehling-Henricks M, Villalta SA, **Wang Y**, Tidball JG (2012). IL-10 triggers changes in macrophage phenotype that promote muscle growth and regeneration. *The Journal of Immunology.* **189**, 3669-3680.

Wang Y, Wehling-Henricks M, Zuo Q, Welc SS, Garcia E, Tidball JG. (2015) Transplantation of young bone marrow cells into old mice slows muscle aging. *Gordon Research Conference-Myogenesis.* Lucca, Italy.

Chapter 1. Introduction

1.1 Skeletal muscle undergoes structural and functional losses during aging, which can cause significant public health and socioeconomic challenges.

Skeletal muscle is the most abundant tissue in human body and accounts for 30 - 45% of adult male and 25 - 35% of female body mass (Janssen *et al.* 2000). It is also a major regulator of whole body metabolism (Zurlo *et al.* 1990; Zurlo *et al.* 1994) and protein homeostasis (Millward 1970; Daniel *et al.* 1977). Age-related changes in skeletal muscle significantly affect the health and life quality of elderly people.

During aging, skeletal muscle undergoes a progressive loss of mass, termed sarcopenia (Rosenberg 1997). The rate of muscle loss accelerates over the age of fifty in healthy humans and reaches a rate of 1 - 2% per year (Forbes & Reina 1970; Sehl & Yates 2001; Hughes *et al.* 2002). Although some studies showed that reductions in muscle strength were not proportionally related to muscle mass loss (Newman *et al.* 2006; Clark & Manini 2008), it is well accepted that sarcopenia beyond certain threshold causes loss of muscle functional capacity and eventually leads to increased disability, morbidity and mortality (Janssen *et al.* 2002; Goodpaster *et al.* 2006; Rippberger *et al.* 2017). For example, identification of sarcopenia and mortality in adults ≥ 60 years old from the 1999 - 2002 National Health and Nutrition Examination Survey (NHANES) showed that subjects with sarcopenia had higher all-cause mortality rates and cardiovascular mortality rates compared to subjects without sarcopenia (Rippberger *et al.* 2017). Furthermore,

sarcopenia can cause a great economic burden on healthcare services of society. The healthcare costs of sarcopenia in the United States in 2000 were estimated to be about $18.5 billion (Janssen *et al.* 2004). These costs are likely to increase significantly due to the extension of life span and the progressive aging of the population (Petterson *et al.* 2012; Wang *et al.* 2017). The presence of sarcopenia is also associated with higher hospital cost in older patients with a variety of diseases (Gani *et al.* 2016; Chang *et al.* 2017; Vugt *et al.* 2017), as well as in older people without long-term illnesses (Steffl *et al.* 2017). Preventing sarcopenia will contribute significantly to health cost savings and to better health in elder people.

Aging also affects muscle fiber type composition. Muscle fibers can be categorized into two main types: slow twitch (Type I) muscle fibers and fast twitch (Type II) muscle fibers (Brooke & Kaiser 1970; Herbison *et al.* 1982). Type I fibers are small, slowly-contracting, and highly resistant to fatigue. Type II fibers are larger (Ingjer 1979) and faster-contracting, usually generate greater power but fatigue quickly (Tesch & Karlsson 1978; Young 1984). In healthy young adults, different fiber types are interspersed and present a “mosaic” appearance. Aging is associated with clustering of fibers of the same type (Lexell & Downham 1991) and increased percentage of type I fibers compared to type II fibers (Larsson *et al.* 1978), probably due to the specific loss of fast-twitch motor neurons and decline of muscle fiber re-innervation during aging (Edström & Larsson 1987; Einsiedel & Luff 1992; Kung *et al.* 2013). The decline in muscle mass during aging primarily results from type II fiber atrophy and loss in the number of muscle fibers (Larsson *et al.* 1978; Nilwik *et al.* 2013). This preferential loss of type II fibers also contributes to

the decline in muscle strength during aging because of the predominance of low tension-producing type I fibers in aging muscle (Frontera *et al.* 1988).

Muscle aging is accompanied with increased accumulation of non-contractile material such as adipose and connective tissues (Brooks & Faulkner 1994; Goldspink *et al.* 1994; Goodpaster *et al.* 2008). Excessive fibrosis in aged muscle increases muscle stiffness and contributes to impaired muscle function (Alnaqeeb *et al.* 1984; Wood *et al.* 2014). Muscle fibers are surrounded by extracellular matrix (ECM) that provides mechanical support for force transmission (Sanes 2003). The ECM of skeletal muscle is primarily composed of collagens together with other connective tissue proteins such as laminins, fibronectin and proteoglycans (Badylak 2007; Frantz *et al.* 2010). Studies of human and model animals such as mice or rats both showed that aging is associated with increased collagen concentration in muscle (Kragstrup *et al.* 2011). Although investigators dispute the primary cause for the increase in connective tissue in aging muscle, the increase in collagen content may result from both increased collagen expression (Babraj *et al.* 2005) and decreased collagen turnover (Mohan & Radha 1980; Pattison *et al.* 2003). Furthermore, enzymatically-mediated collagen cross-linking in muscle increases with aging (Palokangas *et al.* 1992; Zimmerman *et al.* 1993; Gosselin *et al.* 1998), which may contribute to the age-related increase in muscle stiffness and the impairment in contracting force generation by aging muscle (Brown *et al.* 1999).

Although exercise has been proven useful for reversing or preventing sarcopenia (Liu &

Latham 2009) and muscle fibrosis (Zimmerman *et al.* 1993; Gosselin *et al.* 1998), exercise is not always feasible for many elderly subjects with limited physical ability due to illness or weakness. Thus, there is an urgent need to better understand the mechanisms that underlie muscle aging so that new therapies and interventions can be developed.

1.2 Aging of the immune system, especially myeloid cells, may contribute to muscle aging.

Although age-related changes in muscle mass, structure and function may be due to alterations in homeostasis that are intrinsic to muscle cells, they may also reflect changes in other systems that can regulate muscle function. For example, age-related changes in the endocrine system and the nervous system have been clearly implicated in sarcopenia (Doherty *et al.* 1993; Urban *et al.* 1995; Nass & Thorner 2002). However, the immune system also experiences changes in function during senescence (Timaffy 1962; Roubenoff 2003), suggesting the possibility that some age-related changes in muscle structure and function may be secondary to senescence of the immune system.

1.2.1 Aging of the myeloid cells may affect changes in muscle stem cell number and functions during aging.

Myeloid cells may influence muscle aging by regulating the number or regenerative capacity of muscle stem cells, called satellite cells. Satellite cells are located beneath the basement

membranes of muscle fibers and are required for muscle regeneration and growth (Sambasivan *et al.* 2011). In response to extrinsic stimuli like injury, satellite cells exit their quiescent state, proliferate, differentiate and fuse with exiting muscle fibers for tissue repair or with each other to generate new muscle fibers (Relaix & Zammit 2012). Depletion of satellite cells completely ablates the regenerative capacity of muscle (Gibson & Schultz 1983). During aging, the myogenic capacity of satellite cells declines with age (Conboy *et al.* 2003; Machida & Booth 2004), which causes a significant decrease in the regenerative capacity of muscle. Furthermore, aging satellite cells can differentiate towards the fibrogenic lineage, which contributes to the increase of connective tissue accumulation during aging (Brack & Rando 2007; Stearns-Reider *et al.* 2017). Together, the decrease of satellite cell myogenic function and their shift towards a fibrogenic phenotype may contribute significantly to sarcopenia and increased muscle fibrosis during aging.

Myeloid cells have long been recognized as playing important roles in regulating satellite cell proliferation and differentiation, suggesting that age-related changes in myeloid cells could contribute to the change of satellite cell functions during aging. The presence of macrophages or macrophage-conditioned medium in satellite cell cultures can increase satellite cell proliferation (Cantini *et al.* 1994; Merly *et al.* 1999; Chazaud *et al.* 2003; Arnold *et al.* 2007) and differentiation (Cantini *et al.* 1994; Cantini *et al.* 1995; Arnold *et al.* 2007). Macrophages also affect satellite cell activation and promote muscle regeneration in injured muscle. Infiltration of macrophages into injured muscle is indispensable for normal muscle regeneration. For example, our lab

demonstrated previously that depletion of macrophages from muscles by antibody treatment impaired satellite cell activation and slowed muscle growth and regeneration during modified muscle loading (Tidball & Wehling-Henricks 2007). Other methods of blocking macrophage infiltration or function in various types of muscle injuries also result in poor muscle regeneration (Lescaudron *et al.* 1999; Summan *et al.* 2006; Segawa *et al.* 2008; Martinez *et al.* 2010) and more severe fibrosis (Segawa *et al.* 2008). Moreover, boosting the infiltration of macrophages can enhance muscle regeneration (Lescaudron *et al.* 1999). Together, these previous investigations indicate that the decline of satellite cells myogenic capacity and satellite cells shifting to the fibrogenic lineage during aging may be partly attributable to aging of the myeloid cells, supporting the hypothesis that myeloid cell aging contributes to sarcopenia and age-related muscle fibrosis.

1.2.2 Different subtypes of macrophages may play distinct roles in aging muscle.

Macrophages are a highly heterogeneous population of leukocytes. Classical activation of macrophages refers to their activation induced by pro-inflammatory T helper 1 (TH1) cytokines such as tumor necrosis factor-α (TNFα) and interferon-γ (IFNγ), resulting in M1 macrophages that express high levels of CD68 and inducible nitric oxide synthase (iNOS) (Gordon & Taylor 2005; Tidball & Villalta 2010; Tidball 2017). Alternative activation of macrophages refers to the activation of macrophages induced by anti-inflammatory T helper 2 (TH2) cytokines such as interleukin-4 (IL-4) and interleukin-10 (IL-10), resulting in M2 macrophages that express high

levels of CD163 and CD206 (Gordon 2003; Tidball & Villalta 2010; Tidball 2017).

M1 and M2 macrophages play distinct roles in injured and dystrophic muscles. M1 macrophages infiltrate into the injury site at early onset inflammation following acute muscle injury and phagocytose tissue debris resulting from muscle injury (Tidball & Villalta 2010; Tidball 2017). M1 macrophages secrete pro-inflammatory cytokines that promote satellite cell proliferation and suppress their differentiation at the earliest stages of muscle regeneration (Chen *et al.* 2005; Cheng *et al.* 2008; Londhe & Davie 2011). However, M1 macrophages can also have negative effects on muscle regeneration. For example, M1 macrophages promote muscle damage in the *mdx* mouse model of Duchenne muscular dystrophy by the production of nitric oxide (NO) generated by iNOS (Villalta *et al.* 2009). M2 macrophages also play important and complex roles during muscle regeneration. M1 macrophages shift to the M2 phenotype when injured muscle is dominated by the Th2 cytokine response (Deng *et al.* 2012). The transition from an M1-biased to an M2-biased macrophage phenotype in injured muscle is necessary for normal regeneration (Arnold *et al.* 2007; Tidball & Wehling-Henricks 2007; Deng *et al.* 2012). Increases of TH2 cytokines deactivate M1 macrophages and promote the shift to M2 phenotype in *mdx* muscles during the transition from the acute peak of *mdx* pathology to the regenerative stage (Villalta *et al.* 2009; Villalta *et al.* 2011). M2 macrophages also promote muscle fibrosis in *mdx* muscle by arginase-1 (Arg1) mediated arginine metabolism (Wehling-Henricks *et al.* 2010). Collectively, the heterogeneity of macrophages and their distinct functions during regeneration indicates that different populations of macrophages may play

distinct roles during muscle aging.

1.2.3 Increased levels of inflammatory cytokines secreted by aging myeloid cells may be an important contributor to sarcopenia.

Aging is associated with a chronic low-grade systemic inflammation, termed “inflammaging”, which is characterized by a 2- to 3-fold elevation in circulating pro-inflammatory cytokines including TNFα, IL-1β, IL-6 and many others (Roubenoff *et al.* 1998; Calçada *et al.* 2014). Inflammaging has been correlated with loss of muscle regenerative capacity, muscle strength and muscle mass in the elderly (Visser *et al.* 2002; Roubenoff 2003; van der Poel *et al.* 2011). For example, higher plasma concentrations of IL-6 and TNFα were associated with lower muscle mass and lower muscle strength in elderly persons (Visser *et al.* 2002). Increased mortality was also associated with both a higher level of TNFα and greater sarcopenia (Roubenoff *et al.* 2003), suggesting a possible mechanistic relationship between TNFα, sarcopenia and mortality.

The mechanism through which inflammaging leads to decline in muscle mass and function has not been clarified yet. However, *in vivo* and *in vitro* studies indicate that TNFα may mediate the increase in proteolysis during aging and contribute to muscle atrophy (Goodman 1991; Zamir *et al.* 1992; Li & Reid 2000). TNFα activates the NF-κB pathway by activation of IκB kinase (IKK) which phosphorylates and inactivates the inhibitor of the NF-κB (IκB) complex, allowing the translocation of the NF-κB complex into the nucleus (Ozes *et al.* 1999). Increased

NF-κB signaling then activates the ubiquitin-proteasome system, increasing the catalytic function of the 20S proteasome subunit which increases the degradation and removal of proteins (Li & Reid 2000).

TNFα also regulates muscle cell proliferation and differentiation in muscle regeneration. For example, ablation of TNFα or its receptor slows formation of new muscle fibers and causes impaired muscle regeneration following acute injury (Warren *et al.* 2002; Chen *et al.* 2005). However, elevating systemic TNFα levels attenuated myoblast proliferation and differentiation following injury caused by modified muscle use (Langen *et al.* 2006). Furthermore, infusion or injection of TNFα resulted in a pronounced loss of skeletal muscle and body mass (Llovera *et al.* 1993; Ling *et al.* 1997). These data suggest that TNFα has a complex role in regulating muscle regeneration and muscle wasting, and that manipulating systemic level of TNFα strongly affects the outcome of muscle mass and health in different models. Together, these findings support our hypothesis that age-related changes of systemic levels of inflammatory cytokines, especially TNFα, is an important contributor to sarcopenia.

1.3 Specific aims

In this investigation, we examined the role of aging of myeloid cells in muscle aging by addressing the following specific aims:

Aim 1: We tested whether preventing age-related reductions in muscle neuronal nitric oxide

synthase (*nNOS*) would obviate the age-related increase of intramuscular myeloid cell numbers and prevent age-related muscle fibrosis.

Aim 2: We tested whether manipulating the age of the immune system by heterochronic bone marrow transplantations would affect sarcopenia and age-related muscle fibrosis.

Aim 3: We tested whether specifically decreasing the number of M2 macrophages by myeloid specific mutation of the transcription factor *Sfpi1* would affect sarcopenia and age-related muscle fibrosis.

Aim 4: We tested whether genetic ablation of inflammatory cytokine TNFα would affect sarcopenia and whether transplantation of wild-type bone marrow cells into *TNFα*-mutant mice induces muscle aging.

References

Alnaqeeb M, Al Zaid N, Goldspink G (1984). Connective tissue changes and physical properties of developing and ageing skeletal muscle. *Journal of Anatomy*. **139**, 677.

Arnold L, Henry A, Poron F, Baba-Amer Y, Van Rooijen N, Plonquet A, Gherardi RK, Chazaud B (2007). Inflammatory monocytes recruited after skeletal muscle injury switch into antiinflammatory macrophages to support myogenesis. *Journal of Experimental Medicine*. **204**, 1057-1069.

Babraj JA, Cuthbertson DJ, Smith K, Langberg H, Miller B, Krogsgaard MR, Kjaer M, Rennie MJ (2005). Collagen synthesis in human musculoskeletal tissues and skin. *American Journal of Physiology-Endocrinology and Metabolism*. **289**, E864-E869.

Badylak SF (2007). The extracellular matrix as a biologic scaffold material. *Biomaterials*. **28**, 3587-3593.

Brack AS, Rando TA (2007). Intrinsic changes and extrinsic influences of myogenic stem cell function during aging. *Stem Cell Reviews*. **3**, 226-237.

Brooke MH, Kaiser KK (1970). Muscle fiber types: how many and what kind? *Archives of Neurology*. **23**, 369-379.

Brooks SV, Faulkner JA (1994). Skeletal muscle weakness in old age: underlying mechanisms. *Medicine and Science in Sports and Exercise*. **26**, 432-439.

Brown M, Fisher JS, Salsich G (1999). Stiffness and muscle function with age and reduced muscle use. *Journal of Orthopaedic Research*. **17**, 409-414.

Calçada D, Vianello D, Giampieri E, Sala C, Castellani G, de Graaf A, Kremer B, van Ommen B, Feskens E, Santoro A (2014). The role of low-grade inflammation and metabolic flexibility in aging and nutritional modulation thereof: a systems biology approach. *Mechanisms of Ageing and Development*. **136**, 138-147.

Cantini M, Massimino ML, Bruson A, Catani C, Dallalibera L, Carraro U (1994). Macrophages regulate proliferation and differentiation of satellite cells. *Biochemical and Biophysical Research Communications*. **202**, 1688-1696.

Cantini M, Massimino ML, Rapizzi E, Rossini K, Catani C, Dallalibera L, Carraro U (1995). Human satellite cell-proliferation in vitro is regulated by autocrine secretion of IL-6 stimulated by a soluble factor (s) released by activated monocytes. *Biochemical and Biophysical Research Communications*. **216**, 49-53.

Chang C-D, Wu JS, Mhuircheartaigh JN, Hochman MG, Rodriguez EK, Appleton PT, Mcmahon CJ (2017). Effect of sarcopenia on clinical and surgical outcome in elderly patients with proximal femur fractures. *Skeletal Radiology*, 1-7.

Chazaud B, Sonnet C, Lafuste P, Bassez G, Rimaniol A-C, Poron F, Authier F-J, Dreyfus PA, Gherardi RK (2003). Satellite cells attract monocytes and use macrophages as a support to escape apoptosis and enhance muscle growth. *The Journal of Cell Biology*. **163**, 1133-1143.

Chen S-E, Gerken E, Zhang Y, Zhan M, Mohan RK, Li AS, Reid MB, Li Y-P (2005). Role of TNF-α signaling in regeneration of cardiotoxin-injured muscle. *American Journal of Physiology-Cell Physiology*. **289**, C1179-C1187.

Cheng M, Nguyen M-H, Fantuzzi G, Koh TJ (2008). Endogenous interferon-γ is required for efficient skeletal muscle regeneration. *American Journal of Physiology-Cell Physiology*. **294**, C1183-C1191.

Clark BC, Manini TM (2008). Sarcopenia≠ dynapenia. *The Journals of Gerontology Series A: Biological Sciences and Medical Sciences*. **63**, 829-834.

Conboy IM, Conboy MJ, Smythe GM, Rando TA (2003). Notch-mediated restoration of regenerative potential to aged muscle. *Science*. **302**, 1575-1577.

Daniel P, Pratt O, Spargo E (1977). The metabolic homoeostatic role of muscle and its function as a store of protein. *The Lancet*. **310**, 446-448.

Deng B, Wehling-Henricks M, Villalta SA, Wang Y, Tidball JG (2012). IL-10 triggers changes in macrophage phenotype that promote muscle growth and regeneration. *The Journal of Immunology*. **189**, 3669-3680.

Doherty TJ, Vandervoort AA, Taylor AW, Brown WF (1993). Effects of motor unit losses on strength in older men and women. *Journal of Applied Physiology*. **74**, 868-874.

Edström L, Larsson L (1987). Effects of age on contractile and enzyme-histochemical properties of fast- and slow-twitch single motor units in the rat. *The Journal of Physiology*. **392**, 129-145.

Einsiedel L, Luff A (1992). Alterations in the contractile properties of motor units within the ageing rat medial gastrocnemius. *Journal of the Neurological Sciences*. **112**, 170-177.

Forbes GB, Reina JC (1970). Adult lean body mass declines with age: some longitudinal observations. *Metabolism*. **19**, 653-663.

Frantz C, Stewart KM, Weaver VM (2010). The extracellular matrix at a glance. *Journal of Cell Science*. **123**, 4195-4200.

Frontera WR, Meredith CN, O'Reilly KP, Knuttgen HG, Evans WJ (1988). Strength conditioning in older men: skeletal muscle hypertrophy and improved function. *Journal of Applied Physiology*. **64**, 1038-1044.

Gani F, Buettner S, Margonis GA, Sasaki K, Wagner D, Kim Y, Hundt J, Kamel IR, Pawlik TM (2016). Sarcopenia predicts costs among patients undergoing major abdominal operations. *Surgery*. **160**, 1162-1171.

Gibson MC, Schultz E (1983). Age‐related differences in absolute numbers of skeletal muscle satellite cells. *Muscle & Nerve*. **6**, 574-580.

Goldspink G, Fernandes K, Williams PE, Wells DJ (1994). Age-related changes in collagen gene expression in the muscles of mdx dystrophic and normal mice. *Neuromuscular Disorders*. **4**, 183-191.

Goodman MN (1991). Tumor necrosis factor induces skeletal muscle protein breakdown in rats. *American Journal of Physiology-Endocrinology And Metabolism*. **260**, E727-E730.

Goodpaster BH, Chomentowski P, Ward BK, Rossi A, Glynn NW, Delmonico MJ, Kritchevsky SB, Pahor M, Newman AB (2008). Effects of physical activity on strength and skeletal muscle fat infiltration in older adults: a randomized controlled trial. *Journal of Applied Physiology*. **105**, 1498-1503.

Goodpaster BH, Park SW, Harris TB, Kritchevsky SB, Nevitt M, Schwartz AV, Simonsick EM, Tylavsky FA, Visser M, Newman AB (2006). The loss of skeletal muscle strength, mass, and quality in older adults: the health, aging and body composition study. *The Journals of Gerontology Series A: Biological Sciences and Medical Sciences*. **61**, 1059-1064.

Gordon S (2003). Alternative activation of macrophages. *Nature Reviews Immunology*. **3**, 23-35.

Gordon S, Taylor PR (2005). Monocyte and macrophage heterogeneity. *Nature Reviews Immunology*. **5**, 953-964.

Gosselin LE, Adams C, Cotter TA, McCormick RJ, Thomas DP (1998). Effect of exercise training on passive stiffness in locomotor skeletal muscle: role of extracellular matrix. *Journal of Applied Physiology*. **85**, 1011-1016.

Herbison G, Jaweed M, Ditunno J (1982). Muscle fiber types. *Archives of Physical Medicine and Rehabilitation*. **63**, 227-230.

Hughes VA, Frontera WR, Roubenoff R, Evans WJ, Singh MAF (2002). Longitudinal changes in body composition in older men and women: role of body weight change and physical activity. *The American Journal of Clinical Nutrition*. **76**, 473-481.

Ingjer F (1979). Capillary supply and mitochondrial content of different skeletal muscle fiber types in untrained and endurance-trained men. A histochemical and ultrastructural study. *European Journal of Applied Physiology and Occupational Physiology*. **40**, 197-209.

Janssen I, Heymsfield SB, Ross R (2002). Low relative skeletal muscle mass (sarcopenia) in older persons is associated with functional impairment and physical disability. *Journal of the American Geriatrics Society*. **50**, 889-896.

Janssen I, Heymsfield SB, Wang Z, Ross R (2000). Skeletal muscle mass and distribution in 468 men and women aged 18–88 yr. *Journal of Applied Physiology*. **89**, 81-88.

Janssen I, Shepard DS, Katzmarzyk PT, Roubenoff R (2004). The healthcare costs of sarcopenia in the United States. *Journal of the American Geriatrics Society*. **52**, 80-85.

Kragstrup TW, Kjaer M, Mackey A (2011). Structural, biochemical, cellular, and functional changes in skeletal muscle extracellular matrix with aging. *Scandinavian Journal of Medicine & Science in Sports*. **21**, 749-757.

Kung TA, Cederna PS, van der Meulen JH, Urbanchek MG, Kuzon Jr WM, Faulkner JA (2013). Motor unit changes seen with skeletal muscle sarcopenia in oldest old rats. *Journals of Gerontology Series A: Biomedical Sciences and Medical Sciences*. **69**, 657-665.

Langen RC, Schols AM, Kelders MC, van der Velden JL, Wouters EF, Janssen-Heininger YM (2006). Muscle wasting and impaired muscle regeneration in a murine model of chronic pulmonary inflammation. *American Journal of Respiratory Cell and Molecular Biology*. **35**, 689-696.

Larsson L, Sjödin B, Karlsson J (1978). Histochemical and biochemical changes in human skeletal muscle with age in sedentary males, age 22–65 years. *Acta Physiologica*. **103**, 31-39.

Lescaudron L, Peltékian E, Fontaine-Pérus J, Paulin D, Zampieri M, Garcia L, Parrish E (1999). Blood borne macrophages are essential for the triggering of muscle regeneration following muscle transplant. *Neuromuscular Disorders*. **9**, 72-80.

Lexell J, Downham D (1991). The occurrence of fibre-type grouping in healthy human muscle: a quantitative study of cross-sections of whole vastus lateralis from men between 15 and 83 years. *Acta Neuropathologica*. **81**, 377-381.

Li Y-P, Reid MB (2000). NF-κB mediates the protein loss induced by TNF-α in differentiated skeletal muscle myotubes. *American Journal of Physiology-Regulatory, Integrative and Comparative Physiology*. **279**, R1165-R1170.

Ling P, Schwartz JH, Bistrian BR (1997). Mechanisms of host wasting induced by administration of cytokines in rats. *American Journal of Physiology-Endocrinology And Metabolism*. **272**, E333-E339.

Liu Cj, Latham NK (2009). Progressive resistance strength training for improving physical function in older adults. *The Cochrane Library*.

Llovera M, López-Soriano FJ, Argilés JM (1993). Effects of tumor necrosis factor-α on muscle-protein turnover in female Wistar rats. *Journal of the National Cancer Institute*. **85**, 1334-1339.

Londhe P, Davie JK (2011). Gamma interferon modulates myogenesis through the major histocompatibility complex class II transactivator, CIITA. *Molecular and Cellular Biology*. **31**, 2854-2866.

Machida S, Booth FW (2004). Increased nuclear proteins in muscle satellite cells in aged animals as compared to young growing animals. *Experimental Gerontology*. **39**, 1521-1525.

Martinez CO, McHale MJ, Wells JT, Ochoa O, Michalek JE, McManus LM, Shireman PK (2010). Regulation of skeletal muscle regeneration by CCR2-activating chemokines is directly related to macrophage recruitment. *American Journal of Physiology-Regulatory, Integrative and Comparative Physiology*. **299**, R832-R842.

Merly F, Lescaudron L, Rouaud T, Crossin F, Gardahaut MF (1999). Macrophages enhance muscle satellite cell proliferation and delay their differentiation. *Muscle & Nerve*. **22**, 724-732.

Millward DJ (1970). Protein turnover in skeletal muscle. II. The effect of starvation and a protein-free diet on the synthesis and catabolism of skeletal muscle proteins in comparison to liver. *Clinical Science*. **39**, 591-603.

Mohan S, Radha E (1980). Age-related changes in rat muscle collagen. *Gerontology*. **26**, 61-67.

Nass R, Thorner M (2002). Impact of the GH-cortisol ratio on the age-dependent changes in body composition. *Growth Hormone & IGF Research*. **12**, 147-161.

Newman AB, Kupelian V, Visser M, Simonsick EM, Goodpaster BH, Kritchevsky SB, Tylavsky FA, Rubin SM, Harris TB (2006). Strength, but not muscle mass, is associated with mortality in the health, aging and body composition study cohort. *The Journals of Gerontology Series A: Biological Sciences and Medical Sciences*. **61**, 72-77.

Nilwik R, Snijders T, Leenders M, Groen BB, van Kranenburg J, Verdijk LB, van Loon LJ (2013). The decline in skeletal muscle mass with aging is mainly attributed to a reduction in type II muscle fiber size. *Experimental Gerontology*. **48**, 492-498.

Ozes ON, Mayo LD, Gustin JA, Pfeffer SR, Pfeffer LM, Donner DB (1999). NF-κB activation by tumour necrosis factor requires the Akt serine-threonine kinase. *Nature*. **401**, 82-85.

Palokangas H, Kovanen V, Duncan R, Robins S (1992). Age-related changes in the concentration of hydroxypyridinium crosslinks in functionally different skeletal muscles. *Matrix*. **12**, 291-296.

Pattison JS, Folk LC, Madsen RW, Childs TE, Booth FW (2003). Transcriptional profiling identifies extensive downregulation of extracellular matrix gene expression in sarcopenic rat soleus muscle. *Physiological Genomics*. **15**, 34-43.

Petterson SM, Liaw WR, Phillips RL, Rabin DL, Meyers DS, Bazemore AW (2012). Projecting US primary care physician workforce needs: 2010-2025. *The Annals of Family Medicine*. **10**, 503-509.

Relaix F, Zammit PS (2012). Satellite cells are essential for skeletal muscle regeneration: the cell on the edge returns centre stage. *Development*. **139**, 2845-2856.

Rippberger PL, Emeny RT, Mackenzie TA, Bartels SJ, Batsis JA (2017). The association of sarcopenia, telomere length, and mortality: data from the NHANES 1999–2002. *European Journal of Clinical Nutrition*, 1.

Rosenberg IH (1997). Sarcopenia: origins and clinical relevance. *The Journal of Nutrition*. **127**, 990S-991S.

Roubenoff R (2003). Catabolism of aging: is it an inflammatory process? *Current Opinion in Clinical Nutrition & Metabolic Care*. **6**, 295-299.

Roubenoff R, Harris TB, Abad LW, Wilson PW, Dallal GE, Dinarello CA (1998). Monocyte cytokine production in an elderly population: effect of age and inflammation. *The Journals of Gerontology Series A: Biological Sciences and Medical Sciences*. **53**, M20-M26.

Roubenoff R, Parise H, Payette HA, Abad LW, D'Agostino R, Jacques PF, Wilson PW, Dinarello CA, Harris TB (2003). Cytokines, insulin-like growth factor 1, sarcopenia, and mortality in very old community-dwelling men and women: the Framingham Heart Study. *The American Journal of Medicine*. **115**, 429-435.

Sambasivan R, Yao R, Kissenpfennig A, Van Wittenberghe L, Paldi A, Gayraud-Morel B, Guenou H, Malissen B, Tajbakhsh S, Galy A (2011). Pax7-expressing satellite cells are indispensable for adult skeletal muscle regeneration. *Development*. **138**, 3647-3656.

Sanes JR (2003). The basement membrane/basal lamina of skeletal muscle. *Journal of Biological Chemistry*. **278**, 12601-12604.

Segawa M, Fukada S-I, Yamamoto Y, Yahagi H, Kanematsu M, Sato M, Ito T, Uezumi A, Hayashi Si, Miyagoe-Suzuki Y (2008). Suppression of macrophage functions impairs skeletal muscle regeneration with severe fibrosis. *Experimental Cell Research*. **314**, 3232-3244.

Sehl ME, Yates FE (2001). Kinetics of human aging: I. Rates of senescence between ages 30 and 70 years in healthy people. *The Journals of Gerontology Series A: Biological Sciences and Medical Sciences*. **56**, B198-B208.

Stearns-Reider KM, D'Amore A, Beezhold K, Rothrauff B, Cavalli L, Wagner WR, Vorp DA, Tsamis A, Shinde S, Zhang C (2017). Aging of the skeletal muscle extracellular matrix drives a stem cell fibrogenic conversion. *Aging Cell*. **16**, 518-528.

Steffl M, Sima J, Shiells K, Holmerova I (2017). The increase in health care costs associated with muscle weakness in older people without long-term illnesses in the Czech Republic: results from the Survey of Health, Ageing and Retirement in Europe (SHARE). *Clinical Interventions in Aging*. **12**, 2003.

Summan M, Warren GL, Mercer RR, Chapman R, Hulderman T, Van Rooijen N, Simeonova PP (2006). Macrophages and skeletal muscle regeneration: a clodronate-containing liposome depletion study. *American Journal of Physiology-Regulatory, Integrative and Comparative Physiology*. **290**, R1488-R1495.

Tesch P, Karlsson J (1978). Isometric strength performance and muscle fibre type distribution in man. *Acta Physiologica*. **103**, 47-51.

Tidball JG (2017). Regulation of muscle growth and regeneration by the immune system. *Nature Reviews Immunology*. **17**, 165-178.

Tidball JG, Villalta SA (2010). Regulatory interactions between muscle and the immune system during muscle regeneration. *American Journal of Physiology-Regulatory, Integrative and Comparative Physiology*. **298**, R1173-R1187.

Tidball JG, Wehling-Henricks M (2007). Macrophages promote muscle membrane repair and muscle fibre growth and regeneration during modified muscle loading in mice in vivo. *The Journal of Physiology*. **578**, 327-336.

Timaffy M (1962). A comparative study of bone marrow function in young and old individuals. *Gerontologia Clinica*. **4**, 13-18.

Urban RJ, Bodenburg YH, Gilkison C, Foxworth J, Coggan AR, Wolfe RR, Ferrando A (1995). Testosterone administration to elderly men increases skeletal muscle strength and protein synthesis. *American Journal of Physiology-Endocrinology And Metabolism*. **269**, E820-E826.

van der Poel C, Gosselin LE, Schertzer JD, Ryall JG, Swiderski K, Wondemaghen M, Lynch GS (2011). Ageing prolongs inflammatory marker expression in regenerating rat skeletal muscles after injury. *Journal of Inflammation*. **8**, 41.

Villalta SA, Nguyen HX, Deng B, Gotoh T, Tidball JG (2009). Shifts in macrophage phenotypes and macrophage competition for arginine metabolism affect the severity of muscle pathology in muscular dystrophy. *Human Molecular Genetics*. **18**, 482-496.

Villalta SA, Rinaldi C, Deng B, Liu G, Fedor B, Tidball JG (2011). Interleukin-10 reduces the pathology of mdx muscular dystrophy by deactivating M1 macrophages and modulating macrophage phenotype. *Human Molecular Genetics*. **20**, 790-805.

Visser M, Pahor M, Taaffe DR, Goodpaster BH, Simonsick EM, Newman AB, Nevitt M, Harris TB (2002). Relationship of interleukin-6 and tumor necrosis factor-α with muscle mass and muscle strength in elderly men and women: the Health ABC Study. *The Journals of Gerontology Series A: Biological Sciences and Medical Sciences*. **57**, M326-M332.

Vugt JL, Buettner S, Alferink LJ, Bossche N, de Bruin RW, Darwish Murad S, Polak WG, Metselaar HJ, IJzermans JN (2017). Low skeletal muscle mass is associated with increased hospital costs in patients with cirrhosis listed for liver transplantation–a retrospective study. *Transplant International*. doi:10.1111/ tri.13048

Wang C, Li F, Wang L, Zhou W, Zhu B, Zhang X, Ding L, He Z, Song P, Jin C (2017). The impact of population aging on medical expenses: A big data study based on the life table. *Bioscience Trends*, 2017.01243.

Warren GL, Hulderman T, Jensen N, McKinstry M, Mishra M, Luster MI, Simeonova PP (2002). Physiological role of tumor necrosis factor α in traumatic muscle injury. *The FASEB Journal*. **16**, 1630-1632.

Wehling-Henricks M, Jordan MC, Gotoh T, Grody WW, Roos KP, Tidball JG (2010). Arginine metabolism by macrophages promotes cardiac and muscle fibrosis in mdx muscular dystrophy. *PloS One*. **5**, e10763.

Wood LK, Kayupov E, Gumucio JP, Mendias CL, Claflin DR, Brooks SV (2014). Intrinsic stiffness of extracellular matrix increases with age in skeletal muscles of mice. *Journal of Applied Physiology*. **117**, 363-369.

Young A (1984). The relative isometric strength of type I and type II muscle fibres in the human quadriceps. *Clinical Physiology and Functional Imaging*. **4**, 23-32.

Zamir O, Hasselgren P-O, Higashiguchi T, Frederick JA, Fischer JE (1992). Tumour necrosis factor (TNF) and interleukin-1 (IL-1) induce muscle proteolysis through different mechanisms. *Mediators of Inflammation*. **1**, 247-250.

Zimmerman SD, McCormick RJ, Vadlamudi RK, Thomas DP (1993). Age and training alter collagen characteristics in fast-and slow-twitch rat limb muscle. *Journal of Applied Physiology*. **75**, 1670-1674.

Zurlo F, Larson K, Bogardus C, Ravussin E (1990). Skeletal muscle metabolism is a major determinant of resting energy expenditure. *Journal of Clinical Investigation*. **86**, 1423.

Zurlo F, Nemeth PM, Choksi RM, Sesodia S, Ravussin E (1994). Whole-body energy metabolism and skeletal muscle biochemical characteristics. *Metabolism*. **43**, 481-486.

Chapter 2. Increases of M2a macrophages and fibrosis in aging muscle are influenced by bone marrow aging and negatively-regulated by muscle-derived nitric oxide.

2.1 Abstract

Muscle aging is associated with changes in myeloid cell phenotype that may influence age-related changes in muscle structure. We tested whether preventing age-related reductions in muscle neuronal nitric oxide synthase (nNOS) would obviate age-related changes in myeloid cells in muscle. Our findings show that muscle aging is associated with elevations of anti-inflammatory M2a macrophages that can increase muscle fibrosis. Expression of a muscle-specific *nNOS* transgene in mice prevented age-related increases in M2a macrophages. Transgene expression also reduced expression of collagens and decreased muscle fibrosis. The *nNOS* transgene prevented age-related increases in Arg1 but did not influence *TGF*β expression, indicating that the transgene may prevent age-related muscle fibrosis by inhibiting the Arg1-dependent profibrotic pathway. Although aged satellite cells or fibro-adipogenic precursor (FAPs) cells also promote fibrosis, transgene expression had no effect on the expression of key signaling molecules that regulate fibrogenic activity of those cells. Finally, we tested whether increases in M2a macrophages and the associated increase in fibrosis were attributable to aging of myeloid lineage cells. Young bone marrow cells (BMCs) were transplanted into young or old mice and muscles were collected 8-months later. Muscles of young mice receiving young BMCs showed no effect on M2a macrophage number or collagen

accumulation compared to age-matched, non-transplanted controls. However, muscles of old mice receiving young BMCs showed fewer M2a macrophages and less accumulation of collagen. Thus, the age-related increase in M2a macrophages in aging muscle and the associated muscle fibrosis are determined in part by the age of bone marrow cells.

2.2 Introduction

Aging muscle undergoes a shift in the balance between myogenic potential and fibrogenic activity so that senescent muscle suffers from a reduced capacity to repair and regenerate as it becomes increasingly fibrotic. Over time, the shift can lead to substantial accumulations of connective tissue. For example, recent findings show that the concentration of collagen in the muscles of old mice is nearly twice the concentration in young mice, corresponding to a 2-fold increase in muscle stiffness (Alnaqeeb *et al.* 1984; Wood *et al.* 2014). At least some of the increased fibrosis is caused by increased collagen expression in muscle (Babraj *et al.* 2005) although reductions in collagen turn-over in muscle also occur (Pattison *et al.* 2003). Concurrent with this increase in fibrosis, the regenerative capacity in muscle declines, which may reflect a reduction in the numbers of Pax7+ myogenic cells in the muscle (satellite cells) that are necessary for continued myogenesis (Shefer *et al.* 2006), as well as a reduction in the myogenic capacity of aged satellite cells (Schultz *et al.* 1982; Chakravarthy *et al.* 2000).

Much is unknown concerning the mechanisms that drive senescent muscle toward fibrosis, but recent findings concerning fibrotic processes in dystrophic muscle or in wild-type muscle that has experienced acute injury indicate that the immune system can play important roles in regulating the balance between myogenesis and fibrosis. This has been clearly demonstrated in association with chronic muscle injuries in which muscle inflammation can persist for months or years. In Duchenne muscular dystrophy (DMD) or the *mdx* mouse model of DMD muscle,

inflammation continues from the early onset of the pathology through the entire lifetime of the afflicted (Wehling-Henricks *et al.* 2010). In this case, macrophages comprise the most prevalent leukocyte population (Wehling *et al.* 2001). A subpopulation of anti-inflammatory, M2a macrophages is present at highest numbers through stages of the disease when fibrosis is most extensive and they are primarily responsible for the shift toward a more fibrotic state (Villalta *et al.* 2009). Typically, macrophages are activated to the M2 phenotype by the Th2 cytokines interleukin-4 (IL-4) or IL-13. However, during skeletal muscle inflammation, IL-10 is required for their activation to the M2a phenotype, which is characterized by elevated expression of CD163 and Arg1 (Villalta *et al.* 2011; Deng *et al.* 2012). M2a macrophages then promote muscle fibrosis by Arg1-mediated hydrolysis of arginine that drives the production of ornithine that is then metabolized to produce proline required for collagen production (Wehling-Henricks *et al.* 2010). Ablation of Arg1 expression in *mdx* mice greatly reduces the pathological fibrosis of most dystrophic muscles (Wehling-Henricks *et al.* 2010).

Studies of the response of muscle to injury by toxin injection have indicated that other leukocyte populations can influence the balance between muscle regeneration and fibrosis. For example, toxin-injured muscle experiences invasion by SiglecF+ eosinophils that can promote muscle repair (Heredia *et al.* 2013). Those intramuscular eosinophils release IL-4 that activates fibroadipogenic progenitor cells (FAPs) in the muscle to increase their phagocytic removal of cellular debris and lead to more rapid regeneration (Heredia *et al.* 2013). Other studies have shown that muscle injury by toxin injection causes a clonal expansion of anti-inflammatory,

FoxP3+ regulatory T-cells (Tregs) that increase muscle regeneration while reducing fibrosis (Burzyn *et al.* 2013). Thus, these studies show that leukocytes invading young muscle following acute injury promote regeneration and reduce fibrosis.

The amplified, profibrotic inflammatory response in injured or diseased muscle can be exacerbated by the loss of neuronal nitric oxide synthase (nNOS) from muscle. Nitric oxide (NO) generated by muscle nNOS serves many regulatory roles, but in the context of muscle inflammation it plays a role in inhibiting extravasation of leukocytes into the damaged tissue (Wehling *et al.* 2001). Because of the absence of nNOS from dystrophic muscle, inflammation is amplified and persistent which contributes to muscle fibrosis (Wehling-Henricks *et al.* 2010). However, muscle-derived NO can also activate satellite cells, which are a population of muscle-specific stem cells that reside in fully-differentiated muscle (Anderson, 2000; Tatsumi *et al.* 2002). Satellite cell activation is required for normal muscle regeneration and growth (von Maltzahn *et al.* 2013). Thus, loss of nNOS from dystrophic muscle shifts the myogenic / fibrotic balance toward fibrosis by loss of normal NO modulation of leukocytes and satellite cells.

Skeletal muscle aging also causes large reductions in the expression of *nNOS* (Richmonds *et al.* 1999; Samengo *et al.* 2012) that accompany the increase in fibrosis and the reduction of regenerative capacity experienced during muscle senescence. Thus, it is feasible that the age-related decrease in muscle *nNOS* expression contributes to an increase in the numbers and activation of leukocytes that promote muscle fibrosis while also leading to a reduction in the

numbers of satellite cells, which would reduce the regenerative capacity of aging muscle. We test that hypothesis in the present investigation by examining the effects of expressing a muscle-specific *nNOS* transgene on the numbers and phenotype of leukocyte populations in the muscle, the occurrence of fibrosis and the prevalence of satellite cells in aging muscle. We also test whether age-related increases in macrophage populations in muscle are attributable to the age of the hematopoietic stem cell population from which they are derived, or reflect the age of the muscle in which they reside by performing heterochronic bone marrow transplantations (BMT) between young and old mice and analyzing the effects of those transplantations on muscle macrophage phenotype and fibrosis in old muscle. Collectively, our data show that M2a macrophages in muscle increase with aging in association with increased fibrosis and we find that preventing the reduction in *nNOS* expression in aging muscle prevents age-related changes in muscle macrophages and fibrosis, without affecting the prevalence of satellite cells. Our findings also show that the shift of muscle macrophages to an M2a phenotype is strongly influenced by the age of the hematopoietic cells from which they are derived.

2.3 Results

Expression of an nNOS transgene in skeletal muscle prevented age-related increases in pro-inflammatory cytokine expression and increases in muscle macrophage populations.

Previous investigators have reported increases in either the expression of pro-inflammatory or anti-inflammatory cytokines in aging muscle (Peake *et al.* 2010). Our QPCR analysis of hind-limb muscles from adult (12-month-old) and aged (24-month-old) mice showed that aging is associated with increased expression of pro-inflammatory and anti-inflammatory cytokines, although the magnitude of increase varied between muscles (Table 1). Th1 cytokines *IL-1β*, *TNFα* and *IFNγ* were significantly elevated in all senescent muscles analyzed, with the exception of no increase in *IL-1β* expression in old soleus muscle. However, *IL-10* expression was also significantly elevated in old muscle, accompanying the increased expression of the M2a macrophage phenotypic marker, *CD163*. Quantitation of CD68+ and CD163+ macrophages showed approximately a two-fold increase in CD68+ and CD163+ macrophages in wild-type, 24-month-old muscle compared to 12-month-old muscle, in accord with changes in *CD68* and *CD163* mRNA levels (Figures 1A - D). Macrophages were primarily located in perimysium in all treatment groups (Figures 1E, F). Although the histological data indicated that elevations of CD68+ and CD163+ macrophage populations in aging muscle were prevented by nNOS transgene expression (Figures 1A - C), QPCR data showed that transgene expression prevented the age-related increase in transcripts associated with M1 macrophages (*TNFα* and

IFNγ; Figures 1G, H), but did not affect the elevation of *IL-10*, which can be expressed by M2 macrophages (Figure 1M). The lack of concordance between the reduction in M2 macrophages in transgenic, 24-month-muscle and no reduction in *IL-10* expression indicates that M2 macrophages are not the primary source of *IL-10* expression in old muscle. Other transcripts associated with the M1 phenotype (*IL-6, iNOS*) or M2 phenotype (*IL-4, IL-5, IL-13*) were also unaffected by aging (Figures 1I - N).

Expression of an nNOS transgene in skeletal muscle prevented age-related increases in muscle fibrosis.

Because earlier studies showed that loss of nNOS expression in muscle led to greater numbers of macrophages in muscle (Wehling *et al.* 2001; Nguyen & Tidball, 2003) and demonstrated that prolonged elevation of M2a macrophage populations in diseased muscle were associated with increased fibrosis (Wehling *et al.* 2010), we assayed whether the NO-mediated reduction in M2a macrophage numbers in aging muscle influenced fibrosis. Expression of the *nNOS* transgene reduced the level of transcripts encoding collagen type I, collagen type III and collagen type V in 24-month-old muscle (Figures 2A - C). Furthermore, expression of the transgene prevented the age-related increase in the volume fraction of muscle that was comprised of each collagen type (Figures 2D - F) and reduced the thickness of epimysial and perimysial connective tissue that was comprised of collagen types I, III or V (Figure s 2G - L).

The association between reductions in M2a macrophage numbers and the reductions in age-related muscle fibrosis suggested that M2a macrophages could promote fibrosis in aging muscle. Because previous studies showed that M2a macrophages can drive muscle fibrosis via Arg1-mediated metabolism (Wehling-Henricks *et al.* 2010), we assayed for Arg1 expression in aged muscle and found that CD163+ M2a macrophages in old muscle express Arg1 (Figures 2M - O). We also found that *nNOS* transgene expression reduced Arg1 expression in old muscle (Figure 2P) by a magnitude that resembled the reduction of CD163+ M2 macrophage populations caused by transgene expression (Figure 1C). Although M2 macrophages can also express TGFβ, which is a pro-fibrotic cytokine, we observed no age-related increase in *TGFβ* expression and *nNOS* transgene expression did not affect *TGFβ* expression (Figure 2Q).

Expression of an nNOS transgene affected Vangl2 and Pax7 expression in adult, but not aged, muscle.

We further tested whether preventing age-related reductions in muscle nNOS expression affected expression of *Vangl2* or *Pax7* because previous investigations showed that NO can increase numbers of Pax7+ satellite cells via a Vangl2-dependent pathway that required increased transcription of *Vangl2* mRNA (Buono *et al.* 2012). Consistent with those previous reports, we observed that nNOS transgene expression caused significant elevations of *Vangl2* and *Pax7* expression in adult skeletal muscle and a strong trend for increased numbers of satellite cells (Figures 3A - D). However, transgene expression did not affect *Pax7* expression,

Vangl2 expression or satellite cell numbers in aged muscle, indicating that the NO-Vangl2-cGMP pathway for expanding satellite cell populations is not activated by elevated *nNOS* expression in old muscle. We also assayed whether the rescue of aged muscle from fibrosis reflected a reduction of satellite cell switching to a profibrotic phenotype via activation of Wnt signaling characterized by elevated expression of *axin-2* mRNA (Brack *et al.* 2007), but we did not observe elevated *axin-2* expression in aged muscles analyzed in our investigation (Figure 3E).

Expression of an nNOS transgene did not influence eosinophil or Treg numbers in aging muscle.

Because elevation in NO production by diseased muscle can reduce numbers of lymphoid and myeloid cell populations other than macrophages in muscle and other leukocytes such as eosinophils (Heredia *et al.* 2013) and regulatory T-cells (Tregs; Burzyn *et al.* 2013) can influence muscle regeneration and fibrosis following injury or disease, we tested whether transgene expression affected numbers of eosinophils or Tregs in aging muscle. We observed that eosinophils were present in aged, wild-type muscle but only in extremely low numbers and their numbers did not change with aging and transgene expression had no effect on their frequency in adult or aged muscles (Figures 3F - H). Tregs were more prevalent than eosinophils in adult and aged muscles, but their numbers were not significantly affected by age or transgene expression (Figures 3I - K), indicating that the rescue from fibrosis did not result from NO effects on Treg numbers.

Transplantation of young bone marrow cells into adult mice prevented the age-related increase in M2a macrophages in muscle.

The increase in CD163+ cells in aging muscle could reflect either the influence of aging muscle on macrophage phenotype or reflect age-related changes in the differentiation of hematopoietic lineage cells that are independent of influences from the host tissue. We tested whether muscle macrophage phenotype was determined by the age of the host muscle or the age of the marrow from which the cells were derived by transplanting young bone marrow cells (BMCs; 2-month-old donors) into young mice (2-months-old) or adult mice (12-months-old) and then assaying muscle macrophage phenotype and muscle fibrosis 8 months later. Levels of chimerism achieved 8-months after BMT did not differ between young transplant recipients (circulating leukocytes donor-derived: 95.0%; *sem* = 1.9; *N* = 5) or old recipients (circulating leukocytes donor-derived: 97.6%; *sem* = 0.28; *N* = 4). Muscles of mice that were not transplant recipients showed increases in M2a macrophage numbers (Figure 4A) that were similar to the increases that occurred between 12 and 24 months of age (Figure 1C). Although 10-month-old mice that received BMT at 2 months of age showed numbers of M2a macrophages in muscle that were identical to the numbers that occurred in non-transplanted, 10-month-old mice, transplantation of 2-month-old BMCs into 12-month-old mice prevented the increase in intramuscular M2a macrophages that occurs during aging to 20 months of age. The muscles of 20-month-old transplant recipients and 20-month-old non-transplanted both showed similar distributions of M2a macrophages in the perimysium and endomysium (Figures 4B, C). These

findings support the view that the age of the hematopoietic compartment and not the age of the muscle is primarily important in determining the increase of M2a macrophages in aging muscle.

Transplantation of young bone marrow cells into adult mice reduced connective tissue accumulation in old muscle.

Because experimental reductions of M2a macrophages in aging muscle caused coinciding reductions in muscle fibrosis (Figures 1C; 2D - F), we tested whether the reduction of M2a macrophages in 20-month-old mice that received young bone marrow showed similarly reduced levels of fibrosis. As observed between 12- and 24-month-old, wild-type mice (Figure s 2A - C), expression of *collagens 1* and *collagen 3* did not increase significantly between 10 and 20 months, although expression of *collagen 5* showed a significant increase (Figures 4D - F). However, collagen type V expression was identical in 20-month-old mice that received transplantation of young BMCs and in 20-month-old, non-transplanted mice, indicating that aging of the hematopoietic compartment did not influence *collagen 5* expression (Figure 4F).

Similar to our findings in comparing accumulation of connective tissue proteins in aging muscle between 12 and 24 months of age (Figures 2D, E), we found that the volume fraction of muscle occupied by collagens type I, type III and type V increased between 10 and 20 months of age (Figures 4G - O). We also observed that transplantation of young BMCs into adult muscle prevented the age-related accumulation of collagens type I and type III and significantly reduced the accumulation of collagen type V during aging (Figures 4G - I). For each collagen type,

accumulation primarily occurred in the perimysial and endomysial spaces (Figures 4J - O). These findings indicate that the aging of the hematopoietic compartment contributes significantly to the accumulation of connective tissue in aging muscle.

2.4 Discussion

Our findings show that aging of the hemaotopoietic compartment is accompanied by an increase in the numbers of CD163+ M2a macrophages in skeletal muscle and show that the shift toward greater numbers of M2a macrophages is associated with increased muscle fibrosis. Furthermore, the data show that neither the increase in M2a macrophages or muscle fibrosis occurs if the age-related decrease in muscle *nNOS* expression is prevented. Collectively, the results support the hypothesis that loss of NO production in aging muscle enables an increase of M2a macrophages that can promote fibrosis through Arg1-dependent mechanisms (Figure 5). This resembles the mechanism that drives fibrosis in *mdx* muscle, although the magnitude of increase in M2a macrophages in aging muscle is only ~3-fold between 12- and 24-months-old while the increase in dystrophic muscle at the peak of inflammation is several-hundred-fold compared to wild-type muscle (Wehling *et al.* 2001). However, the magnitude of fibrosis during muscle aging is similarly less. The observations suggest that fibrosis of senescent muscle could reflect a low-grade, chronic inflammation that increases tissue fibrosis.

Aging is generally viewed as involving a systemic increase in pro-inflammatory, Th1 cytokines that are associated with promoting many physiological changes associated with aging (Krabbe *et al.* 2004). Prominent among these increases, elevations of levels of the pro-inflammatory cytokine TNFα have been reported most consistently in numerous senescent tissues, including muscle and blood (Greiwe *et al.* 2001; Visser *et al.* 2002; Schaap *et al.* 2009).

We similarly observed elevations of *TNFα* expression in all aging muscles that we examined and found those increases were accompanied by elevations in other potent, pro-inflammatory cytokines including *IFNγ* and *IL1β*. Although IFNγ and TNFα are strong activators of the pro-inflammatory, M1 macrophage phenotype, we observed that the numbers of CD163+ M2a macrophages more than doubled in aging muscle, indicating that macrophage activation to the M2 phenotype is most strongly driven in aging muscle. However, this preferential activation to the M2a phenotype was not closely reflected by increases in IL-4 or IL-13. In contrast, all muscles examined showed significant elevations of *IL-10* expression, supporting previous observations that IL-10 plays a central role in regulating M2a macrophage phenotype in muscle (Villalta *et al.* 2011; Deng *et al.* 2012). Although our findings clearly show preferential activation of macrophages to the M2a phenotype in muscle during aging, the finding is not entirely consistent with some previous observations. For example, comparisons of vastus lateralis biopsies from old (~71-years) and young (~32 years) humans showed no significant difference between the two groups in the number CD163+ macrophages when the data were expressed as number of macrophages per muscle fiber (Przybyla *et al.* 2006). Nevertheless, increases in expression of IL-10 occurred in the aging, human muscles (Przybyla *et al.* 2006), similar to the present study. More recently, histological analysis of vastus lateralis biopsies of old and young human subjects also showed no significant difference in the number of CD68+ macrophages / fiber between the two groups (Tam *et al.* 2012). However, this latter investigation reported that mRNA expression levels of both CD68 and CD206, another marker of the M2 phenotype,

approximately doubled in aged muscle, consistent with our current findings.

We were particularly interested in data obtained in our investigation that failed to implicate other cell types in age-related shifts in muscle myogenesis and fibrosis. For example, recent findings indicating a significant role of SiglecF+ eosinophils in IL-4 mediated activation of FAPs to drive regeneration of young muscle following acute injury (Heredia *et al.* 2013) suggested the possibility that perturbations in eosinophil numbers or IL-4 expression in aging muscle could influence the shift of senescent muscle to a less myogenic phenotype. However, we found eosinophils were rare in muscles at both 12-months and 24-months of age, their numbers did not change during aging, they were located primarily in the epimysium rather than within muscle fascicles and IL-4 levels did not decline with aging. We also anticipated that numbers of FoxP3 Tregs within the muscle could decline during aging, in view of recent findings that T-regs promote muscle regeneration and reduce fibrosis in young muscle following injury (Burzyn *et al.* 2013). However, Tregs numbers and FoxP3 expression were low and did not change during aging, showing that reductions in myogenic capacity and increases in muscle fibrosis during aging were not likely the consequence of reductions in Treg functions within the muscle, as can occur in young, injured muscle.

We were also surprised that we did not detect signs of increased activation of Wnt signaling that would reflect transitions of satellite cells from a myogenic phenotype to a fibrogenic phenotype. This phenotypic transition is driven by a switch from Notch signaling to Wnt signaling,

reflected in a requisite increase in *axin-2* transcription (Brack *et al.* 2007). Previous investigations showed that during mouse aging, this transition corresponded to both a reduction in the regenerative capacity of satellite cells and an increase in muscle fibrosis which was reflected by an approximately 2-fold increase in *axin-2* mRNA as mice aged from about 5-months-old to about 25-months-old (Brack *et al.* 2007). However, we observed no increase in *axin-2* mRNA in muscle between 12- and 24-months of age, indicating that the increased occurrence of fibrosis during muscle aging did not require elevation of *axin-2* expression during that interval.

Reductions in satellite cell numbers have also been associated with shifting the balance between myogenesis and fibrosis in aging muscle, although conclusions vary with regard to whether reductions in satellite cell numbers actually occur during aging. Part of the explanation for the discrepancy reflects the ages selected for comparison. For example, numbers of Pax7 expressing cells per mouse myofiber in extensor digitorum longus muscle significantly declined when comparing 3- to 6-month-old muscles to 18- to 27-months-old muscles, but there was no significant reduction when comparing 11- to 12-months-old muscles to 18- to 27-months-old muscles (Shefer *et al.* 2006). That observation is consistent with the findings in the present investigation, which show no changes in satellite cell number per unit volume of muscle occurred between 12- and 24-months of age in mice. However, we did observe that expression of the *nNOS* transgene increased *Pax7* expression and produced a strong trend ($p = 0.057$) for increased numbers of satellite cells in 12-months-old muscle. This finding is consistent with

previous studies which showed that muscle-derived NO and exogenous NO donors can increase satellite cell numbers in young mice (Anderson, 2000; Buono *et al.* 2012) and *in vitro* (Soltow *et al.* 2010). Furthermore, we observed that the NO-induced elevation of *Pax7* expression in 12-month-old muscles coincided with increases in expression of *Vangl2*. Previous investigators have demonstrated that NO can promote satellite cell proliferation *in vitro* via an NO-Vangl2-cGMP pathway that requires increased transcription of Vangl2 (Buono *et al.* 2012). Curiously, we did not find evidence for NO-Vangl2 induction of satellite cell proliferation in 24-months-old muscles, and the increase in *Pax7* expression that was evident at 12-months of age in transgenic mice returned to wild-type levels at 24-months of age. Previous assays of NO-induction of satellite cell proliferation *in vitro* showed a decline in the inductive effect in satellite cells isolated from old muscle (Leiter & Anderson, 2010). That observation combined with our findings suggest that the defect in NO activation of proliferation in old satellite cells may result from a lack of NO induction of Vangl2 expression that is specific to old muscle.

Our observations that muscle aging is associated with an increase in intramuscular M2a macrophages and increased fibrosis led us to speculate that aging of the hematopoietic lineage cells from which the macrophages were derived could influence the amplification of intramuscular M2a macrophages, independent of the age of the host tissue. We tested this by transplanting young BMCs into young or old recipients and then assaying M2a macrophage numbers and extent of fibrosis 8 months later. Our finding that young BMT into young recipients yielded numbers of intramuscular M2a macrophages that did not differ from non-transplanted,

age-matched controls showed that macrophages derived from transplanted BMCs retained their normal capacity to enter muscle. However, young BMT into old recipients showed numbers of M2a macrophages in muscle that matched the age of the donors, not the recipient. Furthermore, the age-related increases in collagen type 1 and type 3 content of muscle did not occur in the muscles of mice that received young BMT. That finding validates the positive relationship between changes of M2a macrophage prevalence and the extent of muscle fibrosis, but it also tells us that factors endogenous both to aging skeletal muscle and to aging hematopoietic lineage cells work in concert to influence the numbers of M2a macrophages in aging muscle.

Recent, important findings showing that muscle fibrosis is amplified by depleting satellite cells from muscle during aging (Fry *et al.* 2015) combined with observations that satellite cell-derived factors can modulate the activity of fibroblasts in muscle (Fry *et al.* 2014) indicate that cells from multiple lineages may interact to regulate muscle fibrosis during aging. Our findings that implicate cells of the hematopoietic lineage in muscle fibrosis show that cells derived from the bone marrow also participate in that regulatory network. Notably, the extent to which aging muscle fibrosis is promoted by satellite cell depletions (Fry *et al.* 2015) resembles the extent to which aging of hematopoietic lineage cells appear to contribute to muscle fibrosis, in the present study. Continuing studies are directed toward exploring the potential regulatory interactions between satellite cells and bone marrow derived cells that regulate fibrosis and other age-related changes of muscle.

2.5 Materials and methods

Animal treatments

Experiments involving animals were conducted according to the National Institutes of Health Guide for the Care and Use of Laboratory Animals and were approved by the Institutional Animal Care and Use Committee. Muscles were collected from wild-type (C57 BL/6) mice or mice that expressed a muscle-specific transgene encoding nNOS (Wehling *et al.* 2001) at 12- or 24-months of age and then used for analysis. As shown in previous work (Samengo *et al.* 2012), nNOS expression in wild-type, mouse quadriceps muscle declines ~50% at the mRNA level and ~70% at the protein level between 12- and 24-months of age. Expression of the *nNOS* transgene increases nNOS protein expression in muscle by ~50-fold over wild-type levels (Wehling *et al.* 2001). Muscles were analyzed at 10- or 12-months of age which corresponds to ~38 to 43-years of age in humans (Flurkey *et al.* 2007) and at 20- or 24-months-old which corresponds to humans at ~62 to 69-years of age (Flurkey *et al.* 2007). Survivorship of non-irradiated C57 BL/6 mice is greater than 80% at 24-months (Flurkey *et al.* 2007). Survivorship of irradiated C57 BL/6 mice is greater than 60% at 20-months of age (current investigation). We have shown that significant sarcopenia occurs between 10- and 20-months of age in irradiated mice (present investigation) and between 12- and 24-months of age in non-irradiated mice (Samengo *et al.* 2012 and present investigation).

Bone marrow transplantation.

Wild-type mice were used for heterochronic, bone marrow transplantation in which donor mice were 2-months-old, female mice and recipient mice were 2- or 12-months-old male mice. A schematic graph of experimental design for bone marrow transplantation experiments is shown in Figure 6.

Recipient mice were given antibiotic-treated water containing 0.5 mg/ml trimethoprim/ sulfamethoxazole for 6 days before irradiation. The mice then received total body irradiation of 950-1000 R in one dose emanating from a cesium 137 source. 18 hours after irradiation, the mice were injected via tail vein with freshly isolated bone marrow cells (BMCs). BMCs for transplantation were flushed from tibias and femurs of 2-months-old female donor mice after euthanization by isoflurane inhalation. The femurs and tibias were sterilly dissected, cleaned and collected in sterile Petri dishes containing ice-cold sterile Dulbecco's phosphate-buffered saline (DPBS; Gibco). BMCs were collected by flushing the bones with DPBS using a 23G needle. Red blood cells were lysed using 3 ml ACK lysing buffer (BioWhittaker) for 5 minutes on ice before reconstitution to 10 ml with DPBS. The cells were then filtered with a 70 μm cell strainer and then centrifuged at 500 x g for 5 minutes. The cells were then washed and centrifuged two more times in DPBS to assure that non-cellular material was not transferred to the BMC transplant recipient. The final, cell pellet was re-suspended in DPBS at a concentration of 6.7×10^7 cells / ml. Each recipient mouse was then injected with 150 μl containing 10^7 cells

via tail vein. The recipients were provided antibiotic water for 2 weeks after irradiation and then switched to acidified water without antibiotics.

Chimerism assay.

The engraftment of transplanted BMCs was evaluated using fluorescent in situ hybridization analysis for the X and Y chromosomes (Kreatech). Blood samples were collected from the femoral artery at the time of dissection into tubes containing 100 µl of 20 mM EDTA (pH 8.0). Red blood cells were lysed with 0.85% ammonium chloride for 10 minutes and centrifuged for 5 minutes at 800 x g. The pellets were resuspended in 500 µl of 75 mM KCl and incubated for 1 minute at room temperature. Samples were then fixed with ice-cold 3:1 methanol and glacial acetic acid and centrifuged for 5 minutes at 1400 x g. The pellets were resuspended in buffer, placed on slides and left to air dry. Slides were treated in 2X saline-sodium citrate (SSC) buffer with 0.6 M sodium chloride and 60 mM trisodium citrate (pH 7.0) at 37 ºC for 15 minutes and then dehydrated in ethanol for 1 minute and air-dried. Slides were then treated with denaturing solution (70% formamide in 2X SSC (pH 7.0)) at 72 ºC for 2 minutes and dehydrated in ice-cold 70%, 85% and 100% ethanol for 2 minutes each and air-dried. The X/Y chromosome probes (Kreatech) were denatured at 90 ºC for 10 minutes. 2 µl of probe were applied to each slide and incubated overnight at 37 ºC. After incubation, slides were washed successively in 0.4X SSC/ 0.3% Igepal at 72 ºC for 2 minutes, 2X SSC/ 0.1% Igepal at room temperature for 1 minute, and 2X SSC at room temperature for 1 minute. Slides were then dehydrated in 70%, 85% and 100%

ethanol for 1 minute each, air-dried and cover-slipped with Prolong Gold antifade reagent with DAPI (Invitrogen). The numbers of XY immunolabeled cells and XX immunolabeled cells on each slide were counted and chimerism was expressed as the number of XX cells / total cell number for each mouse.

Production of Pax7 antibody and immunohistochemistry.

Pax7 hybridoma cells were purchased from Developmental Studies Hybridoma Bank. Cells were cultured in complete medium consisting of DMEM with 1% penicillin- streptomycin (Gibco) and 20% heat-inactivated fetal bovine serum. After 48 hours, conditioned medium was collected and centrifuged at 400 x g for 3 minutes. Supernatant was then affinity purified on a column containing anti-mouse IgG-agarose beads (Sigma-Aldrich) pretreated with Tris buffered saline (TBS) containing 150 mM NaCl, 50 mM Tris-HCl and 0.1% sodium azide. Bound protein was then eluted in 200 µl fractions in glycine elution buffer containing 100 mM glycine (ACROS Organics) and pH adjusted to 2.2 with HCl. The column was then washed with 10 volumes TBS. Protein concentration of each fraction was determined by testing absorbance at 280 nm. The fraction with highest protein concentration was used for immunohistochemistry. Specificity of the antibody was tested by western blotting with the antibody only or antibody pre-incubated with Pax7 blocking peptide (Aviva Systems Biology).

One quadriceps muscle from each mouse was dissected and rapidly frozen in isopentane cooled in liquid nitrogen. Frozen cross-sections were cut from the midbelly of each muscle at a

thickness of 10 μm. The frozen sections were air-dried for 30 minutes and fixed in ice-cold acetone for 10 minutes, and endogenous peroxidase activity was quenched with 0.3% H_2O_2. Sections were then treated with blocking buffer from a mouse-on-mouse immunohistochemistry kit (M.O.M kit; Vector) for 1 hour and immunolabeled with affinity purified mouse anti-Pax7 antibody (1/200) for 3 hours at room temperature. Sections were washed with 50 mM sodium phosphate buffer (pH 7.4) containing 200 mM sodium chloride (PBS) and then incubated with biotin-conjugated anti-mouse IgG (1/250) from the M.O.M kit for 30 minutes. Sections were subsequently washed with PBS and then incubated for 30 minutes with ABC reagents from the M.O.M kit. Staining was visualized with the peroxidase substrate 3-amino-9-ethylcarbazole (AEC kit; Vector), yielding a red reaction product.

For immunohistochemistry for other antigens, acetone-fixed frozen sections of quadriceps were blocked in 3% bovine serum albumin (BSA) and 2% gelatin in 50 mM Tris buffer (pH 7.2) for 1 hour and then immunolabeled with rat anti-CD68 (1/100; Serotec), rabbit anti-CD163 (1/50; Santa Cruz Biotech), rabbit anti-major basic protein (1/3000; from Dr. James Lee, Mayo Clinic, Scottsdale), rabbit anti-collagen type I (1/50; Chemicon International) or goat anti-collagen type V (1/50; Southern Biotech) for 3 hours at room temperature or with rat anti-FoxP3 (1/10; eBioscience) or goat anti-collagen type III (1/50; Southern Biotech) overnight at 4 ºC. Sections were washed with PBS and then probed with biotin-conjugated secondary antibodies (1/200; Vector) for 30 minutes. Sections were subsequently washed with PBS and then incubated for 30 minutes with avidin D-conjugated horseradish peroxidase (1/1000; Vector). Staining was

visualized with the AEC kit.

The number of immunolabeled cells / volume of muscle tissue was determined by first measuring the total volume of each section using a stereological, point-counting technique to determine section area and then multiplying that value by the section thickness (10 μm) (Wehling *et al.* 2001). The numbers of immunolabeled cells in each section were counted and expressed as the number of cells / unit volume of each section. The volume fraction of muscle that was occupied by specific connective tissue proteins was determined by overlaying a 10 x 10 eyepiece micrometer over microscopic images of cross-sections of entire quadriceps muscle that were immunolabeled with antibodies to collagens type I, type III or type V. The percentage of grid intercepts that overlaid antibody-labeled connective tissue relative to total grid intercepts was determined to assess connective tissue volume fraction.

Double-labeling for arginase-1 and CD163.

Frozen, acetone-fixed sections of quadriceps muscles were treated with blocking buffer from M.O.M kit for 1 hour and then immunolabeled with a combination of mouse anti-arginase-1 (1/100; BD Transduction labs) and rabbit anti-CD163 (1/50; Santa Cruz Biotech) for 3 hours at room temperature. Sections were washed with PBS and then incubated with a combination of FITC conjugated anti-rabbit IgG and Texas Red conjugated anti-mouse IgG (1/100; Vector) for 30 minutes in the dark. Sections were washed with PBS and cover-slipped with Prolong Gold anti-fade reagent with DAPI (Invitrogen).

RNA isolation and quantitative PCR.

Muscles were homogenized in Trizol (Invitrogen) and RNA extracted, isolated and DNase-treated using RNeasy spin columns according the manufacturer's protocol (Qiagen). RNA was then electrophoresed on 1.2% agarose gels and RNA quality assessed by determining 28S and 18S ribosomal RNA integrity. Total RNA was reverse transcribed with Super Script Reverse Transcriptase II using oligo dTs to prime extension (Invitrogen). The cDNA was used to measure the expression of selected transcripts using SYBR green qPCR master mix according to the manufacturer's protocol (Bio-Rad). Real-time PCR was performed on an iCycler thermocycler system equipped with iQ5 optical system software (Bio-Rad). We maximized the rigor of quantifying the relative levels of mRNA by following established guidelines for sample preparation, experimental design, data normalization and data analysis for QPCR (Nolan *et al.* 2006; Bustin *et al.* 2009). Because expression of reference genes that are used to normalize QPCR data can vary between samples (Vandesompele *et al.* 2002), we empirically identified reference genes that did not vary between our experimental groups using geNorm 3.5 software, as described previously (Villalta *et al.* 2011). Based on that analysis, RNPS1 and SRP14 were validated as reference genes. The normalization factor for each sample was calculated by geometric averaging of the Ct values of both reference genes using the geNorm software. The highest relative expression for each gene was set to 1 and the other expression values were then scaled to that value. Primers used for QPCR are listed in Table 5 at the end of this dissertation.

Statistics

Data are presented as mean ± *sem*. One-way analysis of variance was used to test whether differences between groups were significant at $p < 0.05$. Significant differences between groups were identified using Tukey's Post Hoc test.

Figures

Figure 1.

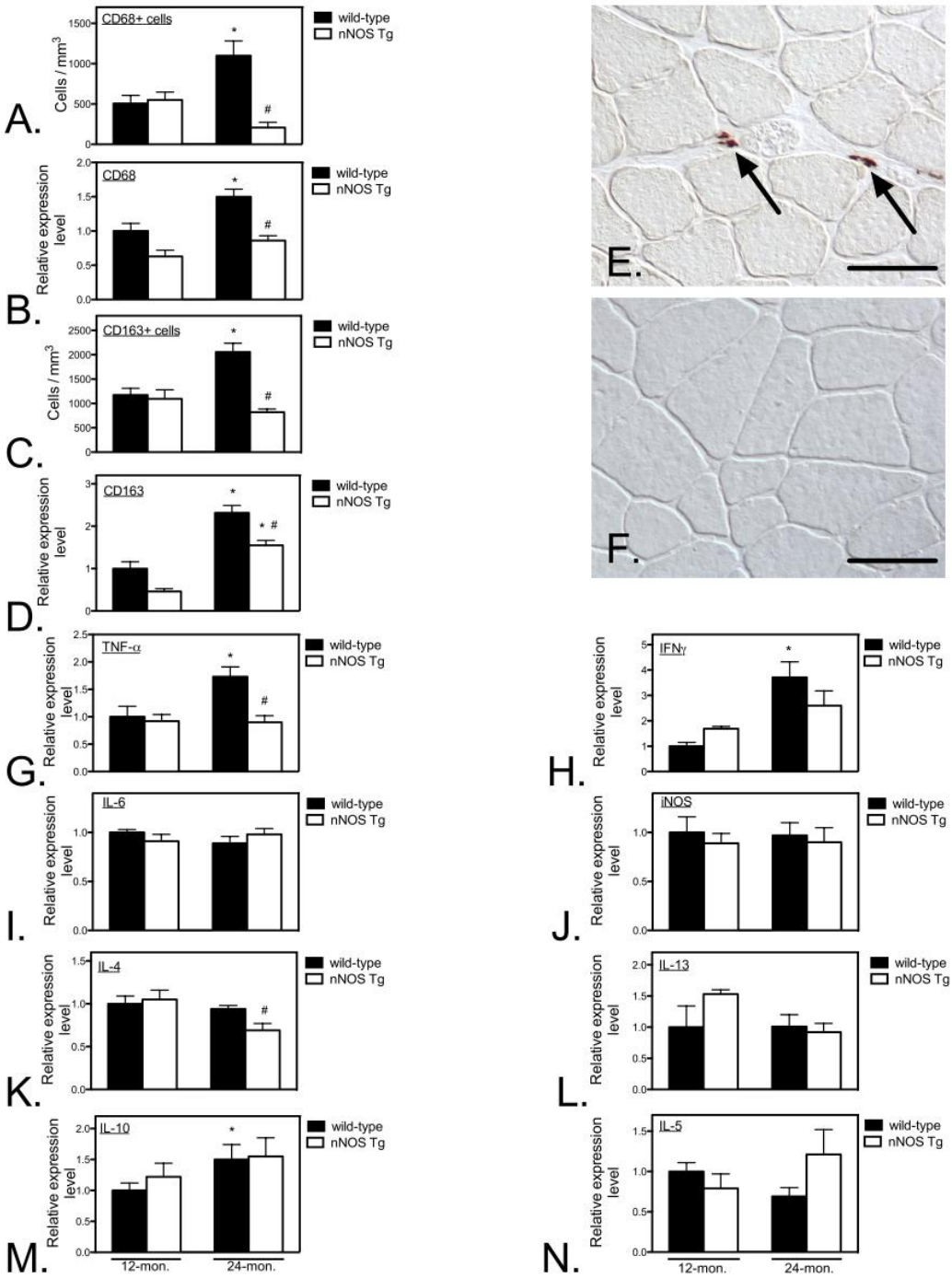

Figure 2.

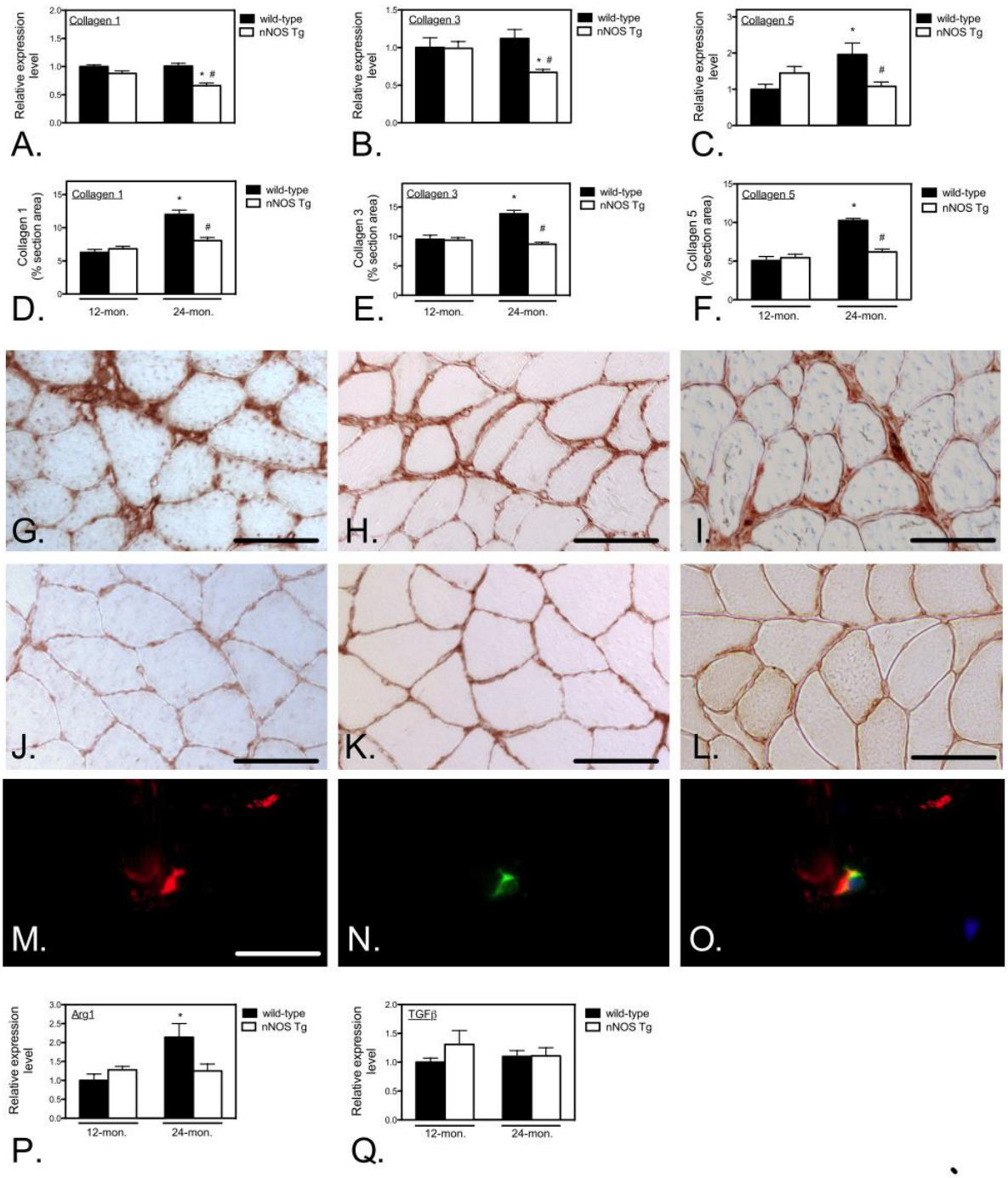
A.
Collagen 1
Relative expression level
wild-type
nNOS Tg
B.
Collagen 3
C.
Collagen 5
D.
Collagen 1 (% section area)
12-mon.
24-mon.
E.
Collagen 3
F.
Collagen 5
G.
H.
I.
J.
K.
L.
M.
N.
O.
P.
Arg1
Q.
TGFβ

Figure 3.

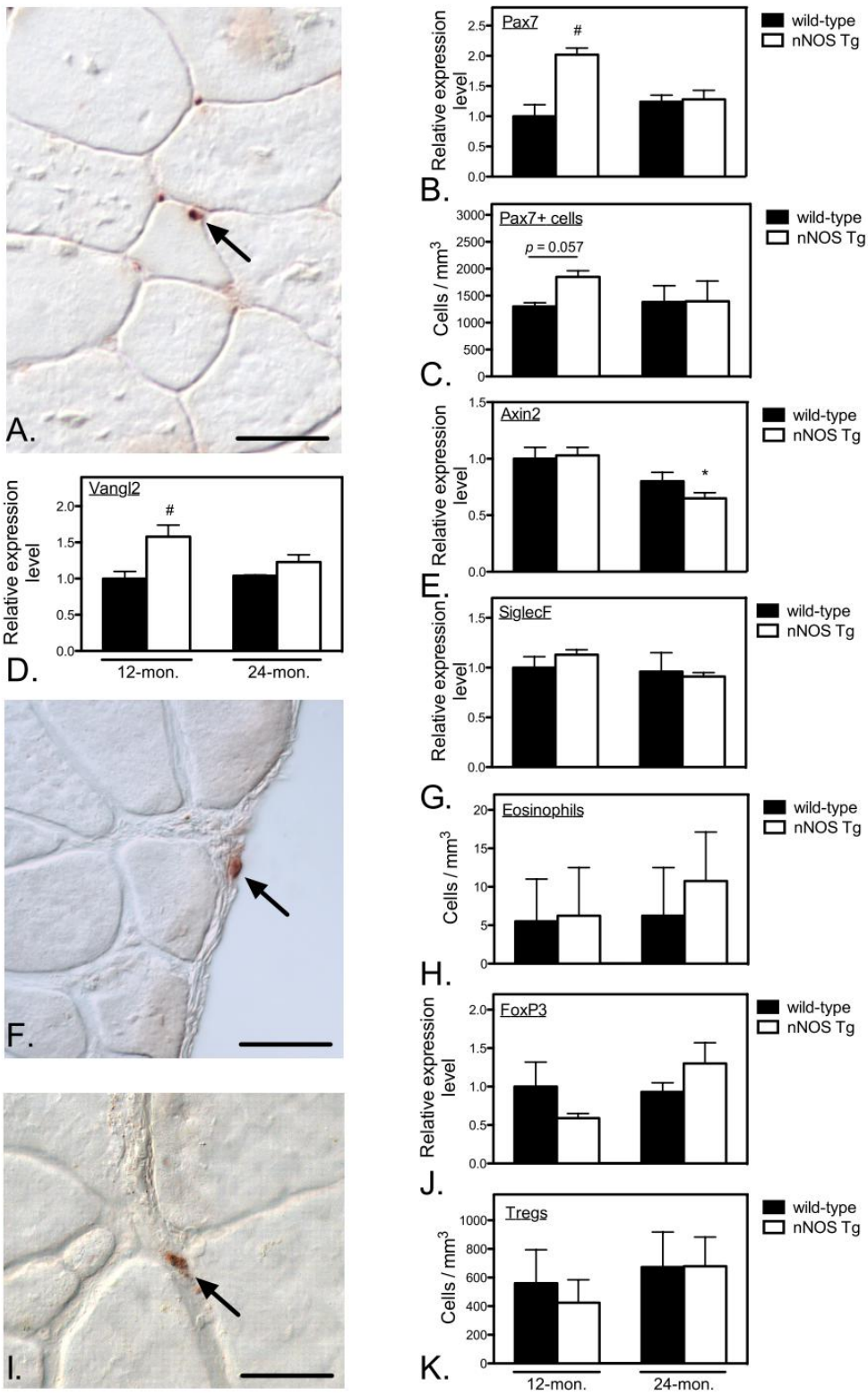
A.
B.
Pax7
#
Relative expression level
wild-type
nNOS Tg
C.
Pax7+ cells
p = 0.057
Cells / mm3
D.
Vangl2
#
12-mon.
24-mon.
E.
Axin2
*
F.
G.
SiglecF
H.
Eosinophils
I.
J.
FoxP3
K.
Tregs

Figure 4.

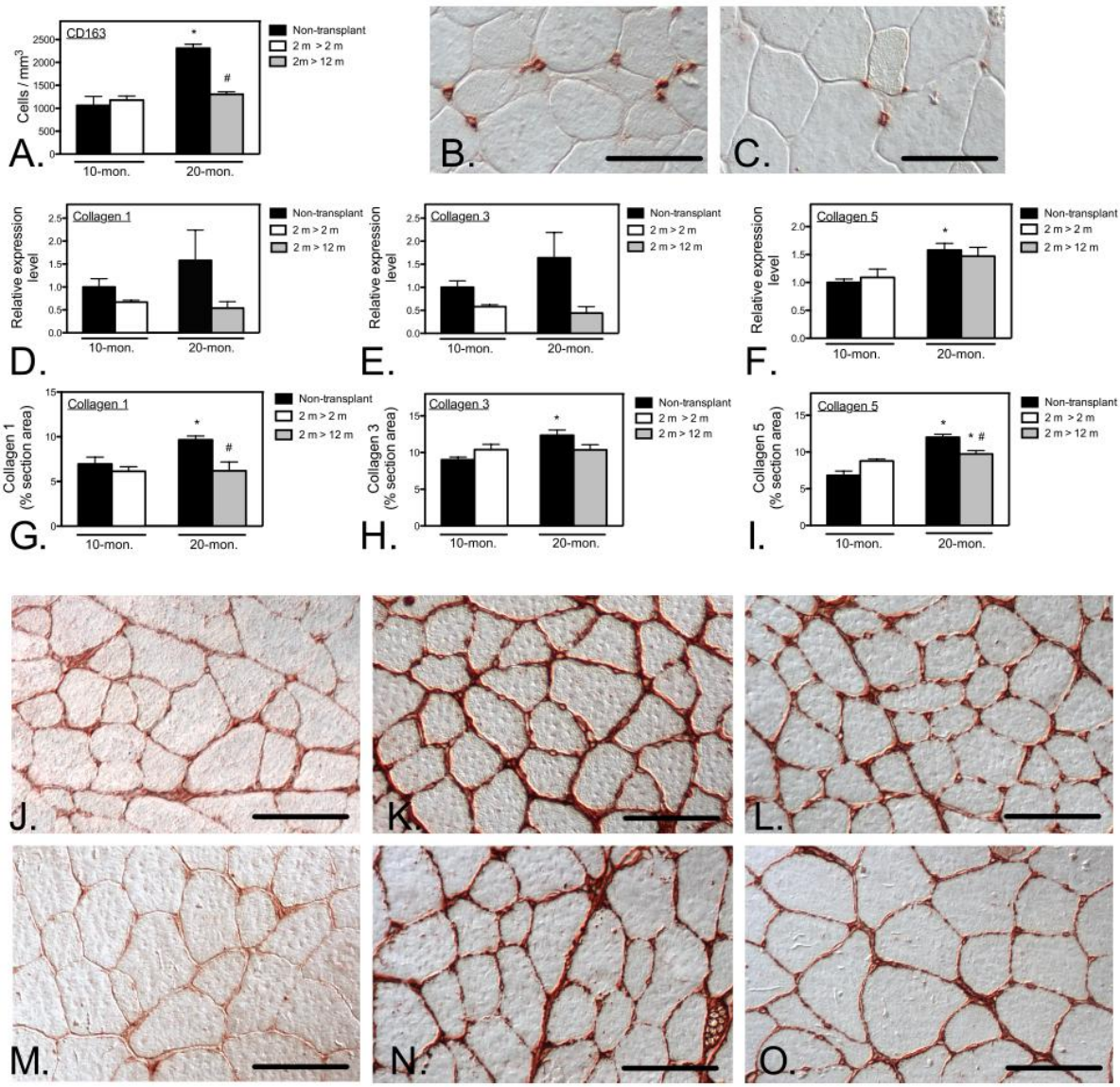
A.
CD163
Cells / mm3
Non-transplant
2 m > 2 m
2m > 12 m
10-mon.
20-mon.
B.
C.
D.
Collagen 1
Relative expression level
E.
Collagen 3
F.
Collagen 5
G.
Collagen 1
(% section area)
H.
Collagen 3
I.
Collagen 5
J.
K.
L.
M.
N.
O.

Figure 5.

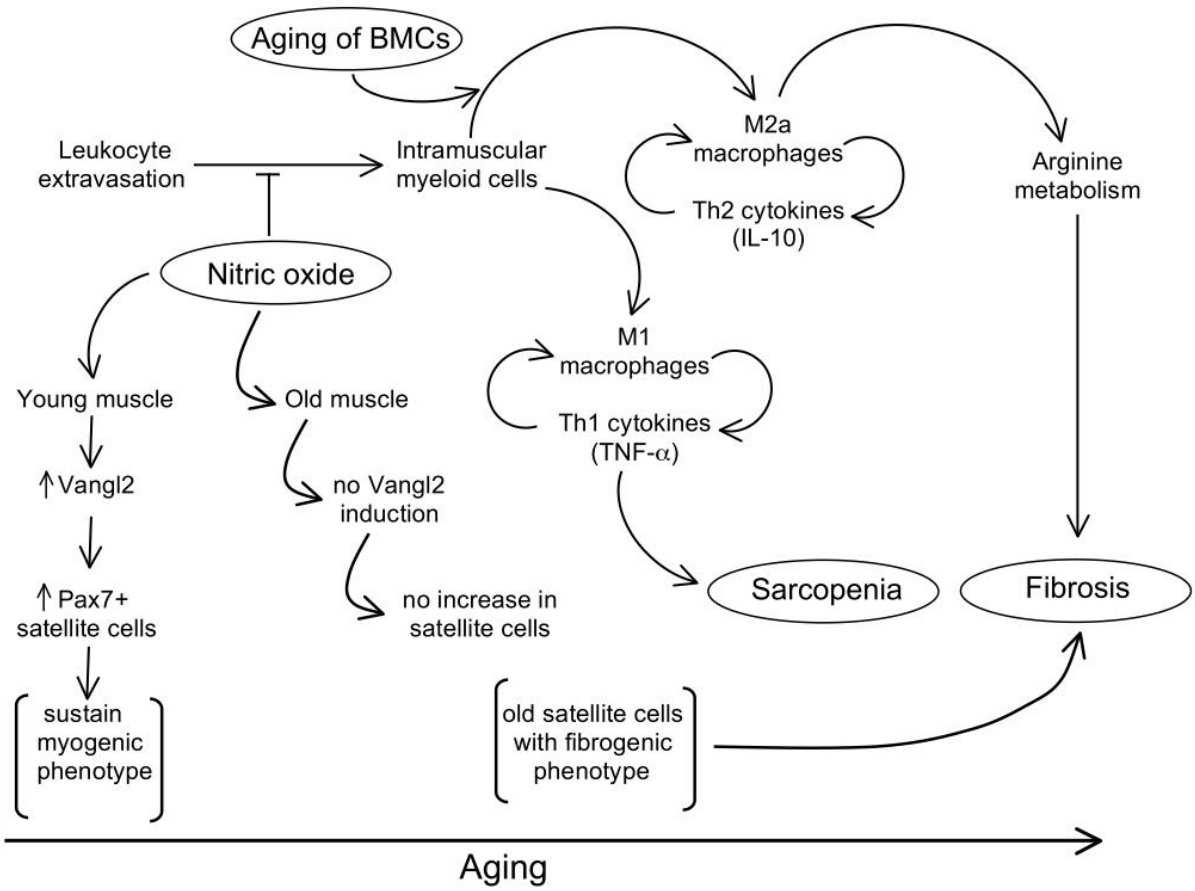
Aging of BMCs
Leukocyte extravasation
Intramuscular myeloid cells
M2a macrophages
Th2 cytokines (IL-10)
Arginine metabolism
Nitric oxide
M1 macrophages
Th1 cytokines (TNF-α)
Young muscle
Old muscle
↑Vangl2
no Vangl2 induction
↑Pax7+ satellite cells
no increase in satellite cells
Sarcopenia
Fibrosis
sustain myogenic phenotype
old satellite cells with fibrogenic phenotype
Aging

Figure 6.

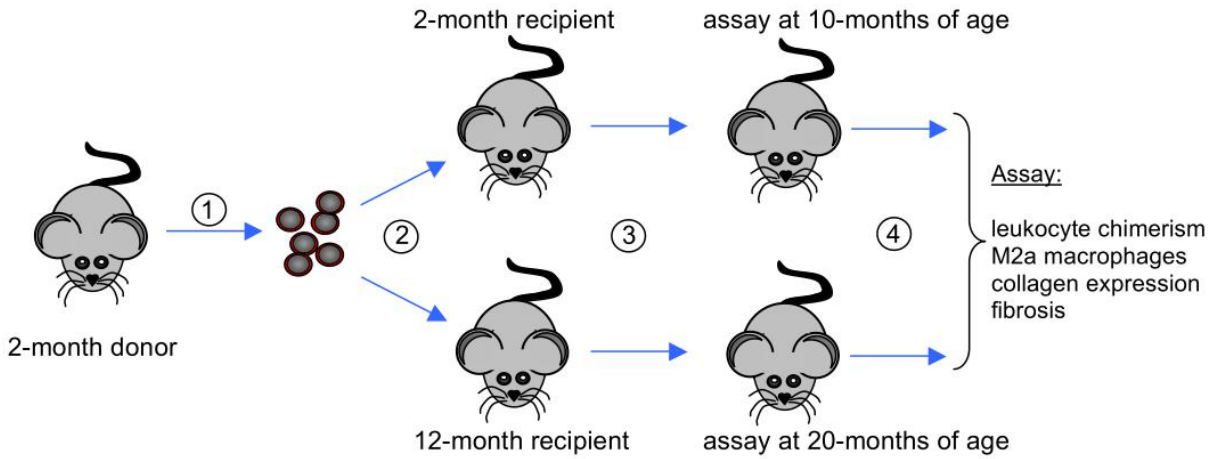
2-month recipient
assay at 10-months of age
Assay:
leukocyte chimerism
M2a macrophages
collagen expression
fibrosis
1
2
3
4
2-month donor
12-month recipient
assay at 20-months of age

Figure legends.

Figure 1. Muscle-derived NO prevents age-related increases of intramuscular macrophages and elevated expression of Th1 cytokines in muscle. A - D. Expression of a muscle-specific *nNOS* transgene prevented the age-related increases in: A. CD68+ macrophage numbers; B. *CD68* mRNA levels assayed by QPCR; C. CD163+ M2a macrophage numbers; D. *CD163* mRNA levels assayed by QPCR. E. Immunohistochemistry showing distribution of M2a macrophages labeled with anti-CD163 (arrows) in the thickened perimysium and epimysium of 24-month-old, wild-type quadriceps. F. Anti-CD163 immunohistochemistry revealed no M2a macrophages in this region of *nNOS* transgenic quadriceps muscle where the thickness of the perimysium and epimysium resembles 12-month-old wild-type mice. Bars = 40 μm. QPCR data showing increases in the mRNA for Th1 cytokines *TNFα* (panel G) and *IFNγ* (panel H) occurred in muscles during aging but the increases were prevented by transgene expression. Other mRNAs associated with M1 macrophages did not increase with aging and were not affected by transgene expression (panel I, *IL-6*; panel J, inducible NOS [*iNOS*]). Expression of mRNA for Th2 cytokines in muscle were differentially affected by aging and transgene expression: K. *IL-4* mRNA did not increase with aging, although transgene expression reduced its concentration in 24-month-old muscle; L. Neither aging or transgene expression affected *IL-13* expression. M. Aging increased *IL-10* expression but the increase was unaffected by transgene expression; N. Neither aging or transgene expression affected *IL-5* expression. N = 5 for all data sets. *

indicates significant difference at $p < 0.05$ compared to same genotype at 12-months-old. # indicates significant difference at $p < 0.05$ compared to wild-type at same age.

Figure 2. Increases in connective tissue accumulation in aging muscle coincided with elevations of *arginase* expression and were prevented by *nNOS* transgene expression. A - C: QPCR data show that *nNOS* transgene expression reduced mRNA encoding collagen types I, III and V in 24-month-old quadriceps. D - F: The volume fractions of muscle tissue occupied by collagen types I, III and V assayed by stereology of muscle cross-sections showed that each connective tissue component accumulates in muscle between 12 and 24-months of age, but the accumulation was prevented by transgene expression. G - I: Representative cross-sections of 24-months-old, wild-type quadriceps muscles labeled with antibodies to collagen type I (panel G), type III (panel H) or type V (panel I). Bar = 50 μm. J - L: Representative cross-sections of 24-months-old, *nNOS* transgenic quadriceps muscles labeled with antibodies to collagen type I (panel J), type III (panel K) or type V (panel L) showing reduction in thickness of perimysium and epimysium in transgenic muscles compared to wild-type. M - O: Immunohistochemistry, double-labeling for CD163 and Arg1. Cross-sections of 24-months-old wild-type quadriceps muscle labeled with anti-Arg1 (red; panel M), anti-CD163 (green; panel N) and the images merged (yellow; panel O) showed that all CD163+ cells expressed Arg1. P. QPCR analysis of *arginase-1* expression in quadriceps showed that the increase in *Arg1* expression with aging and the prevention of elevated *Arg1* expression in *nNOS* transgenic muscles mirrored changes in *CD163* expression. Q. QPCR analysis of *TGFβ* expression showed that there was no effect of

aging or *nNOS* transgene expression on TGFβ levels in muscle. N = 5 for all data sets. * indicates significant difference at $p < 0.05$ compared to same genotype at 12-months-old. # indicates significant difference at $p < 0.05$ compared to wild-type at same age.

Figure 3. Muscle aging is not associated with changes in *Vangl2* or *axin-2* expression or changes in satellite cell, eosinophil or Treg numbers. A. Representative image of Pax7+ satellite cells (red) at the surface of 24-months-old, wild-type muscle fibers. Bar = 25 μm. B. QPCR analysis showed that aging did not affect *Pax7* expression between 12 and 24 months. Expression of the *nNOS* transgene increased *Pax7* expression at 12 months of age but not at 24 months. C. Stereological counts for Pax7+ cells showed that aging did not affect satellite cell numbers between 12 and 24 months. Expression of the *nNOS* transgene caused a strong trend for increased satellite cell numbers at 12 months of age but not at 24 months. D. QPCR analysis showed that aging did not affect *Vangl2* expression between 12- and 24-months-old. Expression of the *nNOS* transgene increased *Vangl2* expression at 12 months of age but not at 24 months, mirroring changes in *Pax7* expression. E. QPCR analysis showed that aging did not affect *axin-2* expression between 12- and 24-months-old. F. Immunohistochemistry for eosinophils using anti-MBP on a section of 24-months-old, wild-type quadriceps. Most eosinophils (arrow) were observed in the epimysium surrounding the muscle, rather than in the parenchyma. Bar = 25 μm. G. QPCR analysis for SiglecF indicated that there was no change in eosinophil presence during muscle aging or as a consequence of *nNOS* transgene expression. H. Stereological counts for MBP+ cells show that neither *nNOS* transgene expression or aging affected eosinophil numbers

between 12 and 24 months. I: Immunohistochemistry for Tregs (arrow) using anti-FoxP3 on a section of 24-months-old wild-type quadriceps. Bar = 25 μm. J. QPCR analysis for *FoxP3* indicated that there was no change in Treg presence during muscle aging or as a consequence of *nNOS* transgene expression. K. Stereological counts for FoxP3+ cells showed that neither *nNOS* transgene expression or aging affected Treg numbers between 12 and 24 months. N = 5 for all data sets. * indicates significant difference at $p < 0.05$ compared to same genotype at 12-months-old. # indicates significant difference at $p < 0.05$ compared to wild-type at same age.

Figure 4. Effects of heterochronic BMT on muscle fibrosis and inflammation. A. Anti-CD163 immunohistochemistry showed intramuscular M2a macrophages increased in number significantly between 10 and 20 months of age, but the increase did not occur in 20-month-old mice that had received transplantation of 2-month-old BMCs when the recipients were 12 months of age. B. Representative anti-CD163 immunohistochemistry of M2a macrophages in quadriceps muscle of 20-month-old, non-transplanted mouse. Bar = 40 μm. C. Representative anti-CD163 immunohistochemistry of M2a macrophages in quadriceps muscle of 20-month-old mouse that received transplantation of 2-month-old BMCs. Bar = 40 μm. D - E. QPCR for mRNA for collagens in muscle showed no significant differences in expression of collagen type I or type III between 10- and 20-months of age between any of the treatment groups. F. QPCR for collagen type V showed that the significant increase in collagen V expression in muscle between 10- and 20-months of age was not affected by transplantation of 2-month-old BMCs. G - I. The volume fractions of muscle tissue occupied by collagen types I, III and V assayed by stereology

of muscle cross-sections showed that 20-month-old, non-transplanted mice had significantly larger volume fraction of the muscle occupied by collagen types I, III or V than occurred in 10-month-old non-transplanted mice. Transplantation of 2-month-old BMCs prevented the age-associated increase in collagen type I in muscle (panel G), did not affect the increase in collagen type 3 (panel H) and reduced, but did not prevent, the increase in collagen V in 20-month-old mice. N = 5 for all groups. * indicates significant difference at $p < 0.05$ compared to 10-month-old mice receiving same treatment. # indicates significant difference at $p < 0.05$ compared to non-transplanted mice at same age. J, K: Representative images of cross-sections of quadriceps from 20-months-old, non-transplanted mice (panels J - L) or 20-months-old mice receiving transplantation of 2-month-old BMCs (panel M - O) after labeling with anti-collagen type I (panels J and M), type III (panels K and N) and type V (panels L and O), showing a decreased volume fraction of muscle occupied by collagens type I and type V in mice receiving BMT from young donors. Bars = 50 μm.

Figure 5. Summary diagram that illustrates potential mechanisms through which muscle-derived NO and bone marrow-derived cells can influence sarcopenia and muscle fibrosis that occurs during aging. In young muscle, relatively-high levels of nitric oxide are capable of: 1) increasing satellite cell numbers through increased, Vangl2-mediated signaling (Anderson, 2000; Buono *et al.* 2012) and 2) inhibiting extravasation of leukocytes into the muscle. Age-related loss of muscle nNOS is associated with an increase intramuscular leukocytes, especially M2a macrophages that can promote muscle fibrosis via arginase-mediated metabolism. Aging of

BMCs leads to a shift in myeloid cells in muscle toward the M2a phenotype that occurs independent of the age of the muscle in which the myeloid cells reside. This shift in macrophage phenotype can further promote muscle fibrosis during aging.

Figure 6. Schematic diagram of the experimental design for bone marrow transplantation experiments. Bone marrow was isolated from female, 2-month-old wild-type mice (1). The isolated cells were then repeatedly washed in buffer and then transplanted to either 2-month-old or 12-month-old, wild-type, male recipients by tail vein injection (2). Mice in both groups were then housed for 8-months to permit bone marrow engraftment and aging (3). Tissues were collected for analysis when the young group was 10-months-old and contained 10-months-old bone marrow-derived cells and the old group was 20-months-old containing 10-months-old bone marrow-derived cells (4).

Tables

Table 1.

Muscles	Transcripts									
	CD68	IL-1β	TNFα	IFNγ	IL-6	CD163	IL-4	IL-5	IL-10	IL-13
Quadriceps	1.5 (0.11)*	2.74 (0.28)§	1.73 (0.18)*	3.71 (0.61)#	0.89 (0.07)	2.18 (0.12)#	0.94 (0.04)	0.69 (0.11)	1.50 (0.10)*	1.06 (0.21)
Soleus	2.55 (0.18)§	1.07 (0.19)	3.24 (0.35)§	3.08 (0.77)*	0.82 (0.12)	2.32 (0.17)§	1.48 (0.24)	1.16 (0.13)	11.66 (0.6)§	1.52 (0.33)
Tibialis anterior	1.64 (0.07)#	1.72 (0.14)#	2.35 (0.13)§	4.21 (0.25)§	0.83 (0.08)	1.66 (0.04)#	1.34 (0.15)	1.18 (0.03)#	7.96 (1.14)§	ND

* Unpaired T-test; $p < 0.05$

Unpaired T-test; $p < 0.01$

§ Unpaired T-test; $p < 0.001$

Table 1. Relative expression levels of inflammation-associated genes in 24-month-old muscles assessed by QPCR. Values shown are expressed relative to the expression levels in 12-month-old wild-type muscles in which the Ct values are normalized to empirically validated reference genes and the log transformation of the normalized mean for the group is adjusted to 1 unit. Standard errors of the mean are shown parenthetically. N = 5 for each group.

References

Alnaqeeb MA, Alzaid NS, Goldspink G (1984) Connective tissue changes and physical properties of developing and ageing skeletal muscle. *Journal of Anatomy*. **139**, 677-689.

Anderson JE (2000) A role for nitric oxide in muscle repair: Nitric oxide-mediated activation of muscle satellite cells. *Molecular Biology of the Cell.* **11**, 1859-1874.

Babraj JA, Cuthbertson DJR, Smith K, Langberg H, Miller B, Krogsgaard MR, Kjaer M, Rennie MJ (2005) Collagen synthesis in human musculoskeletal tissues and skin. *American Journal of Physiology-Endocrinology and Metabolism.* **289**, E864-E869.

Brack AS, Conboy MJ, Roy S, Lee M, Kuo CJ, Keller C, Rando TA (2007) Increased Wnt signaling during aging alters muscle stem cell fate and increases fibrosis. *Science.* **317**, 807-810.

Buono R, Vantaggiato C, Pisa V, Azzoni E, Bassi MT, Brunelli S, Sciorati C, Clementi E (2012) Nitric oxide sustains long-term skeletal muscle regeneration by regulating fate of satellite cells via signaling pathways requiring Vangl2 and cyclic GMP. *Stem Cells.* **30**, 197-209.

Burzyn D, Kuswanto W, Kolodin D, Shadrach JL, Cerletti M, Jang Y, Sefik E, Tan TG, Wagers AJ, Benoist C, Mathis D (2013) A special population of regulatory T cells potentiates muscle repair. *Cell.* **155**, 1282-1295.

Bustin SA, Benes V, Garson JA, Hellemans J, Huggett J, Kubista M, Mueller R, Nolan T, Pfaffl MW, Shipley GL, Vandesompele J. Wittwer CT. (2009) The MIQE guidelines: minimum information for publication of quantitative real-time PCR experiments. *Clinical Chemistry.* **55**,

611–622.

Chakravarthy MV, Davis BS, Booth FW (2000) IGF-I restores satellite cell proliferative potential in immobilized old skeletal muscle. *Journal of Applied Physiology.* **89**, 1365-1379.

Deng B, Wehling-Henricks M, Villalta SA, Wang Y, Tidball JG (2012) IL-10 triggers changes in macrophage phenotype that promote muscle growth and regeneration. *Journal of Immunology*. **189**, 3669-3680.

Flurkey K, Currer JM, Harrison DE (2007) The mouse in aging research. In: *The Mouse in Biomedical Research*. 2nd edition. 637-672.

Fry CS, Lee JD, Jackson JR, Kirby TJ, Stasko SA, Liu H, Dupont-Versteegden EE, McCarthy JJ, Peterson CA (2014) Regulation of the muscle fiber microenvironment by activated satellite cells during hypertrophy. *The FASEB Journal*. **28**, 1654-1665.

Fry CS, Lee JD, Mula J, Kirby TJ, Jackson JR, Liu F, Yang L, Mendias CL, Dupont-Versteegden EE McCarthy JJ, Peterson CA (2015) Inducible depletion of satellite cells in adult, sedentary mice impairs muscle regenerative capacity without affecting sarcopenia. *Nature Medicine.* **21**, 76-82.

Greiwe JS, Cheng B, Rubin DC, Yarasheski KE, Semenkovich CF (2001) Resistance exercise decreases skeletal muscle tumor necrosis factor alpha in frail elderly humans. *The FASEB Journal*. **15**, 475-482.

Heredia JE, Mukundan L, Chen FM, Mueller AA, Deo RC, Locksley RM, Rando TA, Chawla A (2013) Type 2 innate signals stimulate fibro/adipogenic progenitors to facilitate muscle

regeneration. *Cell.* **153**, 376-388.

Krabbe KS, Pedersen M, Bruunsgaard H (2004) Inflammatory mediators in the elderly. *Experimental Gerontology*. **39**, 687-699.

Leiter JRS, Anderson JE (2010) Satellite cells are increasingly refractory to activation by nitric oxide and stretch in aged mouse-muscle cultures. *The International Journal of Biochemistry & Cell Biology.* **42**, 132-136.

Nguyen HX, Tidball JG (2003) Expression of a muscle-specific, nitric oxide synthase transgene prevents muscle membrane injury and reduces muscle inflammation during modified muscle use in mice. *Journal of Physiology*. **550**, 347-356.

Nolan T, Hands RE, Bustin SA. (2006) Quantification of mRNA using real-time RT–PCR. *Nature Protocols.* **1**, 1559–1582.

Pattison JS, Folk LC, Madsen RW, Childs TE, Booth FW (2003) Transcriptional profiling identifies extensive downregulation of extracellular matrix gene expression in sarcopenic rat soleus muscle. *Physiological Genomics* **15**, 34-43.

Peake J, Della Gatta P, Cameron-Smith D (2010) Aging and its effects on inflammation in skeletal muscle at rest and following exercise-induced muscle injury. *American Journal of Physiology-Regulatory, Integrative and Comparative Physiology.* **298**, R1485-R1495.

Przybyla B, Gurley C, Harvey JF, Bearden E, Kortebein P, Evans WJ, Sullivan DH, Peterson CA, Dennis RA (2006) Aging alters macrophage properties in human skeletal muscle both at rest and in response to acute resistance exercise. *Experimental Gerontology*. **41**, 320-327.

Richmonds CR, Boonyapisit K, Kusner LL, Kaminski HJ (1999) Nitric oxide synthase in aging rat skeletal muscle. *Mechanisms of Ageing and Development.* **109**, 177-189.

Samengo G, Avik A, Fedor B, Whittaker D, Myung KH, Wehling-Henricks M, Tidball JG (2012) Age-related loss of nitric oxide synthase in skeletal muscle causes reductions in calpain S-nitrosylation that increase myofibril degradation and sarcopenia. *Aging Cell* **11**, 1036-1045.

Schaap LA, Pluijm SMF, Deeg DJH, Harris TB, Kritchevsky SB, Newman AB, Colbert LH, Pahor M, Rubin SM, Tylavsky FA, Visser M, Hlth ABCS (2009) Higher inflammatory marker levels in older persons: associations with 5-year change in muscle mass and muscle strength. *The Journals of Gerontology. Series A, Biological sciences and medical sciences.* **64**, 1183-1189.

Schultz E, Lipton BH (1982). Skeletal muscle satellite cells: changes in proliferation potential as a function of age. *Mechanisms of Ageing and Development.* **20**, 377-383.

Shefer G, Van de Mark DP, Richardson JB, Yablonka-Reuveni Z (2006) Satellite-cell pool size does matter: defining the myogenic potency of aging skeletal muscle. *Developmental Biology.* **294**, 50-66.

Soltow QA, Lira VA, Betters JL, Long JHD, Selllman JE, Zeanah EH, Criswell DS (2010) Nitric oxide regulates stretch-induced proliferation in C2C12 myoblasts. *Journal of Muscle Research and Cell Motility.* **31**, 215-225.

Tam CS, Sparks LM, Johannsen DL, Covington JD, Church TS, Ravussin E (2012) Low

macrophage accumulation in skeletal muscle of obese type 2 diabetics and elderly subjects. *Obesity*. **20**, 1530-1533.

Tatsumi R, Hattori A, Ikeuchi Y, Anderson JE, Allen RE (2002) Release of hepatocyte growth factor from mechanically stretched skeletal muscle satellite cells and role of pH and nitric oxide. *Molecular Biology of the Cell.* **13**, 2909-2918.

Vandesompele J, De Preter K, Pattyn F, Poppe B, Van Roy N, De Paepe A, Speleman F. (2002) Accurate normalization of real-time quantitative RT–PCR data by geometric averaging of multiple internal control genes. *Genome Biology.* **3**, research/0034.1-0034.11.

Villalta SA, Nguyen HX, Deng B, Gotoh T, Tidball JG (2009) Shifts in macrophage phenotypes and macrophage competition for arginine metabolism affect the severity of muscle pathology in muscular dystrophy. *Human Molecular Genetics.* **18**, 482-496.

Villalta SA, Rinaldi C, Deng B, Liu G, Fedor B, Tidball JG (2011) Interleukin-10 reduces the pathology of mdx muscular dystrophy by deactivating M1 macrophages and modulating macrophage phenotype. *Human Molecular Genetics.* **20**, 790-805.

Visser M, Pahor M, Taaffe DR, Goodpaster BH, Simonsick EM, Newman AB, Nevitt M, Harris TB (2002) Relationship of interleukin-6 and tumor necrosis factor-alpha with muscle mass and muscle strength in elderly men and women: the health ABC study. *The Journals of Gerontology. Series A, Biological Sciences and Medical Sciences.* **57**, M326-M332.

von Maltzahn J, Jones AE, Parks RJ, Rudnicki MA (2013) Pax7 is critical for the normal function of satellite cells in adult skeletal muscle. *Proceedings of the National Academy of Sciences*

of the United States of America. **110**, 16474-16479.

Wehling M, Spencer MJ, Tidball JG (2001) A nitric oxide synthase transgene ameliorates muscular dystrophy in mdx mice. *Journal of Cell Biology*. **155**, 123-131.

Wehling-Henricks M, Jordan MC, Gotoh T, Grody WW, Roos KP, Tidball JG (2010) Arginine metabolism by macrophages promotes cardiac and muscle fibrosis in mdx muscular dystrophy. *PLoS One.* **5**, e10763

Wood LK, Kayupov E, Gumucio JP, Mendias CL, Claflin DR, Brooks SV (2014) Intrinsic stiffness of extracellular matrix increases with age in skeletal muscles of mice. *Journal of Applied Physiology*. **117**, 363-369.

Chapter 3. Aging of the immune system causes reductions in muscle stem cell populations, promotes their shift to a fibrogenic phenotype and modulates sarcopenia

3.1 Abstract

Aging is associated with diminished muscle mass, reductions in muscle stem cell functions and increased muscle fibrosis. The immune system, especially macrophages, can play important roles in modulating muscle growth and regeneration, suggesting that the immune system may also have significant influences on muscle aging. Moreover, the immune system experiences changes in function during senescence, suggesting that regulatory interactions between muscle cells and the immune system may also change during aging. In this study, we performed bone marrow transplantations between age-mismatched donor and recipient mice to test the influence of age of the immune system on muscle aging. Transplantation of young bone marrow cells into old recipients prevented sarcopenia and prevented age-related change in muscle fiber phenotype. Transplantation of old bone marrow cells into young animals reduced satellite cell numbers and promoted satellite cells to switch toward a fibrogenic phenotype. We also demonstrated that conditioned media from young, but not old, bone marrow cells promoted myoblast proliferation *in vitro*. Together, our results demonstrate that aging of the bone marrow cells promotes the age-related reduction of satellite cell number and function and contributes to sarcopenia.

3.2 Introduction

Skeletal muscle undergoes morphological and functional changes during aging, that include the progressive loss of muscle mass and strength (Roubenoff 2001; Cruz-Jentoft *et al.* 2010). Aging muscle also experiences a reduced capacity to repair and regenerate (Conboy *et al.* 2003; Cosgrove *et al.* 2014; Sousa-Victor & Munoz-Canoves 2016), and increased fibrosis and muscle stiffness (Alnaqeeb *et al.* 1984; Wood *et al.* 2014). These age-related changes in skeletal muscle directly contribute to loss of functional independence and increased rates of morbidity and mortality (Marty *et al.* 2017). Furthermore, with the extension of lifespan and the increasing number and percentage of older people in modern society (Petterson *et al.* 2012), muscle aging can lead to great socioeconomic and health challenges. Thus, there is an urgent need to better understand the mechanisms that underlie muscle aging and to develop new therapies and interventions to halt or reverse sarcopenia.

Muscle aging is influenced by intrinsic changes in satellite cells, as well as extrinsic changes in the environment of the satellite cells. Those intrinsic and extrinsic factors work together with extensive crosstalk to determine the outcome of muscle aging (Dumont *et al.* 2015). For example, muscle regenerative capacity is affected by the age of the systemic environment in which regeneration occurs. Previous studies utilizing muscle transplantation experiments (Carlson & Faulkner 1989; Roberts *et al.* 1997) or heterochronic parabiosis (Conboy *et al.* 2005; Brack & Rando 2007) showed that young muscles that regenerated in an

aged environment experienced impaired regeneration and old muscles experience improved regeneration when exposed to a youthful environment.

The immune system has been well-studied for its function in regulating skeletal muscle growth and regeneration in both acute and chronic muscle injury models (Sun *et al.* 2009; Tidball 2017). Because immune cells are important sources of cytokines and other secreted factors in circulation and some of those factors can affect myogenesis (Zamir *et al.* 1992; Cheng *et al.* 2008; Londhe & Davie 2011), it is feasible that the influence of the age of the host environment on muscle regeneration is at least partly attributable to the immune system. Moreover, the immune system also experiences changes in function during senescence, which may affect its proper interaction with the muscle compartment and contribute to muscle aging. For example, the imbalance between inflammatory and anti-inflammatory networks during immunosenescence causes a low-grade, chronic systemic inflammation, termed inflammaging (Franceschi *et al.* 2007). Inflammaging has been associated with many age-related diseases (Franceschi & Campisi 2014; Fülöp *et al.* 2016) including age-dependent muscle wasting (Jo *et al.* 2012; Wilson *et al.* 2017).

Macrophages are important members of the immune system that comprise the vast majority of intramuscular leukocytes and play an indispensable role in regulating muscle repair and regeneration. Previous studies in our lab and by other groups demonstrated that depletion of myeloid cells from injured muscle slows muscle growth and regeneration (Lescaudron *et al.*

1999; Tidball & Wehling-Henricks 2007; Segawa *et al.* 2008; Martinez *et al.* 2010), while boosting the infiltration of macrophages can enhance muscle regeneration (Lescaudron *et al.* 1999). However, aging muscle shows a progressive loss of the ability to regenerate following injury despite the approximately two-fold increase in intramuscular macrophages that occurs during aging (Wang *et al.* 2015). This suggests that qualitative, age-related changes in intramuscular macrophages may influence their ability to support muscle growth and regeneration during aging.

Macrophages may also contribute to muscle aging by influencing satellite cell functions. *In vitro* experiments showed that the presence of macrophages or macrophage-conditioned medium in satellite cell cultures can increase muscle cell numbers, as well as elevating expression of MyoD, a transcription factor expressed by activated, proliferative satellite cells (Merly *et al.* 1999; Arnold *et al.* 2007). In addition, exposing old satellite cells to young serum increased satellite cell proliferation following acute injury (Conboy *et al.* 2005). Although untested, some of the rejuvenating effects of the young serum could be attributable to the factors generated by the immune system, especially macrophages, suggesting that the age-related decrease in number and myogenic capacity of satellite cells may be partly attributed to the aging of macrophages.

Although an influence of macrophages on satellite cell aging has not been explored previously, we have shown that aging of the immune system affects muscle fibrosis during aging.

Transplantation of BMCs from young donors into old recipients reduced muscle fibrosis (Wang *et al.* 2015). Previous investigations have identified mechanisms through which macrophages facilitate fibrosis in injured and dystrophic muscles, including elevated secretion of transforming growth factor-β (TGFβ) by macrophages (Shen *et al.* 2008; Serrano & Muñoz-Cánoves 2010) and increased arginine metabolism by arginase expressed by M2a macrophages (Wehling-Henricks *et al.* 2010). However, the mechanisms through which aging of immune cells contributes to fibrosis of aging muscle are not clear, and aging satellite cells may be a component of pro-fibrotic processes that are influenced by macrophages. Satellite cells undergo myogenic-to-fibrogenic trans-differentiation during aging that results in the impaired regenerative capacity and increased fibrosis of old muscle (Brack *et al.* 2007), although the factors that regulate that transdifferentiation are unknown. Because bone marrow derived cells reside in muscle and have the potential to influence satellite cell numbers and function (Tidball & Villalta 2010; Tidball 2017), they are a potential source of factors that affect satellite cell shifts to a fibrogenic phenotype.

In the present study, we tested whether the age of the immune system contributes to sarcopenia and satellite cell function using heterochronic bone marrow transplantation (BMT). Our results show that transplantation of young BMCs into old recipients prevented sarcopenia and prevented age-related shifts in muscle fiber phenotype. Transplantation of old BMCs did not induce sarcopenia in young recipients, but did decrease satellite cell numbers despite the young age of the recipients. Moreover, we showed that the presence of conditioned media collected

from young BMCs promotes myoblast proliferation, whereas conditioned media from old BMCs did not have the pro-proliferative effect. Finally, we measured the prevalence of fibrogenic-converted satellite cells in the muscles of heterochronic BMT recipient mice and found that mice into which old BMCs were transplanted had significantly higher percentage of fibrogenic-converted satellite cells. In summary, our results indicate that aging of the immune system plays an important role in regulating muscle aging and contributes to sarcopenia through multiple mechanisms including the regulation of satellite cell proliferation and phenotype switch.

3.3 Results

Effects of bone marrow transplantation on the expression of macrophage phenotypic markers and cytokines.

Male mice that were 10-month- or 20-months old were subjected to myeloablative irradiation prior to bone marrow transplantation. Whole bone marrow cells (BMCs) isolated from 2-month-old and 18-month-old female mice were transplanted into recipients by tail vein injection of 10^7 BMCs/ mouse. Transplanted recipients were then housed in a sterile facility for 8 months before euthanasia and dissections (Figure 7). Chimerism was assessed by fluorescent *in situ* hybridization for X and Y chromosomes in leukocytes isolated from blood of each recipient mouse. The proportion of XX immunolabeled cells, which were derived from bone marrow of donor mice, was greater than 70% for all the animals used in the current investigation. At the time of tissue collection, the age of the recipients was 10-months old (if receiving BMT at 2-months of age) or 20-months old (if receiving BMT at 12-months of age). Non-transplanted mice at 10-months and 20-months of age were used as controls.

We assayed whether BMT affected the expression of macrophage phenotypic markers or cytokines by quantitative polymerase chain reaction (QPCR) for selected transcripts in quadriceps muscles of transplant recipients or age-matched, non-transplanted controls. Notably, expression levels of all transcripts assayed was very low, reflecting the absence of inflammation in the muscles. Significantly, we observed no effect of BMT into 2-months-old recipients on the

expression of the pan-macrophage marker, *F4/80* (Figure 8A), indicating that the numbers of resident macrophages in each treatment group were similar to controls. Assays for levels of expression of transcripts associated with a pro-inflammatory environment showed variable treatment effects. Although expression of *IFNγ* was unaffected by BMT, compared to non-transplanted controls, the expression levels of *TNFα, IL-1β* and *inducible nitric oxide synthase (iNOS)* were all significantly elevated in recipients of 2-month-old donor cells but not in recipients of 18-month-old donor cells (Figures 8B - E). In contrast, BMT had little effect on the expression of transcripts associated with an anti-inflammatory environment (Figures 8F - J). Although 2-month-old recipients of 18-months-old donor BMCs showed significantly less expression of *CD163* (Figure 8F), a marker of anti-inflammatory M2 macrophages, no effect was observed on the expression of *CD206* (Figure 8G) or *arginase-1 (Arg1)* (Figure 8J) which are also expressed by anti-inflammatory M2 macrophages. In addition, BMT into 2-month-olds recipients had no significant effect on the expression of the anti-inflammatory cytokines *IL-4* or *IL-10* (Figures 8H, I).

BMT had little effect on the expression of macrophage phenotypic markers or cytokines in 12-month-old recipient mice. Again, *F4/80* expression levels did not differ between BMT recipients and non-transplanted controls (Figure 8K), indicating that the numbers of resident macrophages were similar. Among all other transcripts assayed (Figures 8L - T), the only transcript expression that varied in a BMT group compared to non-transplanted mice was *IFNγ*, which was significantly higher in 12-months-old recipients of 18-months-old BMCs (Figure 8T).

Transplantation of young BMCs into old recipients prevents the age-related reduction in muscle fiber size and changes in fiber type composition.

We then tested whether aging of the bone marrow affects sarcopenia. We quantified the mass of soleus and quadriceps muscles of transplanted and non-transplanted mice. In non-transplanted controls, the mass of soleus muscles was significantly less in 20-month-old mice than 10-month-old mice (Figure 9A; white bars), indicating measureable sarcopenia during that period of aging. Similarly, the mass of soleus muscles from 20-month-old mice that received old BMT was significantly less than the mass of soleus muscles from 10-month-old mice that received old BMT (Figure 9A; black bars), reflecting a magnitude of sarcopenia that was similar to non-transplanted controls. However, the mass of soleus muscles from 20-month-old mice that received young BMT did not differ from the mass of soleus muscles from 10-month-old mice that received young BMT (Figure 9A; grey bars). These observations indicate that cells derived from young BMCs can significantly reduce sarcopenia.

We also observed that the mass of non-transplanted, control quadriceps muscles declined between 10- and 20-months of age (Figure 9B; white bars), indicating sarcopenia. Consistent with our observations on soleus muscles, we found that the mass of quadriceps muscles from 20-month-old mice that received young BMT did not differ from the mass of quadriceps muscles from 10-month-old mice that received young BMT (Figure 9B; grey bars), which would indicate young BMT reduced sarcopenia. However, unlike our observations on soleus muscles, the

masses of quadriceps muscles from 20-month-old mice and 10-month-old mice that received old BMT did not differ (Figure 9B; black bars).

Although quadriceps mass showed no significant differences between 10-month-old and 20-month-old mice that had received old BMT, histological observations indicated that the fiber cross-sectional area (CSA) of muscle fibers in quadriceps was less in 20-month-old mice receiving old BMT than 10-month-old mice receiving old BMT (Figures 9C, D). This would indicate sarcopenia had occurred in mice receiving BMT from old donors and suggest an increase in the mass of a non-contractile component of muscle during aging of those mice could underlie the discrepancy between the interpretation of mass data versus CSA measurement.

We tested more specifically whether sarcopenia occurred in mice that received BMT, by measuring the CSA of muscle fibers in cross sections of quadriceps muscle from each experimental group. In non-transplanted mice, CSA of quadriceps muscle fibers were significantly less at 20-months old than at 10-months old (Figure 9E; white bars). At 10-months of age, transplantation of neither young nor old BMCs affected myofiber CSA (Figure 9E; 10-mon old). However, 20-months-old mice that received young BMCs when the recipients were 12-month-old showed a significantly greater myofiber CSA compared to 20-month-old, non-transplanted mice (Figures 9C - E; 20-mon old). In fact, myofiber CSA of 20-month-old mice that received young BMT was similar to that of 10-month-old transplanted and control mice, suggesting that transplantation of young BMCs into old recipients prevented the decrease in

fiber size that normally happens during aging (Figure 9E). Moreover, transplantation of 18-month-old BMCs into old recipients did not have this protective effect, shown by a myofiber CSA similar to that of non-transplanted 20-month-old mice (Figure 9E; 20-mon old). Myofiber CSA of 20-month-old mice that received BMCs from old donors was significantly less than the myofiber CSA of 10-month-old mice (transplanted or non-transplanted) and 20-month-old mice transplanted with young BMCs (Figure 9E).

Aging muscle also undergoes a preferential loss of type-II fast-twitch fibers due to the specific loss of fast-twitch motor neurons (Kung *et al.* 2013; Kwon & Yoon 2017). We performed slow myosin heavy chain (sMHC) staining on cross sections of soleus muscle (Figures 9G, H) and found that the ratio of sMHC+ fibers / total fibers increased by 21% in 20-month-old non-transplanted mice compared to 10-month-old non-transplanted mice (Figure 9F; white bars). Similarly, the proportion of sMHC+ fibers was 31% greater in quadriceps of 20-month-old mice that had BMT of old BMCs, compared to 10-month-old mice that had received old BMT (Figure 9F; black bars). However, the proportion of sMHC+ fibers in young and old recipients that received young BMT did not differ (Figure 9F; grey bars) and proportion of sMHC+ fibers in neither young or old transplant recipients differed from quadriceps muscles of 10-month-old non-transplanted mice. Together, these data indicated that transplantation of young, but not old, BMCs into adult mice prevents changes in muscle fiber phenotype that normally occur during aging, in addition to preventing sarcopenia.

Transplantation of old BMCs decreases satellite cell numbers.

Because macrophage-derived factors can affect the expression of myogenic transcription factors that regulate satellite cell proliferation and differentiation, we tested whether heterochronic transplantation affected the expression of key transcription factors that control myogenesis. Our qPCR analysis of quadriceps muscles from non-transplanted mice showed that *Pax7, MyoD*, and *myogenin* expression did not differ between 10- and 20-month-old mice (Figure 10A; white bars). Ten-month-old mice that received transplantation of old BMCs had significantly lower expression of *Pax7* compared to 10-month-old, non-transplanted mice, while transplantation of young BMCs did not change *Pax7* messenger RNA level (Figure 10B). Heterochronic bone marrow transplantation did not affect the expression of *MyoD* and *myogenin* in 10-month-old mice (Figure 10B). In 20-month-old mice, we observed a similar decrease in *Pax7* expression in the recipients that received the transplantation of old BMCs compared to non-transplanted mice (Figure 10C; Pax7). Interestingly, we also found that transplantation of BMCs from 2-month-old donors into old recipients significantly decreased *Pax7* expression, although the reduction was less than that caused by transplantation of old BMCs (Figure 10C). Expression levels of *MyoD* and *myogenin* were not significantly affected by heterochronic BMT in 20-month-old mice (Figure 10C).

We also assayed whether age of the immune system influences satellite cell number because satellite cells are necessary for muscle growth and muscle regeneration following injury.

We performed immunohistochemistry of Pax7 and quantified number of Pax7+ cells per unit volume in cross-sections of quadriceps muscles. Our results show that satellite cell numbers did not differ in non-transplanted mice between 10 and 20 months (Figure 10D; white bars). Transplantation of old BMCs into both young (2-month-old) and adult (12-month-old) recipients caused significant reductions in Pax7+ cell numbers at 10- and 20-months of age, compared to non-transplanted mice (Figure 10D). However, transplantation of young BMCs did not affect satellite cell numbers (Figure 10D). These changes were in accord with changes in *Pax7* mRNA levels (Figures 10B, C). We also quantified satellite cell numbers per hundred myofibers because heterochronic BMT may have influences on fiber size (Figure 9E) and observed a similar treatment effect (Figure 10E).

In summary, our qPCR and histological data show that transplantation of old BMCs decreased Pax7+ satellite cell numbers compared to non-irradiated mice, while transplantation of young BMCs did not affect number of Pax7+ cells.

Macrophages from young mice promote myoblast proliferation.

The decrease of *Pax7* mRNA quantity and decrease in Pax7+ cell numbers in transplanted mice receiving old BMCs may reflect reductions in satellite cell proliferation, or may result from decreased Pax7 expression in each satellite cell. Moreover, Pax7+ satellite cell numbers may be influenced by direct effects of aging of BMCs or by unidentified, indirect effects. We utilized an *in vitro* model to test directly the influence on muscle cells of bone marrow-derived macrophages

(BMDMs) isolated from young or old mice (Figure 11A). Western-blotting data from myoblast cultures treated with conditioned media from cultures of young BMDMs (Young-CM) or old BMDMs (Old-CM) showed no effect on Pax7 protein levels after 2- hours treatment with the conditioned media (Figures 11B, C). However, proliferation of myoblasts in cultures, reflected by Ki67 expression, was significantly elevated in cultures treated with Young-CM, compared to Old-CM after 24-hours treatment (Figure 11D). At 48 hours after treatment, Young-CM treatment significantly increased myoblast numbers compared to myoblasts treated with non-conditioned media (Figure 11E). However, Old-CM did not significantly affect myoblast numbers compared to myoblasts cultured with non-conditioned media and myoblast cell numbers in Old-CM cultures were significantly lower from those in Young-CM cultures (Figure 11E). These data show that macrophages from young, but not old mice, promoted myoblast proliferation, indicating that aging of the bone marrow can contribute to reductions in satellite cell number caused by a reduction in pro-proliferative macrophage-derived factors.

Transplantation of old BMCs into young and adult recipients biased satellite cells toward a fibrogenic phenotype.

Aging of bone marrow may also affect myogenic capacity and may contribute to muscle aging by promoting satellite cell shifts towards a fibrogenic, non-myogenic phenotype. Because previous investigations showed that this phenotypic switch is reflected by the expression of ER-TR7, an extracellular matrix protein, by Pax7+ satellite cells (Brack *et al.* 2007), we assayed

the percentage of Pax7+ cells that expressed ER-TR7 in each of our treatment groups. We observed that the proportion of Pax7+ cells that expressed ER-TR7 was not different in non-transplanted mice at 10- and 20-months of age but more than doubled between 20- and 24-months of age (Figure 12A; white bars). We also found that transplantation of young BMCs did not influence the proportion of satellite cells that expressed the fibrogenic marker at either 10- or 20-months of age (Figure 12A). However, transplantation of old BMCs into young and adult recipients more than doubled the proportion of ER-TR7-expressing satellite cells, to levels similar to 24-month-old, non-transplanted controls (Figure 12A).

Because ER-TR7 is also secreted by fibroblast and binds to the extracellular matrix between the myofibers, distinguishing between ER-TR7 within satellite cells and versus extracellular ER-TR7 was occasionally obscured in immunolabelled sections. We chose to further validate the ER-TR7 data by assaying for HSP47, a collagen-specific molecular chaperone and marker of fibrogenic cells. Data obtained by assaying HSP47/Pax7 double positive cells were nearly identical to the data obtained for ER-TR7/Pax7 double positive cells (Figures 12B - E). In addition, we observed that mice that received transplantation of old BMCs had similar proportion of Pax7+/HSP47+ cells as 26-month-old non-transplanted mice (Figure 12B); this is intriguing because the age of the bone marrow in both the 10-month-old and 20-month-old recipients was 26-month-old because the donor BMCs were isolated from 18-month-old mice and were transplanted into the recipients for 8 months before tissue collection. Collectively, these findings show that the conversion of satellite cells toward a more

fibrogenic lineage is accelerated by the aging of the bone marrow, which may provide an additional mechanism through which aging of the bone marrow contributes to muscle aging.

3.4 Discussion

In the present study, we tested whether the age of the immune system contributes to sarcopenia and satellite cell function utilizing the heterochronic bone marrow transplantation (BMT) model. Unlike muscle transplantation or parabiosis, the BMT experiments specifically altered the immune cells, which are derived from the hematopoietic stem cells in bone marrow, which shows more specifically the role of age of the immune cells in muscle aging. Other advantages of the BMT model include no direct damage to the muscles and the possibility to keep the recipient mice alive after transplantation for a long enough time (8 months in the present study) to ensure that we are assessing the influence of the donor-derived immune system during the aging process.

Our results showed that intrinsic changes in the skeletal muscle compartment during aging are strongly influenced by aging of the immune cells. One intriguing aspect of our results is the asymmetric effects on muscle aging caused by transplantation of young versus old bone marrow cells. For example, transplantation of young BMCs into old recipients prevented the decrease of myofiber size and prevented the increase of the percentage of slow-twitch fibers seen when the recipients were 20-months old (Figures 9E, F). However, the presence of old BMCs in young recipients did not induce the change in myofiber size or slow-twitch fiber percentage at 10-months old (Figures 9E, F). These data indicate that aging of the immune system alone is not sufficient to induce sarcopenia in a young host, while aged muscles in the old recipients also did

not experience sarcopenia if a young immune system is present. Thus, an aged immune compartment and aged muscle compartment are both required for sarcopenia to occur in 20-month-old mice.

Although aging of the immune system alone is insufficient to induce sarcopenia, it is sufficient to cause the reduction in satellite cell numbers and the switch of satellite cells to a fibrogenic phenotype. Transplantation of 18-months-old BMCs into young recipients decreased the number of Pax7+ satellite cells per unit volume of muscle or satellite cell number per 100 myofibers (Figures 10D, E), which may be due to old immune cells losing the ability to secrete macrophage-derived soluble factors that promote myoblast proliferation. Moreover, we also observed that 20-month-old non-transplanted mice did not have fewer satellite cell than 10-month-old non-transplanted mice, but they did have smaller myofiber CSA and an increased proportion of slow-twitch myofibers. These data suggest that reductions in satellite cell numbers is not sufficient or necessary to induce sarcopenia. On the other hand, we observed that at both 10- and 20-months of age, the presence of 26-month-old bone marrow cells more than doubled the proportion of satellite cells that switched to a fibrogenic phenotype compared to age-matched, non-transplanted mice (Figures 12A, B), suggesting that aging of the bone marrow cells may contribute to age-related muscle fibrosis by affecting satellite cell phenotype. A previous investigation showed that lifelong reduction of satellite cells in sedentary mice did not affect the rate or extent of changes in muscle mass, myofiber CSA or fiber type composition during aging, but did cause increased fibrosis (Fry *et al.* 2015). Those observations are

consistent with our findings in the present investigation, indicating that aging of the immune system affects satellite cell proliferation and phenotype switch, which then contributes to age-related muscle fibrosis but not sarcopenia.

Interestingly, controversy exists concerning whether satellite cell numbers decrease during aging (Snow 1977; Gibson & Schultz 1983; Conboy *et al.* 2003; Shefer *et al.* 2006; Day *et al.* 2010). Different muscles and various methods used to quantify satellite cell numbers may underlie part of the discrepancy in results, but the age of mice chosen for comparison is also an important variable. For example, electron microscopy showed that the percentage of satellite cells in total myonuclei in soleus muscle that were comprised by satellite cell nuclei did not decrease when comparing 8- to 10-month-old muscles with 19- to 20-month-old muscles, but a significant decline was seen between 19- to 20-month-old muscles and 29- to 30-month-old muscles (Snow 1977). Quantifying satellite cell number per myofiber in soleus muscles with Pax7 staining of freshly isolated myofibers, Shefer *et al.* (2006) showed that the number of satellite cells per myofiber did not change significantly when comparing 7- to 10-month-old muscles to 18- to 27-month-old muscles, but there was a significant decline when comparing 18- to 27-month-old muscles to 28- to 33-month-old muscles. Those observations suggest that the reduction of satellite number does not occur during early stages of aging, but is obvious when the mice reach senescence. Those results are consistent with our findings in the present investigation, which showed no difference between 10- and 20-month-old mice in the number of satellite cell per unit volume of muscle or their number per 100 myofibers. Although observations

in previous investigations and the present study suggest that reducing satellite cell numbers by either genetic manipulation of Pax7 (Fry *et al.* 2015) or by manipulating the age of the immune system did not induce sarcopenia at 20- to 24-months of age, it is unknown whether reductions in satellite cell numbers contribute to sarcopenia at later, senescent stages of aging.

We also observed in the present investigation that young bone marrow-derived macrophages secrete soluble factors into the media that increase myoblast proliferation. Conditioned media collected from old BMDMs did not promote myoblast proliferation. However, the identity of the macrophage-derived factor that is responsible for the age-related differences in regulating myoblast proliferation remains unclear and is subject of our continuing studies. A recent study identified macrophage-derived ADAMTS1 as an extracellular regulator that promotes satellite cell activation by inhibiting Notch signaling (Du *et al.* 2017). The failure to activate Notch signaling following injury in old satellite cells led to a decreased myogenic ability of satellite cells and impaired regeneration in old muscle (Conboy *et al.* 2003), which could be rescued by exposing the old satellite cells to young serum through heterochronic parabiosis (Conboy *et al.* 2005). However, whether Notch signaling is involved in sarcopenia of sedentary mice without injury is unknown and the observation that the expression of Notch-1 is similar in satellite cells isolated from resting muscles of young and aged mice (Conboy *et al.* 2003) argues against the possibility. Further studies are needed to determine whether the age of macrophages affects ADAMTS1 expression, its function in regulating Notch signaling and whether this mechanism contributes to satellite cell proliferation ability in aging muscles.

Understanding the communication between cells in the myogenic lineage and other systems is critical for understanding mechanisms of muscle aging, including sarcopenia and age-related muscle fibrosis. The immune system is a suitable target for the development of medical interventions because of its easy accessibility and the adequate choice of drugs to alter the function of immune cells. In addition, bone marrow transplantation has been used with success in both experimental models and clinical practice as a procedure to replace host hematopoietic stem cells. However, bone marrow transplantation as a therapeutic approach for muscle diseases has not been explored previously. The data presented in this and our previous investigation (Wang *et al.* 2015) suggest that age of the immune system has a critical influence on sarcopenia, satellite cell number and phenotype and muscle fibrosis, indicating that rejuvenating the immune system through bone marrow transplantation may be a feasible way to help sustain muscle health in old age.

3.5 Materials and Methods

Mice

C57 BL/6 mice were obtained from the National Institute on Aging mouse colony. All experimental protocols were conducted according to the National Institutes of Health Guide for the Care and Use of Laboratory Animals and were approved by the University of California, Los Angeles Institutional Animal Care and Use Committee.

Bone marrow transplantation

BMCs from 2-month-old or 18-month-old C57 BL/6 mice were aseptically flushed from femurs and tibia with Dulbecco's phosphate buffered saline (DPBS; Sigma, St. Louis, MO). The cells were then treated with ACK lysing buffer (BioWhittaker) to lysis red blood cells before filtered through a 70 μm cell strainer (BD Falcon). BMCs were washed 3 times with DPBS, counted and used immediately for transplantation.

Recipient mice at the age of 2- or 12-months old were given antibiotic-treated water containing 0.5 mg/ml trimethoprim/sulfamethoxazole for 6 days before irradiation. The mice then received total body irradiation of 950-1000 R one day prior to bone marrow transplantation. Freshly isolated BMCs were transplanted through tail vein injection at the dose of 10^7 BMCs/mouse. The recipients were maintained on antibiotic water for 2 weeks after irradiation and then switched to acidified water without antibiotics for the rest of their lives. A more detailed

protocol was described in our previous paper (Wang *et al.* 2015). Survival of irradiated and transplanted mice was greater than 70% at eight months following bone marrow transplantation when muscles and blood were collected from recipient mice.

Chimerism assay

Engraftment of transplanted cells was assessed by fluorescent *in situ* hybridization for X and Y chromosome markers (Kreatech, Leica Labs, Buffalo Grove, IL, USA) using leukocytes isolated from blood that was collected from each recipient mouse. In brief, after red blood cells lysis with 0.85% ammonium chloride and sample fixation with ice-cold fix buffer (3:1 methanol and glacial acetic acid), isolated leukocytes were adhered to microscope slides and stained with the X/Y chromosomes probe following the manufacturer protocol. XY immunolabeled cells and XX immunolabeled cells on each slide were counted. Chimerism was expressed as the number of XX cells/total cell number for each mouse. The percentage of donor derived-cells was greater than 70% for all the animals used in the current investigation.

Myofiber cross-sectional area measurement

One quadriceps muscle of each mouse was dissected and rapidly frozen in isopentane cooled in liquid nitrogen. Frozen cross-sections were cut from the mid-belly of each muscle at a thickness of 10 μm. Sections were then stained with hematoxylin (Vector) for 10 minutes. The muscle fiber cross-sectional area was measured for 500 fibers randomly sampled from complete

cross-sections using a digital imaging system (Bioquant).

Anti-sMHC immunohistochemistry and counting

Frozen sections cut from the mid-belly of soleus muscles were air-dried for 30 minutes and fixed in ice-cold acetone for 10 minutes. Endogenous peroxidase activity was quenched with 0.3% H_2O_2. Sections were then blocked in Mouse on Mouse blocking (M.O.M) kit (Vector) and 2% gelatin in 50 mM Tris buffer (pH 7.2) for 1 hour and then immunolabeled with mouse anti-slow myosin heavy chain (sMHC) (Vector) for 3 hours at room temperature. Sections were washed with PBS and then probed with biotin-conjugated anti-mouse IgG antibody from the M.O.M kit (1/200; Vector) for 30 minutes. Sections were subsequently washed with PBS and then incubated for 30 minutes with ABC reagent from the M.O.M kit. Staining was visualized with AEC kit (Vector). Images were taken from sMHC stained sections and merged to cover the complete cross-sections on which total fiber and sMHC+ fibers were counted.

RNA isolation and quantitative PCR.

One quadriceps muscle of each mouse was dissected and rapidly frozen in liquid nitrogen. Frozen muscles were homogenized in Trizol (Invitrogen). RNA was extracted and isolated with chloroform separatory extraction and isopropyl alcohol participation. The RNA samples were then DNase-treated and cleaned up using RNeasy spin columns according to the manufacturer's protocol (Qiagen). Total RNA was reverse transcribed with SuperScript Reverse

Transcriptase II using oligo dTs to prime extension (Invitrogen) to produce cDNA, which was then used for qPCR using SYBR green qPCR master mix according to the manufacturer's protocol (Bio-Rad). QPCR was performed on an iCycler thermocycler system equipped with iQ5 optical system software (Bio-Rad). *RSP4X* and *SRP14* were used as reference genes. The normalization factor for each sample was calculated by geometric averaging of the Ct values of both reference genes using the geNorm software. Primers used for QPCR are listed in Table 5 at the end of this dissertation.

Pax7+ antibody preparation and immunohistochemistry

Pax7 hybridoma cells were purchased from Developmental Studies Hybridoma Bank (Iowa City Iowa). Cells were cultured in complete medium consisting of DMEM with 1% penicillin-streptomycin (Gibco) and 20% heat-inactivated fetal bovine serum (FBS). Conditioned medium was collected from the cultures and used for purification of antibodies to Pax7, as described previously (Wang *et al.* 2015).

Pax7 antibody was used for immunohistochemistry staining of cross-sections from quadriceps muscles that had been rapidly frozen in liquid nitrogen-cooled isopentane. Sections were fixed in 2% paraformaldehyde for 10 minutes and then immersed in antigen retrieval buffer (10 mM sodium citrate, 0.05% Tween 20, pH 6.0) at 95 – 100 ºC for 40 minutes. Endogenous peroxidase activity in the sectioned tissue was quenched by immersion in 0.3% H_2O_2. Sections were then treated with blocking buffer from a mouse-on-mouse immunohistochemistry kit

(M.O.M kit; Vector) for 1 hour and immunolabeled with mouse anti-Pax7 antibody overnight at 4 ˚C. Sections were subsequently incubated with biotin-conjugated anti-mouse IgG followed by incubation with ABC reagents from the M.O.M kit following manufacturer instruction. Staining was visualized with the AEC kit (Vector). The number of satellite cells/sectioned muscle fiber was determined by counting the number of Pax7+ cells in mid-belly cross-sections of muscles. For Pax7+ cells /mm^3, the volume of muscle tissue was determined by measuring the total volume of each section using a stereological, point-counting technique to determine section area and then multiplying that value by the section thickness (10 μm). To express the data as Pax7+ cells/ 100 fibers, the total number of fibers for each section was counted on the merged image of the whole section.

Myoblast proliferation assay with conditioned media from bone marrow-derived macrophages

Bone marrow cells (BMCs) were isolated from young (10-months old) and old (20-months old) mice as described above in the bone marrow transplantation section. Freshly isolated BMCs were seeded at 5 x 10^6 per 6-cm dish in RPMI-1640 (Sigma) with 20% heat-inactivated fetal bovine serum (FBS; Omega Scientific), penicillin (100 U/ml; Gibco), streptomycin (100 μg/ml; Gibco) and 10 ng/ml M-CSF (R&D) at 37 ºC with 5% CO_2 for 6 days. Media was changed on day 3 and day 5. On day 6, BMDMs were stimulated for 24-hours with activation media consisting of Dulbecco's Modified Eagle Medium (DMEM) with 0.25% heat-inactivated FBS, penicillin, streptomycin and 10 ng/ml M-CSF. Conditioned media were collected following

activation and spun at 500 x g for 5 minutes to remove floating cells and then kept frozen at -20 ˚C.

C2C12 cells were obtained from American Type Culture Collection (ATCC). C2C12 cells were seeded at 6 x 10^4 cell/ well in 6-well plate with sterile glass coverslips coated with 0.01% collagen, type I (Life Technologies) and 2% gelatin in DMEM with 10% FBS. Seeding medium was removed from cultures at 24 hours after seeding and the cells were washed with DPBS before adding conditioned media from young or old BMDMs at 2 ml / well. Coverslips were collected 24 hours after treatment with conditioned media and then immunolabeled with goat-anti-Ki67 (Santa Cruz, M-19). The staining protocol was similar to that described above for sMHC immunohistochemistry except that coverslips were fixed by immersion in cold methanol for 15 minutes. Ki67+ cells and total cell numbers were counted for each slide in at least 5 randomly chosen fields. Proliferation index was expressed as the percentage of Ki67+ cells / total cells.

A separate set of C2C12 cells were seeded at 6 x 10^4 cells/well in 6-well plate without coverslips and maintained in DMEM with 10% FBS for 24 hours. The cells then received 48 hours of treatment with conditioned media collected from young or old BMDM cultures with media change at 24 hours. After treatment, cells were washed twice with DPBS and treated with 0.05% trypsin-EDTA (Sigma) for 3 minutes. Unattached cells were collected in centrifuge tubes, spun and resuspended in 200 µl of DPBS before diluted 1:1 with trypan blue (BioWhittaker) and

counted using hemocytometer.

Western blotting and analysis

After 24-hour treatment with conditioned media or control media C2C12 cells were collected in reducing buffer (80 mM Tris-HCl pH 6.8, 0.1 M dithiothreitol, 70 mM SDS, 1.0 mM glycerol). Samples were boiled for 1 minute, then centrifuged at 12,000 x g for 1 minute. The supernatant fraction of each sample was removed and used to determine protein concentration by filter paper assay. Homogenates containing 20 pg of total protein were separated on 12% sodium dodecyl sulfate-polyacrylamide gel electrophoresis (SDS-PAGE) gels. Proteins were electrophoretically transferred onto nitrocellulose membranes while immersed in transfer buffer (39 mM glycine, 48 mM Tris). After transfer, membranes were stained with Ponceau S (Sigma) to validate uniformity of protein loading and efficiency of transfer. After destain of Ponceau S with 0.5% Tween-20 in PBS, membranes were blocked in buffer containing 0.5% Tween-20, 0.2% gelatin, and 3.0% dry milk (blocking buffer) for at least 1 hour at room temperature. Membranes were probed with mouse-anti Pax7 antibody prepared as described above (1:400) for 3 hours at room temperature. Subsequently, membranes were overlaid with ECL™ horseradish peroxidase linked anti-mouse IgG (GE Healthcare) for 1 hour at room temperature. After each incubation, membranes were washed six times for 10 minutes in wash buffer (0.5% Tween-20, 0.2% gelatin, and 0.3% dry milk). Blots were developed using Chemglow West Chemiluminescence Substrate Kit (Proteinsimple). The relative concentration of Pax7 protein in each sample was determined

by scanning densitometry using ImageJ software.

Double-labeling for Pax7 and ER-TR7 or HSP47.

The immunofluorescence, double-staining protocol was similar to the anti-Pax7 immunohistochemistry method described above, with the following differences. No endogenous peroxidase activity quench was used. After blocking, mouse anti-Pax7 antibody (1:50, purified as stated above) was applied together onto the section with rabbit-anti-HSP47 (1:1000, Abcam) antibody or rat-anti-ER-TR7 (1:1000, Santa Cruz) antibody for overnight incubation at 4 ^{o}C. Sections were subsequently washed with PBS and incubated with a combination of Dylight 488 anti-rat IgG and Dylight 594 anti-mouse IgG (1/100; Vector) for 30 minutes in the dark, followed by DPBS wash and cover-slipped with Prolong Gold anti-fade reagent with DAPI (Invitrogen). The percentage of satellite cells that had switched towards the fibrogenic phenotype was expressed as the percentage of Pax7+/ER-TR7+ or Pax7+/HSP47+ cells in total Pax7+ cells.

Statistics

Data are presented as mean ± SEM. One-way ANOVA (GraphPad) was used to test whether differences between groups were significant at $p < 0.05$. Comparisons of two groups of values were analyzed using the unpaired, two-tailed t test. Differences were considered significant at $p < 0.05$.

Figures

Figure 7.

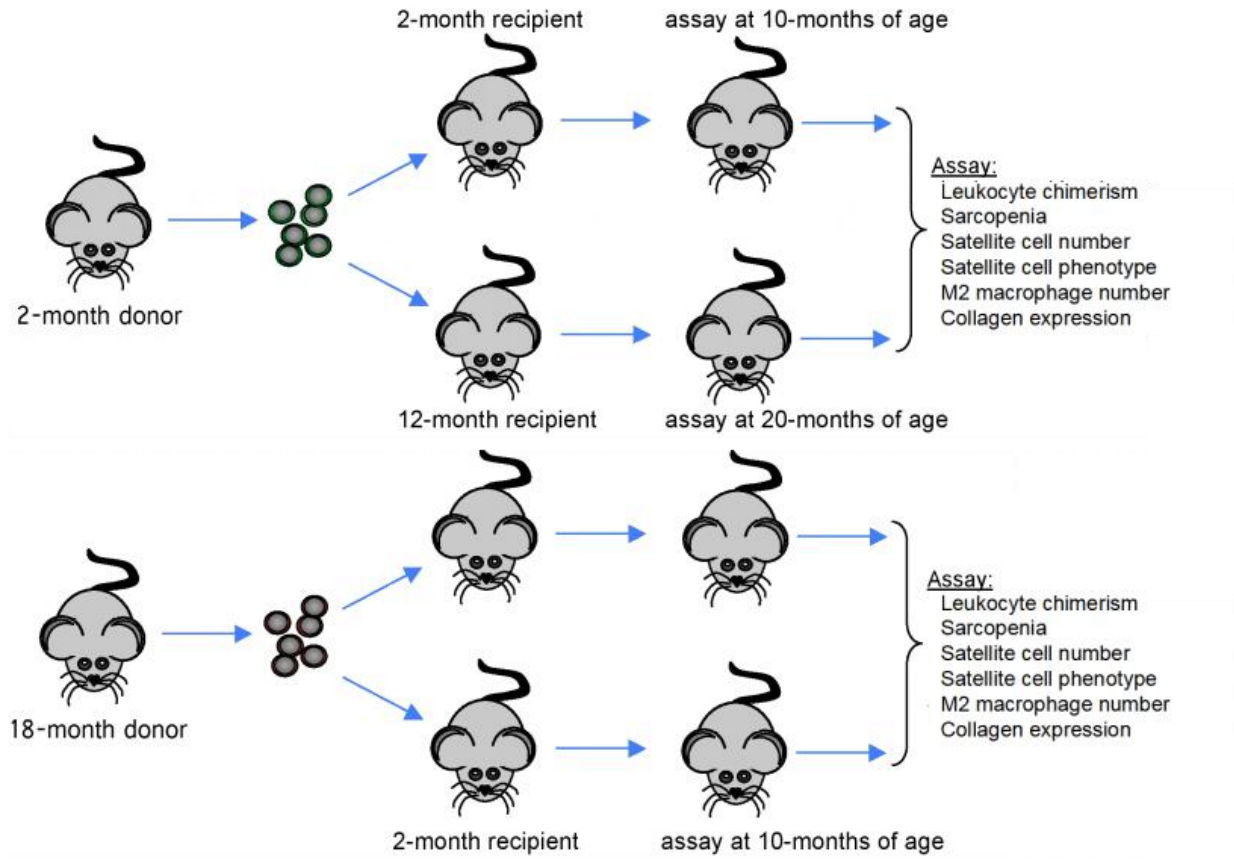

Figure 8.

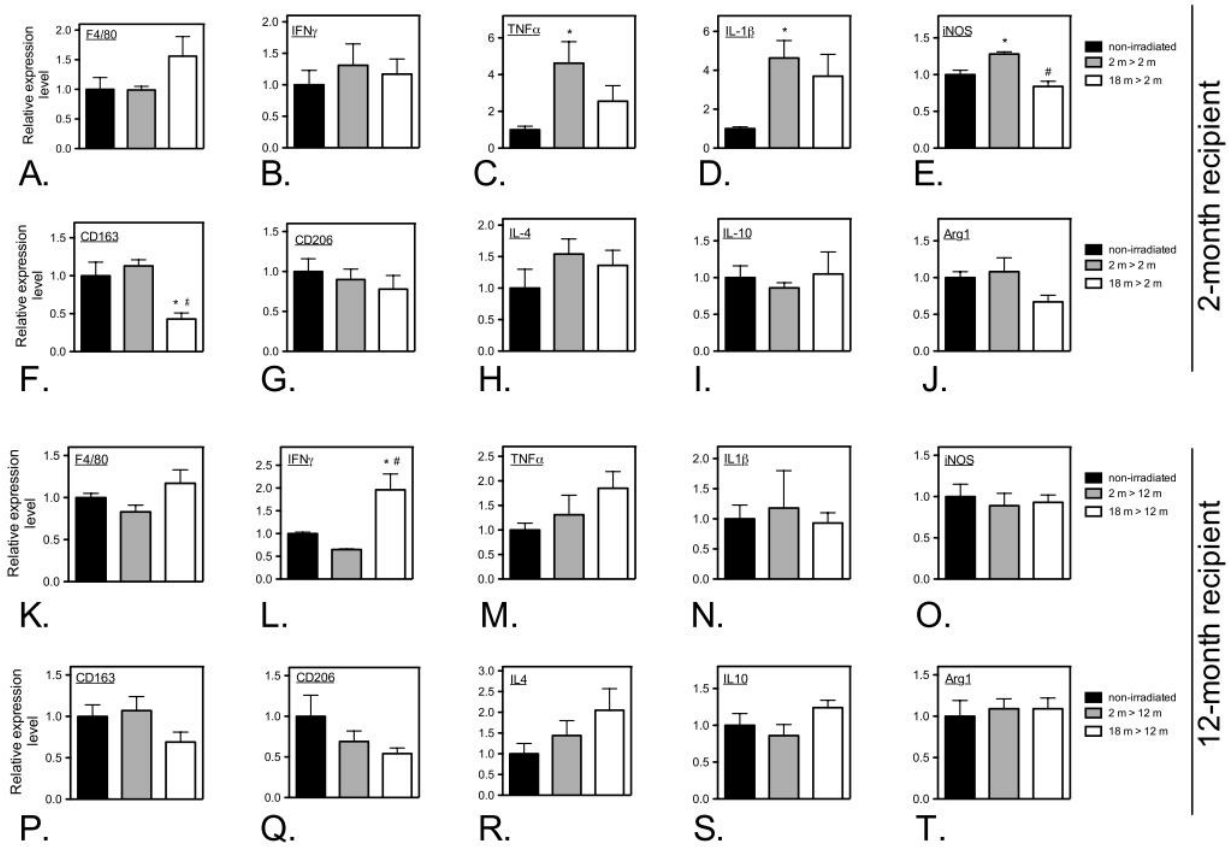
Relative expression level
F4/80
IFNγ
TNFα
IL-1β
iNOS
non-irradiated
2 m > 2 m
18 m > 2 m
2-month recipient
A.
B.
C.
D.
E.
CD163
CD206
IL-4
IL-10
Arg1
F.
G.
H.
I.
J.
F4/80
IFNγ
TNFα
IL1β
iNOS
non-irradiated
2 m > 12 m
18 m > 12 m
12-month recipient
K.
L.
M.
N.
O.
CD163
CD206
IL4
IL10
Arg1
P.
Q.
R.
S.
T.

Figure 9.

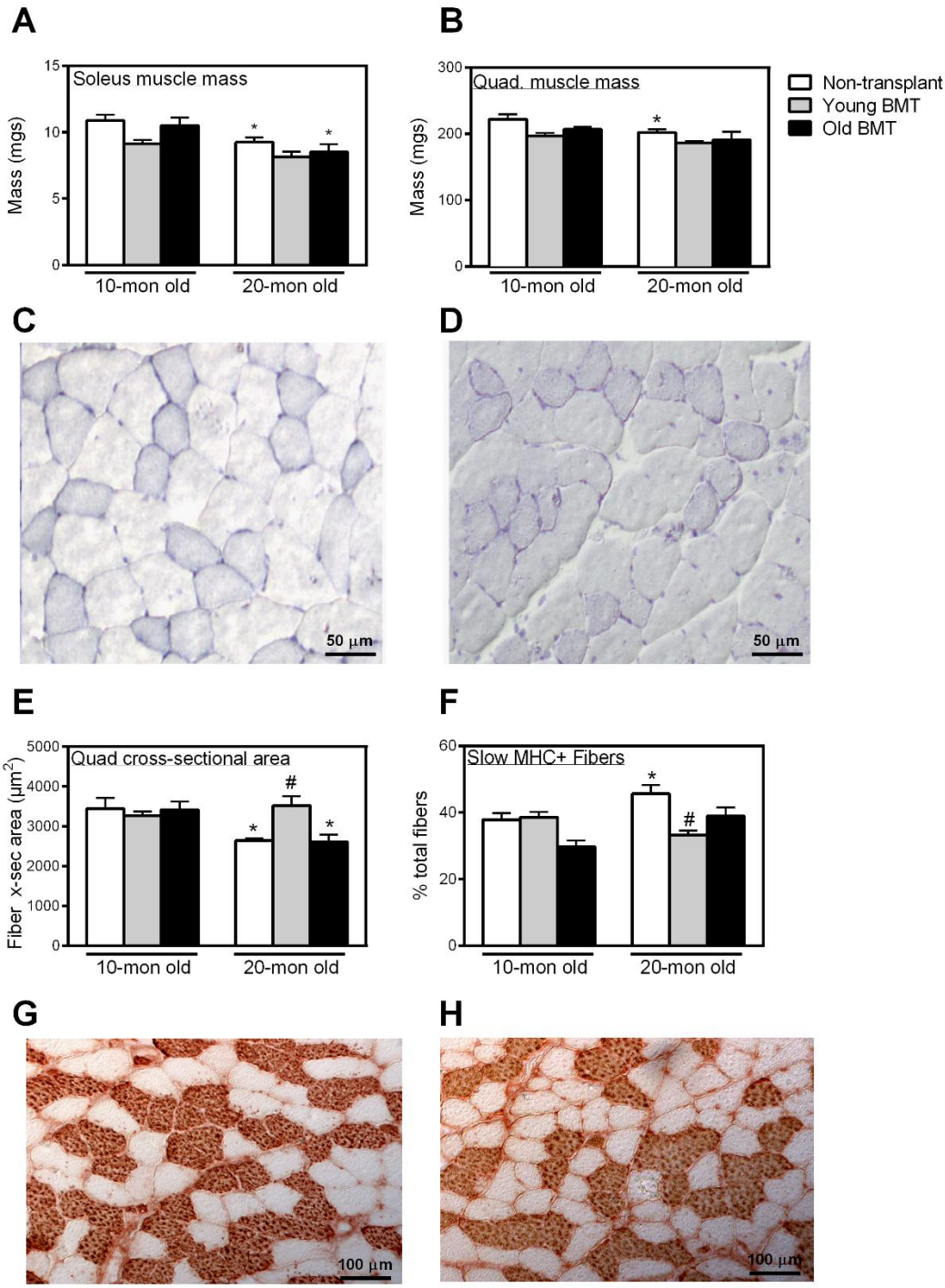
A
Soleus muscle mass
Mass (mgs)
15
10
5
0
*
*
10-mon old
20-mon old
B
Quad. muscle mass
Mass (mgs)
300
200
100
0
*
10-mon old
20-mon old
Non-transplant
Young BMT
Old BMT
C
50 μm
D
50 μm
E
Quad cross-sectional area
Fiber x-sec area (μm2)
5000
4000
3000
2000
1000
0
*
#
*
10-mon old
20-mon old
F
Slow MHC+ Fibers
% total fibers
60
40
20
0
*
#
10-mon old
20-mon old
G
100 μm
H
100 μm

Figure 10.

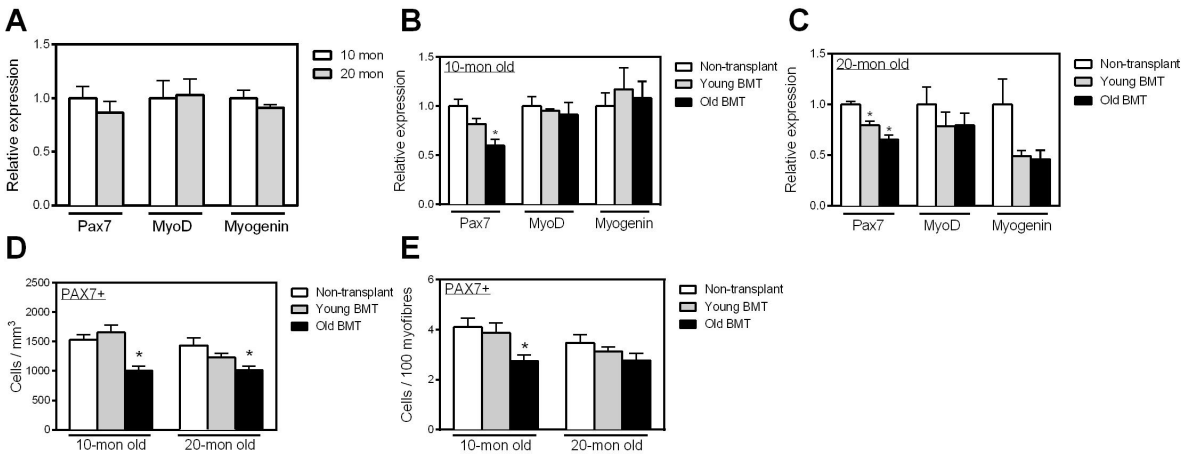
A
B
C
D
E
Relative expression
10 mon
20 mon
Pax7
MyoD
Myogenin
10-mon old
20-mon old
Non-transplant
Young BMT
Old BMT
PAX7+
Cells / mm3
Cells / 100 myofibres
10-mon old
20-mon old

Figure 11.

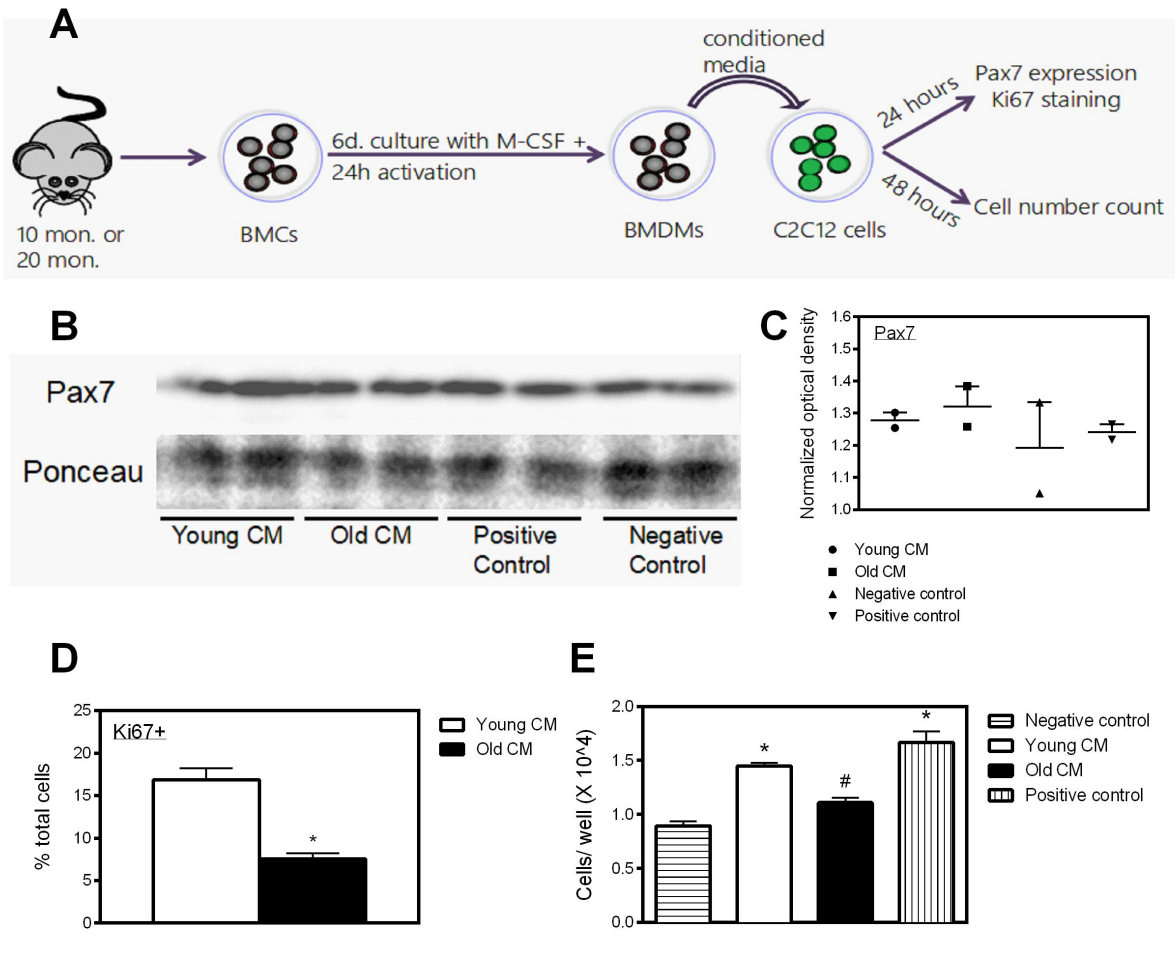
A
conditioned media
6d. culture with M-CSF +
24h activation
24 hours
Pax7 expression
Ki67 staining
48 hours
Cell number count
10 mon. or
20 mon.
BMCs
BMDMs
C2C12 cells
B
Pax7
Ponceau
Young CM
Old CM
Positive Control
Negative Control
C
Pax7
Normalized optical density
Young CM
Old CM
Negative control
Positive control
D
Ki67+
% total cells
Young CM
Old CM
E
Cells/ well (X 10^4)
Negative control
Young CM
Old CM
Positive control

Figure 12.

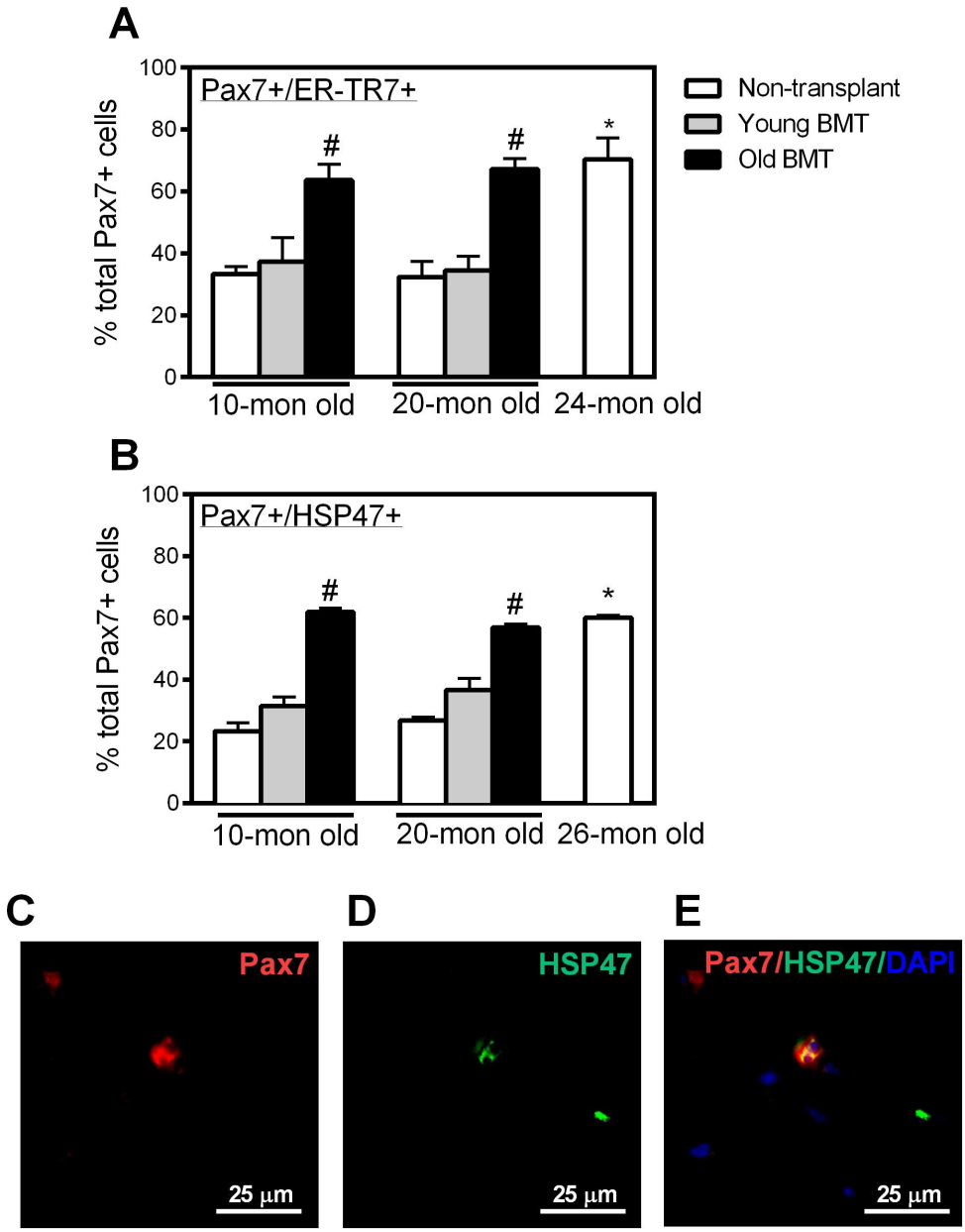
A
Pax7+/ER-TR7+
% total Pax7+ cells
100
80
60
40
20
0
#
#
*
10-mon old
20-mon old
24-mon old
Non-transplant
Young BMT
Old BMT
B
Pax7+/HSP47+
% total Pax7+ cells
100
80
60
40
20
0
#
#
*
10-mon old
20-mon old
26-mon old
C
Pax7
25 μm
D
HSP47
25 μm
E
Pax7/HSP47/DAPI
25 μm

Figure legends

Figure 7. A schematic diagram showing the experimental design of heterochronic bone marrow transplantations.

Figure 8. Expression levels of cytokines and macrophage phenotypic markers in muscles of non-transplanted and BMC transplanted mice. A. Expression levels of F4/80 did not differ significantly between in transplanted and non-transplanted, 10-month-old mice. B - E. Expression levels of transcripts associated with a pro-inflammatory environment in non-transplanted, 10-month-old (black bars), 10-month-old mice that had received BMT of young BMCs (grey bars) and 10-month-old mice that had received BMT of old BMCs. Transcripts assayed are: *IFNγ*(B), *TNFα* (C), *IL-1β* (D) and *iNOS* (E). F - J. Expression levels of transcripts associated with an anti-inflammatory environment in non-transplanted, 10-month-old (black bars), 10-month-old mice that had received BMT of young BMCs (grey bars) and 10-month-old mice that had received BMT of old BMCs. Transcripts assayed are: *CD163* (F), *CD206* (G), *IL-4* (H), *IL-10* (I) and *arginase-1* (*Arg1*; J). K. Expression levels of F4/80 did not differ significantly between in transplanted and non-transplanted, 20-month-old mice. L - O. Expression levels of transcripts associated with a pro-inflammatory environment in non-transplanted, 20-month-old (black bars), 20-month-old mice that had received BMT of young BMCs (grey bars) and 20-month-old mice that had received BMT of old BMCs. Transcripts assayed are: *IFNγ* (L), *TNFα* (M), *IL-1β* (N) and *iNOS* (O). P - T. Expression levels of

transcripts associated with an anti-inflammatory environment in non-transplanted, 20-month-old (black bars), 20-month-old mice that had received BMT of young BMCs (grey bars) and 20-month-old mice that had received BMT of old BMCs. Transcripts assayed are: *CD163* (P), *CD206* (Q), *IL-4* (R), *IL-10* (S) and *Arg1* (T). All data in each set were normalized relative to expression levels in muscles of non-transplanted mice, which were set at 1.0. * indicates significant difference from age-matched, non-transplanted group. # indicates significant difference from age-matched mice that received young BMCs. N = 4-5 per data set.

Figure 9. Transplantation of young BMCs into old recipients prevents age-related reduction in myofiber size and change of fiber type composition. A. Soleus muscle mass of non-transplanted control mice decreased from 10- to 20-months of age (white bars). Mice that received transplantation of young BMCs (grey bars) or old BMCs (black bars) did not show significant differences in soleus muscle mass compared to age-matched, non-transplanted mice. B. Quadriceps muscle mass of 20-month-old, non-transplanted mice was significantly less than that of 10-month-old, non-transplanted mice (white bars). Mice that received transplantation of young BMCs (grey bars) or old BMCs (black bars) did not show significant differences in quadriceps muscle mass compared to age-matched, non-transplanted mice. C. Representative image of a hematoxylin-stained cross section of a quadriceps muscle from a 10-month-old mouse receiving transplantation of old BMCs. D. Representative image of a hematoxylin-stained cross section of a quadriceps muscle from a 20-month-old mouse receiving transplantation of old BMCs. Bars = 50 μm. E. The average myofiber cross-sectional area (CSA) measured in

quadriceps muscles of transplanted and control mice. Transplantation of young but not old BMCs into adult recipients significantly increased fiber CSA at 20-months of age compared to 20-month-old, non-transplanted mice. F. Quantification of the percentage of sMHC+ fibers in total fibers of soleus muscles. Ten-month-old non-transplanted mice had lower proportion of sMHC+ fibers/ total fibers than 20-month-old non-transplanted mice. Transplantation of young BMCs into old mice reduced sMHC+ fiber ratio, while transplantation of old BMT did not cause significant difference in sMHC+ fiber percentage compared to control mice. G. Representative image of sMHC immunohistochemistry staining using the soleus muscle cross section from 20-month-old, non-transplanted mouse. H. Representative image of sMHC staining of the soleus muscle cross section from 20-month-old mouse that had received transplantation of young BMCs, showing a lower percentage of sMHC+ fibers compared with that seen in control mice shown in panel G. Bars = 100 μm. In all panels except for images, * indicates significant difference from 10-month-old mice that received the same treatment. # indicates significant difference from age-matched, non-transplanted mice. N = 5 per data set.

Figure 10. Transplantation of old BMCs reduces *Pax7* expression and the number of Pax7+ cells in both young and old recipients. A. Expression of *Pax7, MyoD* and m*yogenin* did not differ in quadriceps muscles of 10- and 20-month-old, non-transplanted mice. Values normalized to 10-month-old mice. B. QPCR analysis for myogenic transcription factors in quadriceps muscles of 10-month-old mice without transplantation (white bars), with transplantation of young BMCs (gray bars), and with transplantation of old BMCs (black bars). Values normalized to

non-transplanted mice. C. QPCR analysis for myogenic transcription factors in quadriceps muscles of 20-month-old mice without transplantation (white bars), with transplantation of young BMCs (gray bars), and with transplantation of old BMCs (black bars). Values normalized to non-transplanted mice. D. Stereological counts for Pax7+ cells. Satellite cell numbers in 10- or 20-month-old non-transplanted mice did not differ (white bars). Transplantation of old, but not young BMCs decreases satellite cell numbers at both 10- and 20-months of age. * indicates significant difference from age-matched, non-transplanted mice. E. Quantification of satellite cell numbers per 100 myofibers. * indicates significant difference from age-matched, non-transplanted mic. N = 5 per data set for all groups in all panels.

Figure 11. Conditioned media collected from bone marrow-derived macrophages from young mice promote myoblast proliferation. A. A schematic diagram showing the experimental design of BMDM culture, collection of conditioned media, culturing of myoblast and the quantification of myoblast proliferation. B. Western blotting for Pax7 showed that 24-hour treatment with conditioned media collected from either young or old BMDMs did not affect Pax7 protein levels. Ponceau S staining was used as internal control for protein content. C. Optical density of Pax7 western blots normalized to Ponceau S staining. D. Quantification of myoblasts that were entering cell cycle with 24 hours of conditioned media treatment by anti-Ki67 staining. Myoblasts cultured with conditioned media from old BMDMs showed lower Ki67+ cell ratio compared to myoblasts treated with young BMDM conditioned media. * indicates significant difference from young BMDM conditioned media treated group. N= 24 per data set. E. Total cell number count of

myoblasts with 48 hours treatment of conditioned media or control media showed that conditioned media collected from young BMDMs significantly increased cell numbers compared to the negative control. Conditioned media from old BMDMs did not increase cell numbers * indicates significant difference from the negative control group. # indicates significant difference from the young BMDM conditioned media treated group. N = 6 per data set.

Figure 12. Transplantation of old BMCs biased satellite cells toward a fibrogenic phenotype. A. Quantification of the proportion of Pax7+/ER-TR7+ cell in total Pax7+ cells. Transplantation of old, but not young BMCs increased the ratio of Pax7+/ER-TR7+ cells in both 10-month-old recipients and 20-month-old recipients. * indicates significant difference from 10-month-old, non-transplanted group at $P < 0.05$. # indicates significant difference from age-matched mice that received young BMCs at $P < 0.05$. N = 5 per data set. B. Quantification of the proportion of Pax7+/HSP47+ cells in total Pax7+ cells showed nearly identical results as shown in panel A. C - E. Immunofluorescence, double-labeling for Pax7 and HSP47. Cross sections of quadriceps muscle from 20-month-old, non-transplanted mice labeled with anti-Pax7 (red; panel C) and anti-HSP47 (green; panel D) and the merged images (yellow; panel E) showed that satellite cells that had converted to a fibrogenic phenotype were Pax7+/HSP47+.

References

Alnaqeeb M, Al Zaid N, Goldspink G (1984). Connective tissue changes and physical properties of developing and ageing skeletal muscle. *Journal of Anatomy*. **139**, 677-689.

Arnold L, Henry A, Poron F, Baba-Amer Y, Van Rooijen N, Plonquet A, Gherardi RK, Chazaud B (2007). Inflammatory monocytes recruited after skeletal muscle injury switch into antiinflammatory macrophages to support myogenesis. *Journal of Experimental Medicine*. **204**, 1057-1069.

Brack AS, Conboy MJ, Roy S, Lee M, Kuo CJ, Keller C, Rando TA (2007). Increased Wnt signaling during aging alters muscle stem cell fate and increases fibrosis. *Science*. **317**, 807-810.

Brack AS, Rando TA (2007). Intrinsic changes and extrinsic influences of myogenic stem cell function during aging. *Stem Cell Reviews*. **3**, 226-237.

Carlson B, Faulkner J (1989). Muscle transplantation between young and old rats: age of host determines recovery. *American Journal of Physiology-Cell Physiology*. **256**, C1262-C1266.

Conboy IM, Conboy MJ, Smythe GM, Rando TA (2003). Notch-mediated restoration of regenerative potential to aged muscle. *Science*. **302**, 1575-1577.

Conboy IM, Conboy MJ, Wagers AJ, Girma ER, Weissman IL, Rando TA (2005). Rejuvenation of aged progenitor cells by exposure to a young systemic environment. *Nature*. **433**, 760-764.

Cosgrove BD, Gilbert PM, Porpiglia E, Mourkioti F, Lee SP, Corbel SY, Llewellyn ME, Delp SL, Blau HM (2014). Rejuvenation of the muscle stem cell population restores strength to injured aged muscles. *Nature Medicine*. **20**, 255-264.

Cruz-Jentoft AJ, Baeyens J-P, Bauer JM, Boirie Y, Cederholm T, Landi F, Martin FC, Michel J-P, Rolland Y, Schneider SM (2010). Sarcopenia: european consensus on definition and diagnosis: report of the european working group on sarcopenia in older people. *Age and Ageing*. **39**, 412-423

Day K, Shefer G, Shearer A, Yablonka-Reuveni Z (2010). The depletion of skeletal muscle satellite cells with age is concomitant with reduced capacity of single progenitors to produce reserve progeny. *Developmental Biology*. **340**, 330-343.

Du H, Shih C-H, Wosczyna MN, Mueller AA, Cho J, Aggarwal A, Rando TA, Feldman BJ (2017). Macrophage-released ADAMTS1 promotes muscle stem cell activation. *Nature Communications*. **8**, 669.

Dumont NA, Wang YX, Rudnicki MA (2015). Intrinsic and extrinsic mechanisms regulating satellite cell function. *Development*. **142**, 1572-1581.

Franceschi C, Campisi J (2014). Chronic inflammation (inflammaging) and its potential contribution to age-associated diseases. *Journals of Gerontology Series A: Biomedical Sciences and Medical Sciences*. **69**, S4-S9.

Franceschi C, Capri M, Monti D, Giunta S, Olivieri F, Sevini F, Panourgia MP, Invidia L, Celani L, Scurti M (2007). Inflammaging and anti-inflammaging: a systemic perspective on aging

and longevity emerged from studies in humans. *Mechanisms of Ageing and Development*. **128**, 92-105.

Fry CS, Lee JD, Mula J, Kirby TJ, Jackson JR, Liu F, Yang L, Mendias CL, Dupont-Versteegden EE, McCarthy JJ (2015). Inducible depletion of satellite cells in adult, sedentary mice impairs muscle regenerative capacity without affecting sarcopenia. *Nature Medicine*. **21**, 76-80.

Fülöp T, Dupuis G, Witkowski JM, Larbi A (2016). The role of immunosenescence in the development of age-related diseases. *Revista de Investigacion Clinica.* **68**, 84-91.

Gibson MC, Schultz E (1983). Age‐related differences in absolute numbers of skeletal muscle satellite cells. *Muscle & Nerve*. **6**, 574-580.

Jo E, Lee S-R, Park B-S, Kim J-S (2012). Potential mechanisms underlying the role of chronic inflammation in age-related muscle wasting. *Aging Clinical and Experimental Research*. **24**, 412-422.

Kung TA, Cederna PS, van der Meulen JH, Urbanchek MG, Kuzon Jr WM, Faulkner JA (2013). Motor unit changes seen with skeletal muscle sarcopenia in oldest old rats. *Journals of Gerontology Series A: Biomedical Sciences and Medical Sciences*. **69**, 657-665.

Kwon YN, Yoon SS (2017). Sarcopenia: Neurological Point of View. *Journal of Bone Metabolism*. **24**, 83-89.

Lescaudron L, Peltékian E, Fontaine-Pérus J, Paulin D, Zampieri M, Garcia L, Parrish E (1999). Blood borne macrophages are essential for the triggering of muscle regeneration

following muscle transplant. *Neuromuscular Disorders*. **9**, 72-80.

Martinez CO, McHale MJ, Wells JT, Ochoa O, Michalek JE, McManus LM, Shireman PK (2010). Regulation of skeletal muscle regeneration by CCR2-activating chemokines is directly related to macrophage recruitment. *American Journal of Physiology-Regulatory, Integrative and Comparative Physiology*. **299**, R832-R842.

Marty E, Liu Y, Samuel A, Or O, Lane J (2017). A review of sarcopenia: Enhancing awareness of an increasingly prevalent disease. *Bone*. **105**, 276-286

Merly F, Lescaudron L, Rouaud T, Crossin F, Gardahaut MF (1999). Macrophages enhance muscle satellite cell proliferation and delay their differentiation. *Muscle & Nerve*. **22**, 724-732.

Petterson SM, Liaw WR, Phillips RL, Rabin DL, Meyers DS, Bazemore AW (2012). Projecting US primary care physician workforce needs: 2010-2025. *The Annals of Family Medicine*. **10**, 503-509.

Roberts P, McGeachie JK, Grounds MD (1997). The host environment determines strain-specific differences in the timing of skeletal muscle regeneration: cross-transplantation studies between SJL/J and BALB/c mice. *The Journal of Anatomy*. **191**, 585-594.

Roubenoff R (2001). Origins and clinical relevance of sarcopenia. *Canadian Journal of Applied Physiology*. **26**, 78-89.

Segawa M, Fukada S-i, Yamamoto Y, Yahagi H, Kanematsu M, Sato M, Ito T, Uezumi A, Hayashi Si, Miyagoe-Suzuki Y (2008). Suppression of macrophage functions impairs skeletal

muscle regeneration with severe fibrosis. *Experimental Cell Research*. **314**, 3232-3244.

Serrano AL, Muñoz-Cánoves P (2010). Regulation and dysregulation of fibrosis in skeletal muscle. *Experimental Cell Research*. **316**, 3050-3058.

Shefer G, Van de Mark DP, Richardson JB, Yablonka-Reuveni Z (2006). Satellite-cell pool size does matter: defining the myogenic potency of aging skeletal muscle. *Developmental Biology*. **294**, 50-66.

Shen W, Li Y, Zhu J, Schwendener R, Huard J (2008). Interaction between macrophages, TGF‐β1, and the COX‐2 pathway during the inflammatory phase of skeletal muscle healing after injury. *Journal of Cellular Physiology*. **214**, 405-412.

Snow MH (1977). The effects of aging on satellite cells in skeletal muscles of mice and rats. *Cell and Tissue Research*. **185**, 399-408.

Sousa-Victor P, Munoz-Canoves P (2016). Regenerative decline of stem cells in sarcopenia. *Molecular Aspects of Medicine*. **50**, 109-117.

Sun D, Martinez CO, Ochoa O, Ruiz-Willhite L, Bonilla JR, Centonze VE, Waite LL, Michalek JE, McManus LM, Shireman PK (2009). Bone marrow-derived cell regulation of skeletal muscle regeneration. *The FASEB Journal*. **23**, 382-395.

Tidball JG (2017). Regulation of muscle growth and regeneration by the immune system. *Nature Reviews Immunology*. **17**, 165-178.

Tidball JG, Wehling-Henricks M (2007). Macrophages promote muscle membrane repair and muscle fibre growth and regeneration during modified muscle loading in mice in vivo.

The Journal of Physiology. **578**, 327-336.

Wang Y, Wehling-Henricks M, Samengo G, Tidball JG (2015). Increases of M2a macrophages and fibrosis in aging muscle are influenced by bone marrow aging and negatively regulated by muscle-derived nitric oxide. *Aging Cell*. **14**, 678-688.

Wehling-Henricks M, Jordan MC, Gotoh T, Grody WW, Roos KP, Tidball JG (2010). Arginine metabolism by macrophages promotes cardiac and muscle fibrosis in mdx muscular dystrophy. *PloS One*. **5**, e10763.

Wilson D, Jackson T, Sapey E, Lord JM (2017). Frailty and sarcopenia: the potential role of an aged immune system. *Ageing Research Reviews*. **36**, 1-10

Wood LK, Kayupov E, Gumucio JP, Mendias CL, Claflin DR, Brooks SV (2014). Intrinsic stiffness of extracellular matrix increases with age in skeletal muscles of mice. *Journal of Applied Physiology*. **117**, 363-369.

Chapter 4. Myeloid-cell-specific mutation of Sfpi1 selectively reduces M2 macrophage numbers in skeletal muscle, prevents sarcopenia and reduces age-related muscle fibrosis.

4.1 Abstract

We generated a mouse model that harbors a myeloid-cell-specific mutation of *Sfpi1*, which is a transcription factor that is essential for myeloid cell development, to specifically test whether disrupting myelopoiesis affects muscle aging. Myeloid-cell-specific mutation of *Sfpi1* reduced the numbers of M2 macrophages in muscles of 12- and 22-month-old mice without affecting the numbers of CD68-expressing macrophages, and reduced the expression of transcripts associated with M2 polarization of macrophages. The mutation of *Sfpi1* did not affect the colony forming ability or the frequency of specific subpopulations of bone marrow hematopoietic cells and did not affect myeloid / lymphoid cell ratios in peripheral blood leukocyte populations. Cellularity of most subpopulations of hematopoietic lineage cells in the bone marrow, including monocytes, was not influenced by the mutation. The *Sfpi1* mutation in bone marrow-derived macrophages *in vitro* also did not affect expression of transcription factors that indicate M2 polarization of macrophages. Thus, the myeloid-cell-targeted mutation of *Sfpi1* influences macrophage phenotype in muscle, but did not affect earlier stages of differentiation of cells in the monocyte-macrophage lineage. Myeloid-cell-specific mutation of *Sfpi1* reduced age-related muscle fibrosis, which is consistent with the reduction of M2 macrophages numbers and

reduced expression of arginase. Furthermore, myeloid-cell-specific mutation of *Sfpi1* prevented sarcopenia and reduced satellite cell activation. Together, our observations indicate that reducing the number of M2 macrophages in aging muscle by myeloid-cell-specific ablation of *Sfpi1* has a protective effect against muscle aging.

4.2 Introduction

Our observations presented in previous chapters suggested that muscle aging is partly attributable to aging of myeloid cells and the increased number of macrophages in aging muscle. For example, expression of an *nNOS* transgene in skeletal muscle prevents age-related increases in macrophage numbers and reduces the accumulation of collagens in muscle during aging (Wang *et al.* 2015). We also showed in chapter 3 that transplantation of young bone marrow cells reduces sarcopenia and muscle fibrosis in old mice. Furthermore, those data were consistent with the functions of myeloid cells in regulating myogenesis and fibrosis during muscle repair and in dystrophic muscles (Villalta *et al.* 2009; Wehling-Henricks *et al.* 2010; Villalta *et al.* 2011). However, the *nNOS* transgene may affect muscle aging through pathways other than regulating macrophage numbers, such as increasing calpain S-nitrosylation in aging muscle, which may also reduce sarcopenia (Samengo *et al.* 2012). Moreover, other populations of immune cells including CD8+ cytotoxic T (Zhang *et al.* 2014) and regulatory T cells (Burzyn *et al.* 2013; Villalta *et al.* 2014; Wang *et al.* 2015) are also present in skeletal muscle and play important roles in regulating myogenesis. Changes in those populations that may be caused by heterochronic bone marrow transplantation could also contribute to the protective effects against muscle aging. To examine more specifically the function of myeloid cells in muscle aging, we sought to design a mouse model that would specifically affect myeloid cell numbers or activation in aging muscle without affecting other leukocyte populations.

Sfpi1 encodes the Ets family transcription factor PU.1, which is essential in the lineage specification and determining the differentiation fate of hematopoietic cells (Klemsz *et al.* 1990; DeKoter *et al.* 2007; Burda *et al.* 2010). Increased PU.1 concentration is required for the differentiation of common myeloid progenitors (CMPs) into mature granulocytes and monocytes/macrophages (Lichanska *et al.* 1999; Fiedler & Brunner 2012) and disruptions in the *Sfpi1* gene results in a complete ablation of mature macrophages and neutrophils (Scott *et al.* 1994; McKercher *et al.* 1996). However, *Sfpi1* mutation also affects erythroblast maturation and the generation of B cells and complete ablation of *Sfpi1* causes fetal or perinatal lethality (Scott *et al.* 1994; McKercher *et al.* 1996). To create a viable mouse line with *Sfpi1* mutation exclusively in myeloid cells, we crossed the $LysM^{Cre}$ mouse line with the $Sfpi1^{Lox}$ mouse line. Cre recombinase in $LysM^{Cre}$ mice was specifically driven by the promoter of *lysozyme2* gene *(Lyz2)* which is expressed exclusively in myeloid cells. Previous investigation showed crossing $LysM^{Cre}$ mice with mice with loxP-flanked target genes results in high deletion efficiency of target genes in mature macrophages and granulocytes (Clausen *et al.* 1999).

Our findings in the present investigation revealed unexpected effects of *Lyz2*-driven deletion of *Sfpi1*. We found that the targeted mutation did not cause a reduction in the numbers of fully-differentiated macrophages in aging muscle; instead the mutation reduced the numbers of intramuscular macrophages that were activated to the M2 phenotype. This outcome provided us a tool for assessing the role of M2 macrophages in muscle aging and allowed us to validate the important role of M2 macrophages in sarcopenia and fibrosis of aging muscle.

4.3 Results

Sfpi1 mutation driven by Lyz2 promoter reduces the number of M2 macrophages in muscle

LysM^{Cre}/ *Sfpi1*^{Lox} mice (referred to as *Sfpi1*-mutants hereafter) survive normally and show no obvious morphological or behavioral differences during development and throughout life until 22 months-of age, compared to their *LysM*^{wildtype}/ *Sfpi1*^{Lox} littermates (referred to as floxed controls hereafter). We assayed for *Sfpi1*-expressing cells in quadriceps muscles of 12- and 22-month-old mice by immunohistochemistry and found that *Sfpi1*-mutant mice had more than a 90% reduction in PU.1+ cells compared to age-matched floxed control mice (Figure 13A).

Because intramuscular macrophages consist of heterogeneous subpopulations that play distinct roles in regulating muscle growth and regeneration (Tidball 2017), we examined the number of different subtypes of macrophages in *Sfpi1*-mutant mice. Surprisingly, we found that the number of M1 macrophages, shown by the immunohistochemical labeling of the M1 macrophage marker CD68, was not different in quadriceps of *Sfpi1*-mutant mice compared to floxed control mice at 12- and 22-months of age (Figure 13B). Moreover, the mRNA expression level of *CD68* did not differ between floxed controls and *Sfpi1*-mutant mice at 12- and 22-months of age (Figure 13C). These data suggested that myeloid specific mutation of *Sfpi1* did not affect the terminal differentiation of monocytes/macrophage and did not affect the number of M1 macrophages. However, the numbers of CD163+ M2 macrophages were significantly lower in 12- and 22-month-old *Sfpi1*-mutant mice compared to age-matched floxed control mice (Figures

13D - F). Our QPCR results showed a trend for reduced mRNA expression of *CD163* in quadriceps of *Sfpi1*-mutant mice compared to floxed control mice at both 12- and 22-months old (Figure 13G). We also tested the expression of another widely-accepted M2 macrophage marker CD206 (Tidball & Villalta 2010; Villalta *et al.* 2011) in *Sfpi1*-mutant and floxed control mice and found that CD206+ M2 macrophage numbers were significantly reduced by *Sfpi1* mutation in both 12- and 22-month-old muscles (Figure 13H). *CD206* mRNA also showed a trend for lower expression in *Sfpi1*–mutant mice compared to floxed control mice at both 12- and 22-months of age (Figure 13I).

Although the decreases in CD163+ and CD206+ cell numbers could reflect the reduction of macrophage differentiation into the M2 phenotype, they may also reflect the downregulation of *CD163* and *CD206* expression in M2 macrophages because both *CD163* and *CD206* genes have PU.1 binding sites in their promoter regions and their promoter activity is directly regulated by PU.1 (Eichbaum *et al.* 1997; Lloberas *et al.* 1999; Ritter *et al.* 1999; Jego *et al.* 2014). We tested the expression level of *Fizz-1* and *arginase-1* (*Arg1*), which are M2 macrophage related genes that have not been shown to be direct target genes of PU.1. Our QPCR results showed that both *Fizz-1* and *Arg1* expressions were significantly reduced by myeloid specific mutation of *Sfpi1* in 22-month-old muscles and that *Fizz-1* expression was also decreased in 12-month-old *Sfpi1*-mutant mice compared to age-matched floxed controls (Figure 13J, K). These data indicate that myeloid cell specific mutation of *Sfpi1* selectively reduced M2 macrophage numbers in muscles at both 12- and 22-months of age.

Effects of myeloid cell specific mutation of Sfpi1 on hematopoiesis

Sfpi1 gene expression is tightly regulated within the hematopoietic system, and concentration of PU.1 determines the fate of cell differentiation in a dose-dependent manner (Dahl & Simon 2003; DeKoter *et al.* 2007; Mak *et al.* 2011). Although the mutation of *Sfpi1*in our *Sfpi1*-mutant mice was driven by promoter of the *lyz2* gene which is expressed exclusively in myeloid cells, it may affect fates of other hematopoietic cells through feedback pathways (McCabe & MacNamara 2016; Chen *et al.* 2017) or if the activity of the Cre-recombinase is leaky, causing *Sfpi1*-mutation in non-myeloid cells.

We tested the proportion of myeloid cells in total peripheral blood leukocytes and found that the proportion of myeloid cells increases in floxed control mice between 12 and 22 months (Figure 14A). In the *Sfpi1*-mutant mice, we see a similar trend of age-related increase of macrophage proportion, but the difference was not significant (Figure 14A). The proportion of myeloid cells in total peripheral blood leukocytes was not affected by the myeloid specific mutation of *Sfpi1* at 12 and 22 months (Figure 14A), suggesting that *Sfpi1*-mutant mice have normal hematopoiesis.

We then tested whether hematopoiesis was affected in old (22 months) *Sfpi1*-mutant mice compared to floxed control mice. Total numbers of bone marrow cells isolated from hind limb bones were not affected by myeloid specific mutation of *Sfpi1* (data not shown). The ability of hematopoietic cells to proliferate *in vitro* and differentiate into colonies were tested using the

methylcellulose colony forming assay (Pereira *et al.* 2007) and no differences were found between the colony forming ability of bone marrow cells isolated from *Sfpi1*-mutant and floxed control mice (Figure 14B).

We next examined the frequency and cellularity of functionally-defined subpopulations of hematopoietic cells in 22-month-old *Sfpi1*-mutant and floxed control mice by multiparametric flow cytometry (Montecino-Rodriguez *et al.* 2006; Challen *et al.* 2009). Myeloid-cell-specific mutation of *Sfpi1* did not affect the frequency or cellularity of lymphoid-biased hematopoietic stem cells and myeloid-biased hematopoietic stem cells (Figures 14C, D). *Sfpi1*-mutant mice also showed unaffected frequency and cellularity of subpopulations of myeloid progenitors including common myeloid progenitors, granulocyte macrophage progenitors and megakaryocyte erythrocyte progenitors (Figures 14E, F). The cellularity of granulocytes was significantly reduced by *Sfpi1* mutation, although granulocyte frequency was not affected (Figure 14G). Importantly, no differences were seen in frequency or cellularity of monocytes in *Sfpi1*-mutant mice compared to floxed control mice (Figure 14H), indicating the mutation did not disrupt early differentiation of cells in the monocyte / macrophage lineage. Surprisingly, we observed significant reduction in the cellularities of common lymphoid progenitors and of naive / mature B cells (Figures 14J - L). The frequencies of common lymphoid progenitors and naive / mature B cells were not affected by *Sfpi1* mutation (Figures 14I - K), nor were the frequency and cellularities of immature B cells (Figures 14K, L). Together, these data showed that most subpopulations of hematopoietic cells were not affected by myeloid-cell-specific *Sfpi1* mutation,

including cells early in monocyte lineage. However, cellularity of granulocytes, common lymphoid progenitors and naive / mature B cells were reduced in old *Sfpi1*-mutant mice compared to floxed control mice.

Myeloid-cell-specific Sfpi1 mutation has little effect on the phenotype of bone marrow derived macrophages and their response to cytokine-induced M2 polarization

The reduction in M2 macrophage numbers in muscles of *Sfpi1*-mutant mice compared to floxed control mice could reflect the intrinsic defects of macrophages caused by the mutation, or it could reflect the difference of macrophages differentiation in response to the immune environment in muscles. We tested whether the *Sfpi1* mutation caused intrinsic changes to macrophages *in vitro*. BMCs isolated from 12-month-old *Sfpi1*-mutant and floxed control mice were cultured in the presence of macrophage colony-stimulating factor (M-CSF). Although *Sfpi1* has een reported to increase the expression of M-CSF receptors (Olson *et al.* 1995; Li *et al.* 2005; Aikawa *et al.* 2010) and *Sfpi1*-null myeloid progenitors are unresponsive to M-CSF *in vitro* (DeKoter *et al.* 1998), our results showed that BMCs isolated from *Sfpi1*-mutant mice were able to proliferate and differentiate into macrophages in the presence of M-CSF despite the reduced expression of *Sfpi1* (Figure 15A). Polarizing the bone marrow derived macrophages (BMDMs) to a M2 phenotype with Th2 cytokines IL-4 and IL-10 increased *Sfpi1* expression in both *Sfpi1*-mutant and floxed control BMDMs (Figure 15A). However, the *Sfpi1*-mutant BMDMs still showed lower expression of *Sfpi1* after M2 polarization compared to the floxed control BMDMs

with the same treatment (Figure 15A). The expression level of *CD68* was slightly lower in *Sfpi1*-mutant BMDMs compared to floxed control BMDMs (Figure 15B). M2 polarization decreased *CD68* expression in floxed control BMDMs but the expression of *CD68* in *Sfpi1*-mutant BMDMs were not affected by IL-4 and IL-10 (Figure 15B). The expression levels of *CD163* showed an insignificant trend to increase in *Sfpi1*-mutant BMDMs compared to the floxed control BMDMs (Figure 15C). M2 polarization reduced *CD163* expression in *Sfpi1*-mutant BMDMs, but not in floxed control BMDMs (Figure 15C). Expression of the M2 related genes *CD206, Fizz-1* and *Arg1* were significantly increased by M2 polarization in BMDMs from both *Sfpi1*-mutant and floxed control mice (Figures 15D - F). However, their expression levels were not different in *Sfpi1*-mutant and floxed control BMDMs with the same treatments (Figure 15D - F). Together, these data show that the myeloid-cell-specific mutation of *Sfpi1* has little influence on the expression of some macrophage-related genes in BMDMs cultured *in vitro* and their response to M2 polarization. Interestingly, the effects of *Sfpi1* mutation on macrophage phenotype in *Sfpi1*-mutant BMDMs were different from the effect of *Sfpi1* mutation on macrophages in muscles of *Sfpi1*-mutant mice, suggesting that the reduction in M2 macrophage numbers in *Sfpi1*-mutant muscles were affected by the muscle environment *in vivo*.

Myeloid-cell-specific mutation of Sfpi1 reduced connective tissue accumulation in old muscle

We have shown in a previous investigation that the age-related shift toward greater numbers of M2 macrophages in muscle is associated with increased muscle fibrosis (Wang *et al.*

2015). Because *Sfpi1*-mutant mice showed reduced numbers of M2 macrophages in both adult and old muscles compared to age-matched floxed control mice, we tested whether this reduction in M2 macrophages affects muscle fibrosis during aging. Expression of collagen types I and III did not change significantly between 12- and 22-months in floxed control or *Sfpi1*-mutant mice (Figures 16A, B). However, the expression of collagen type III was significantly lower in 22-month-old *Sfpi1*-mutant mice compared to age-matched floxed control mice (Figure 16B). The volume fraction of muscle occupied by collagens type I and type III increased between 12 and 22 months of age (Figures 16C, D). Furthermore, we observed that myeloid specific mutation of *Sfpi1* prevented the age-related accumulation of collagen type I and significantly reduced the accumulation of collagen type III during aging (Figures 16C, D). These findings indicate that the increase of M2 macrophages during aging contributes to age-related muscle fibrosis and that myeloid specific *Sfpi1* mutation can reduce the accumulation of connective tissue in aging muscle by decreasing M2 macrophage numbers.

Myeloid specific mutation of Sfpi1 prevented sarcopenia

We then tested whether the myeloid-cell-specific mutation affected sarcopenia. We quantified the cross-sectional area (CSA) of muscle fibers in 12- and 22-month-old muscles of *Sfpi1*-mutant and floxed control mice. CSA of quadriceps decreased significantly between 12- and 22-months in floxed control mice (Figure 17A). At 12-months of age, quadriceps CSA in *Sfpi1*-mutant mice showed a decreased trend compared to floxed control mice, although the

difference was not significant (Figure 17A). However, quadriceps CSA did not differ between 12- and 22-months old *Sfpi1*-mutant mice (Figures 17A - C), suggesting that *Sfpi1*-mutant mice were able to maintain muscle fiber size during aging despite of the smaller muscle fiber size in adulthood compared to floxed control mice.

Similarly, CSA of tibialis anterior decreased significantly between 12- and 22-months in floxed control mice (Figure 17D). Tibialis anterior CSA did not differ between 12- and 22-months old *Sfpi1*-mutant mice, although the tibialis anterior CSA in 12-month-old *Sfpi1*-mutant mice were smaller compared to 12-month-old floxed control mice (Figure 17D). Together, these data indicate that myeloid-cell-specific mutation of *Sfpi1* prevented sarcopenia.

Myeloid-cell-specific mutation of Sfpi1 reduced satellite cell activation in adult and aging muscles

We tested whether reducing M2 macrophage numbers by myeloid-cell-specific mutation of *Sfpi1* affected satellite cell numbers or function in aging muscle by assaying for the numbers of muscle cells that expressed the myogenic transcription factors Pax7 and MyoD. Pax7 is expressed by quiescent satellite cells or by recently activated satellite cells that have the potential to return to the reserve population of quiescent satellite cells (Olguin & Olwin 2004; Zammit *et al.* 2006). MyoD is expressed by recently activated satellite cells that have the potential to withdraw from the cell cycle and proceed through terminal differentiation (Puri *et al.* 1997; Kitzmann *et al.* 1998; Zhang *et al.* 1999) . Although the *Sfpi1* mutation did not affect the

number of Pax7+ satellite cells per unit muscle volume or per 100 muscle fibers in 12- and 22-month-old mice (Figures 18A, B), the number of activated satellite cells that expressed MyoD was significantly less in *Sfpi1*-mutant mice compared to floxed control mice at both 12- and 22-months old (Figures 18C, D). Furthermore, mRNA expression level of *Pax7* was not affected by the *Sfpi1* mutation in 12- and 22-month-old muscles (Figure 18E), while the *MyoD* expression level was significantly reduced in 12- and 22-month-old muscles of *Sfpi1*-mutant mice compared to age-matched floxed control mice (Figure 18F). Together, these data show that the reduction of M2 macrophages in muscle caused by the *Sfpi1* mutation in myeloid cells influenced the activation of satellite cells, but not their number, at least at the ages examined in the present investigation. Thus, M2 macrophages may contribute to sarcopenia by regulating satellite cell activation.

4.4 Discussion

In the present study, we have demonstrated that the number of M2 macrophages in aging muscle is selectively and significantly reduced by a myeloid-cell-specific mutation *of Sfpi1*. Importantly, this specific perturbation of M2 macrophage numbers was sufficient to reduce sarcopenia and fibrosis of aging muscle. Although we showed in chapters 2 and 3 that interventions that reduced the numbers of macrophages in aging muscle also produced reductions in connective tissue accumulation, the experimental approaches that we used could have affected non-myeloid cell populations that may have unknown roles in muscle aging. Using the myeloid-cell-specific mutation of *Sfpi1*, our findings show more directly that the age-related increase of M2 macrophages is a direct cause of fibrosis in aging muscle. Furthermore, we showed in chapter 3 that the severity of sarcopenia is affected by aging of the immune system. However, we were not able to identify which specific, aging immune cells were responsible for increasing sarcopenia. We have now shown that the selective reduction in M2 macrophage numbers prevented sarcopenia, suggesting that age-related changes in M2 macrophages numbers and functions contribute significantly to sarcopenia.

Our observation that the reduction of M2 macrophages in *Sfpi1*-mutant mice prevented sarcopenia is consistent with previous investigations showing that M2 macrophages play important roles in myogenesis. In injured and dystrophic muscles, M2 macrophages promote muscle repair and regeneration by deactivating pro-inflammatory M1 macrophages and

releasing factors such as IGF1 and Klotho that directly promote myogenesis (Deng *et al.* 2012; Tonkin *et al.* 2015; Wehling-Henricks *et al.* 2018). For example, decreasing the number of M2 macrophages in injured muscle by ablating IL-10 led to fewer regenerating fibers and decreased muscle CSA during the regenerative stages following injury, supporting the possibility that M2 macrophages are required for proper muscle growth regeneration in injured muscle (Deng *et al.* 2012). Whether M2 macrophages have any functions in myogenesis and maintaining muscle health in aging muscle has not been investigated before. In this study, we observed that *Sfpi1*-mutant mice were able to maintain or even slightly increase their muscle fiber size during aging (Figure 17). At 22-months old, the muscle CSAs of both quadriceps and tibialis anterior of the *Sfpi1*-mutant mice were larger compared to age-matched floxed control mice, although the differences are not significant (Figure 17). These data suggest that M2 macrophages play a significant role in myogenesis in non-injured, aging muscle.

Interestingly, we found that the *Sfpi1*-mutant mice have smaller muscle CSA at 12-months old compared to floxed control mice. Furthermore, we found that the expression of *MyoD* gene and the number of MyoD+ cells were lower in mutant mice compared to control mice at both 12- and 22-months, suggesting that reducing M2 macrophage numbers in muscle has a negative effect on muscle stem cell activation. Together, these observations suggest that M2 macrophages may have distinct effects on muscle fiber size at different stages of life. This may be partially explained by the large number of subpopulations of M2 macrophages that serve non-identical functions in numerous tissues (Murray *et al.* 2014).

Although the relationships between changes in macrophage number and the occurrence of fibrosis and sarcopenia during muscle aging are generally consistent in each of the models used in this dissertation work, there is an apparent discrepancy in the age-related changes in intracellular, M2 macrophages in wild-type, C57 BL/6 mice (chapter 2) and in floxed control mice for the *Sfpi1* line. We found that C57 BL/6 mice experienced an 80% increase in intramuscular M2 macrophages between 12- and 24-months of age, although we did not see significant increases in macrophages numbers in floxed control mice between 12- and 22-months of age. Although we do not know why aging did not cause similar increases in intramuscular, M2 macrophages in the two models, the apparent discrepancy could reflect differences between C57 BL/6 and the floxed control mouse lines or the differences in sampling age used in these two projects.

We were surprised that myeloid specific mutation of *Sfpi1* specifically reduced M2 macrophage numbers in muscle without affecting the numbers of M1 macrophages. Previous investigations using conditional null or hypomorphic alleles of *Sfpi1* have shown that ablation or decreasing *Sfpi1* expression at different stages of myeloid lineage determination causes various abnormalities in myeloid cell development (McIvor *et al.* 2003; Rosenbauer *et al.* 2004; Dakic *et al.* 2005; DeKoter *et al.* 2007), although *Sfpi1* manipulation has rarely been reported to affect macrophage phenotype. However, a conditional PU.1-deficient mice line displayed attenuated allergic airway inflammation and reduced gene expression of M2 macrophage markers *Ym-1* and *Fizz-1* in lung tissues following exposure to allergens; this suggested that *Sfpi1* expression

plays a critical role in alternative activation of macrophages to an M2 phenotype (Qian *et al.* 2015). A recent study identified two distinct subtypes of Ly6C^{hi}CD115^{+} monocytes by different expression levels of PU.1 together with other markers (Menezes *et al.* 2016). The PU.1^{hi} subsets differentiate into monocyte-derived dendritic cells in a GM-CSF-dependent manner, while as the PU.1^{lo} subsets of monocytes differentiated into iNOS+ M1 macrophages upon microbial stimulation (Menezes *et al.* 2016). Furthermore, *Sfpi1*+/- mice had reduced numbers of blood CD115^{+}Ly6C^{lo} cells and when presented with inflammatory stimulation, *Sfpi1*+/- mice generated iNOS+ macrophages in the spleen more efficiently than wild-type mice (Menezes *et al.* 2016). These observations are generally consistent with the observations in our *Sfpi1*-mutant mice, suggesting that decreasing the expression of *Sfpi1* reduces M2 polarization of macrophages.

The mechanism through which *Sfpi1* regulates macrophage polarization remains unclear. Our qPCR results of intramuscular macrophages showed that not only did myeloid-cell- specific mutation of *Sfpi1* reduce the expression of M2 associated genes with *Sfpi1* binding sites in their promoter regions, such as CD163 and CD206 (Eichbaum *et al.* 1997; Lloberas *et al.* 1999; Ritter *et al.* 1999; Jego *et al.* 2014), the mutation also caused decreases in the expression levels of *Fizz-1* and *Arg-1,* which are not direct targets of the PU.1 transcription factor activity. Moreover, M1 macrophage related gene CD68 is a target of *Sfpi1* (Li *et al.* 1998; O'Reilly *et al.* 2003), but its expression in muscle was not reduced by the myeloid specific *Sfpi1* mutation. These data suggest that *Sfpi1* regulates macrophage polarization through an indirect pathway instead of directly binding to the promoters and regulating the expression of macrophage phenotype

specific genes.

Another particularly intriguing observation in our present study is that the phenotypes of BMDMs *in vitro* and macrophages in muscles were affected differently by myeloid-cell-specific mutation of *Sfpi1*. Although intramuscular macrophages showed a specific reduction in M2 macrophages, BMDMs from *Sfpi1*-mutant mice showed no differences in M2 macrophage related genes compared to floxed control BMDMs. This discrepancy may be attributable to the different environments in which these macrophages developed and were activated. BMDMs were cultured *in vitro* with recombinant M-CSF to stimulate them towards macrophage differentiation, while intramuscular macrophages in aging muscle developed in a more complex inflammatory environment. We also observed that the response of *Sfpi1*-mutant BMDMs to forced M2 polarization with IL-4 and IL-10 treatment did not differ from the response of floxed control BMDMs. However, previous investigation showed that $Sfpi1^{+/-}$ BMDMs displayed blunted response to IL-4 treatment in M2 gene expressions (Qian *et al.* 2015). A major difference between these two models is that the *Sfpi1* mutation in our model is driven by $LysM^{Cre}$, whereas $Sfpi1^{+/-}$ BMDMs have reduced *Sfpi1* expressions throughout all stages of hematopoiesis. These observations suggest that reducing *Sfpi1* levels at different stages of hematopoiesis affect the response of macrophage to M2 polarization. The different choices of cytokine concentrations and duration of treatments may also contribute to the distinct outcomes.

Although further investigations are needed to uncover the process of *Sfpi1* regulation of

macrophage polarization and phenotype switch, our investigations identified a previously unrecognized tool for directly targeting macrophage phenotype to prevent muscle aging. Our present studies support that M2 macrophages contribute to sarcopenia and the accumulation of connective tissue in aging muscle. Together, these observations shed light on novel understanding of the relationship between aging of the immune system and muscle aging.

4.5 Materials and Methods

Mice

All experimental protocols involving the use of mice were conducted according to the National Institutes of Health Guide for the Care and Use of Laboratory Animals and were approved by the University of California, Los Angeles Institutional Animal Care and Use Committee. *LysM*^{Cre} mice and *Sfpi1*^{lox} mice were obtained from Jackson Laboratories (Bar Harbor, ME, USA).

Dissection and muscle mass measurement

Sfpi1-mutant and floxed control mice were euthanized by inhalation of isoflurane and the hind-limb muscles were dissected rapidly after euthanization. Muscles were then either frozen in liquid nitrogen or embedded in optimal cutting temperature compound (OCT) and rapidly frozen in isopentane cooled in liquid nitrogen.

RNA isolation and quantitative PCR.

Muscles were homogenized in Trizol (Invitrogen) and RNA extracted, isolated and DNase-treated using RNeasy spin columns according to the manufacturer's protocol (Qiagen). RNA was then electrophoresed on 1.2% agarose gels and RNA quality assessed by determining 28S and 18S ribosomal RNA integrity. Total RNA was reverse transcribed with Super Script

Reverse Transcriptase II using oligo dTs to prime extension (Invitrogen) to produce cDNA. The cDNA was used to measure the expression of selected transcripts using SYBR green qPCR master mix according to the manufacturer's protocol (Bio-Rad). Real-time PCR was performed on an iCycler thermocycler system equipped with iQ5 optical system software (Bio-Rad). Reference genes were chosen following previously described methods (Wang *et al.* 2015). Based on that analysis, *RSP4X* and *SRP14* were used as reference genes for QPCR experiments with quadriceps muscles. The normalization factor for each sample was calculated by geometric averaging of the Ct values of both reference genes using the geNorm software. Primers used for QPCR are listed in Table 5 at the end of the dissertation.

Immunohistochemistry and quantification of positive cells

Frozen cross-sections were cut from the mid-belly of quadriceps or soleus muscle at a thickness of 10 μm. The frozen sections were air-dried for 30 minutes and fixed in ice-cold acetone for 10 minutes, and endogenous peroxidase activity was quenched with 0.3% H_2O_2. Sections were then blocked in 3% bovine serum albumin (BSA) and 2% gelatin in 50 mM Tris buffer (pH 7.2) for 30 minutes and then immunolabeled with primary antibodies at concentrations as shown in Table 5, for 3 hours at room temperature. Sections were washed with PBS and then probed with biotin-conjugated secondary antibodies (1/200; Vector) for 30 minutes. Sections were subsequently washed with PBS and then incubated for 30 minutes with avidin D-conjugated horseradish peroxidase (1/1000; Vector). Staining was visualized with the

peroxidase substrate 3-amino-9-ethylcarbazole (AEC kit; Vector), yielding a red reaction product. Positive cells were counted using a bright-field microscope. The numbers of immunolabeled cells in each section were counted and expressed as the number of cells/unit volume of each section. The volume of total muscle and the volume of muscle that consisted of connective tissue was determined using a stereological, point-counting technique to determine section area and then multiplying that value by the section thickness (10 μm). To quantify Pax7+ cells / 100 fibers and MyoD+ cells / 1000 fibers, the total number of fibers for each section was counted on the merged image of the whole section.

Peripheral blood leukocytes counting

Whole blood was collected from a femoral bleed using 1 ml syringe without a needle. Red blood cells were lysed with ACK lysis buffer (Biowhitaker) that had been precooled on ice for 5 minutes. Blood samples were then washed with Dulbecco's phosphate buffered saline (DPBS; Sigma) and then centrifuged for 5 minutes in clinical centrifuge at 1000 rpm. The supernatant was discarded and the pellet resuspended in 1 ml of DPBS. Two-hundred μl of cell resuspension were used for cytospin using Shandon 3 cytofuge for 5 minutes at 380 rpm. Samples were then rinsed briefly in DPBS, fixed with 2% formaldehyde solution for 5 minutes and stained with hematoxylin for 10 minutes. Slides were rinsed with distilled water and coversliped. Cell counts were performed based on cell morphology.

Bone marrow cell isolation and colony forming assay

Bone marrow cells (BMCs) were aseptically flushed from femurs and tibias with DPBS and treated with ACK lysing buffer (Biowhitaker) to clear red blood cells. Following a DPBS wash and filtration through a 70 μm filter, BMCs were counted with hemocytometer and were resuspended in DPBS at the concentration of 2.5 x 10^6 cells / ml. The content and reagents used in the methycellulose medium was shown in Table 2. BMCs were added to the methycellulose medium at a final cell density of 2 x 10^5 cells / ml. The methycellulose medium containing BMCs were then vortexed and left sitting for 10 minutes to get rid of air bubbles. Methycellulose medium containing BMCs were then seeded in 3.5 cm culture dish at 1 ml / dish and cultured at 37 ºC with 5% CO_2 for 11-14 days. Number of colonies were counted under a stereomicroscope.

Flow cytometry

BMCs were isolated as described above. Cells were then washed and incubated with combinations of antibodies as listed in Table 3. All incubations were for 30 - 40 minutes at 4 ºC in DPBS. Flow cytometry were performed on a LSRII (Becton Dickenson).

Bone marrow-derived macrophages culture and M2 polarization

BMCs isolated as described above were seeded at 5 x 10^6 per 6-cm dish in RPMI-1640 (Sigma) with 20% heat-inactivated fetal bovine serum (FBS; Omega Scientific), penicillin (100 U/ml; Gibco), streptomycin (100 μg/ml; Gibco) and 10 ng/ml M-CSF (R&D, Minneapolis, MN) at

37˚C with 5% CO_2 for 6 days. BMDMs were then stimulated for 6-hours with activation media consisting of Dulbecco's Modified Eagle Medium (DMEM) with 0.25% heat-inactivated FBS, penicillin, streptomycin and 10 ng/ml MCSF with or without IL-4 (25 ng/ml; Sigma) and IL-10 (10 ng/ml; Sigma). RNA was collected in Trizol for QPCR analysis as descried above. PPIA and TPT1 were used as reference genes for QPCR experiments using myoblasts or BMDMs.

Cross-sectional area measurement

Frozen cross-sections were cut from the mid-belly of quadriceps femoris muscle at a thickness of 10 μm. Sections were then stained with hematoxylin (Vector) for 10 minutes. The muscle fiber cross-sectional area was measured for 500 fibers randomly sampled from complete cross-sections using a digital imaging system (Bioquant).

Statistics

Data are presented as mean ± sem. One-way analysis of variance was used to test whether differences between 3 or more groups were significant at $p < 0.05$. Significant differences between groups were identified using Tukey's Post Hoc test. Comparisons of two groups of values were analyzed using the unpaired, two-tailed t test.

Figures

Figure 13

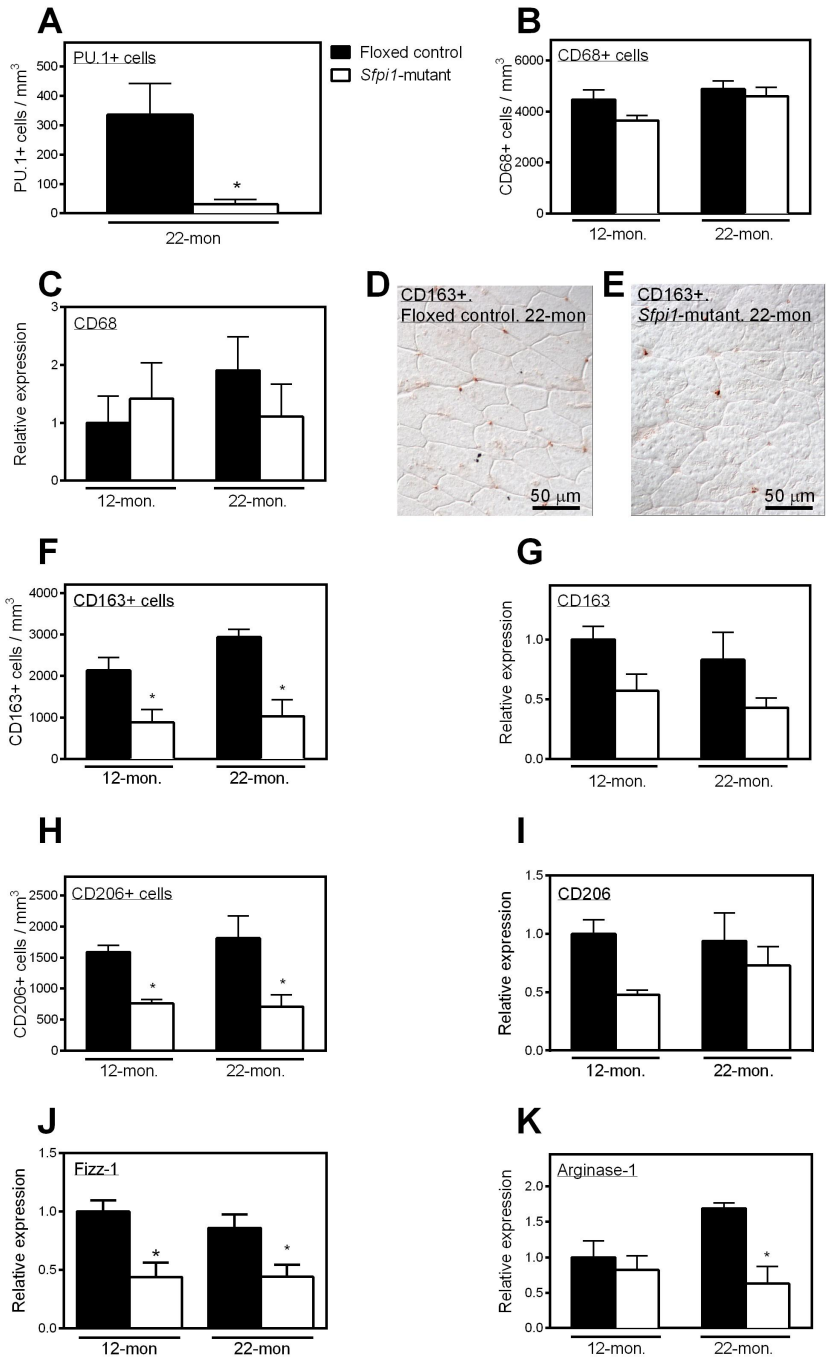

.

Figure 14.

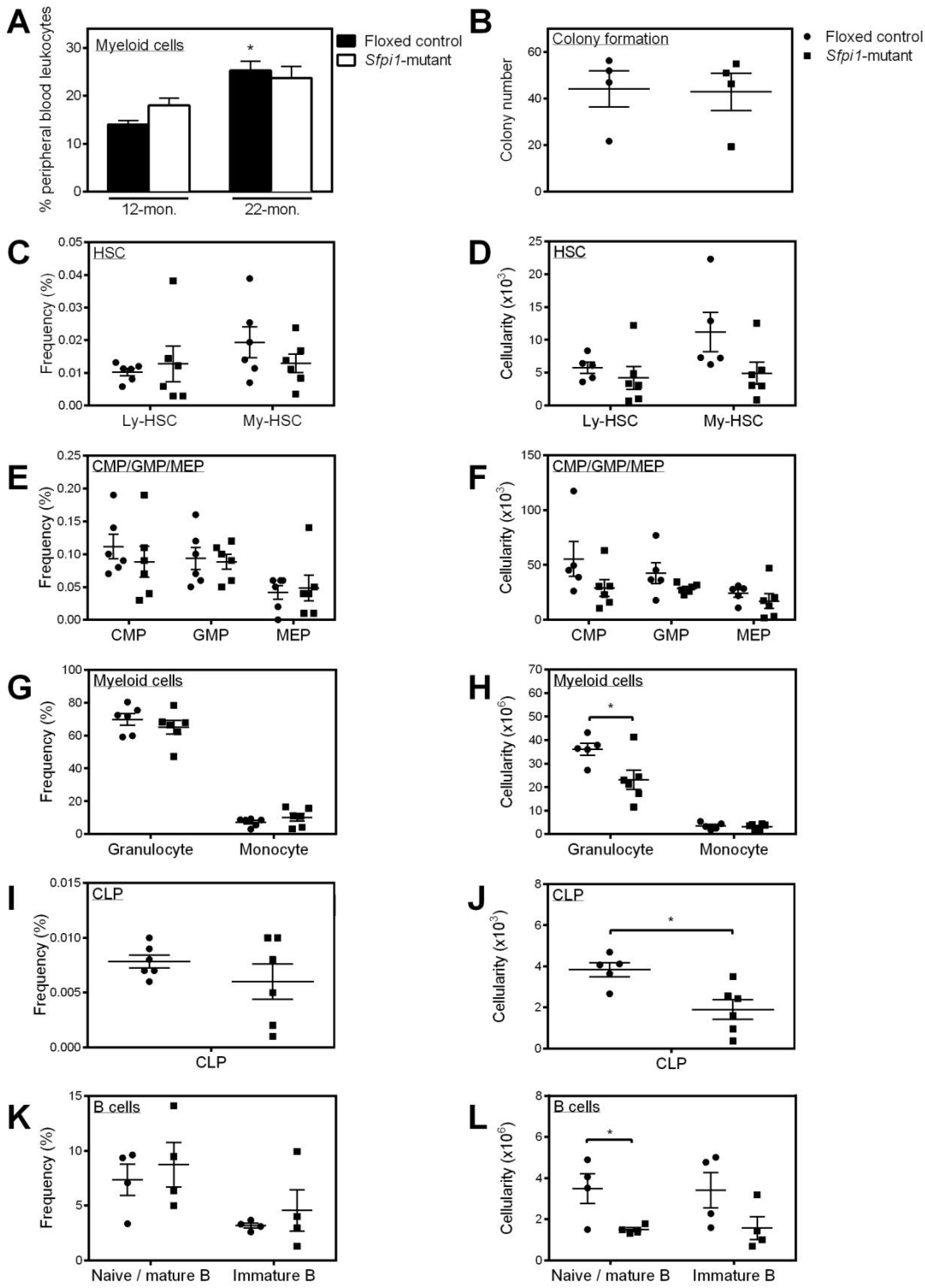
A
Myeloid cells
% peripheral blood leukocytes
Floxed control
Sfpi1-mutant
12-mon.
22-mon.
B
Colony formation
Colony number
Floxed control
Sfpi1-mutant
C
HSC
Frequency (%)
Ly-HSC
My-HSC
D
HSC
Cellularity (x10^3)
Ly-HSC
My-HSC
E
CMP/GMP/MEP
Frequency (%)
CMP
GMP
MEP
F
CMP/GMP/MEP
Cellularity (x10^3)
CMP
GMP
MEP
G
Myeloid cells
Frequency (%)
Granulocyte
Monocyte
H
Myeloid cells
Cellularity (x10^6)
Granulocyte
Monocyte
I
CLP
Frequency (%)
CLP
J
CLP
Cellularity (x10^3)
CLP
K
B cells
Frequency (%)
Naive / mature B
Immature B
L
B cells
Cellularity (x10^6)
Naive / mature B
Immature B

Figure 15.

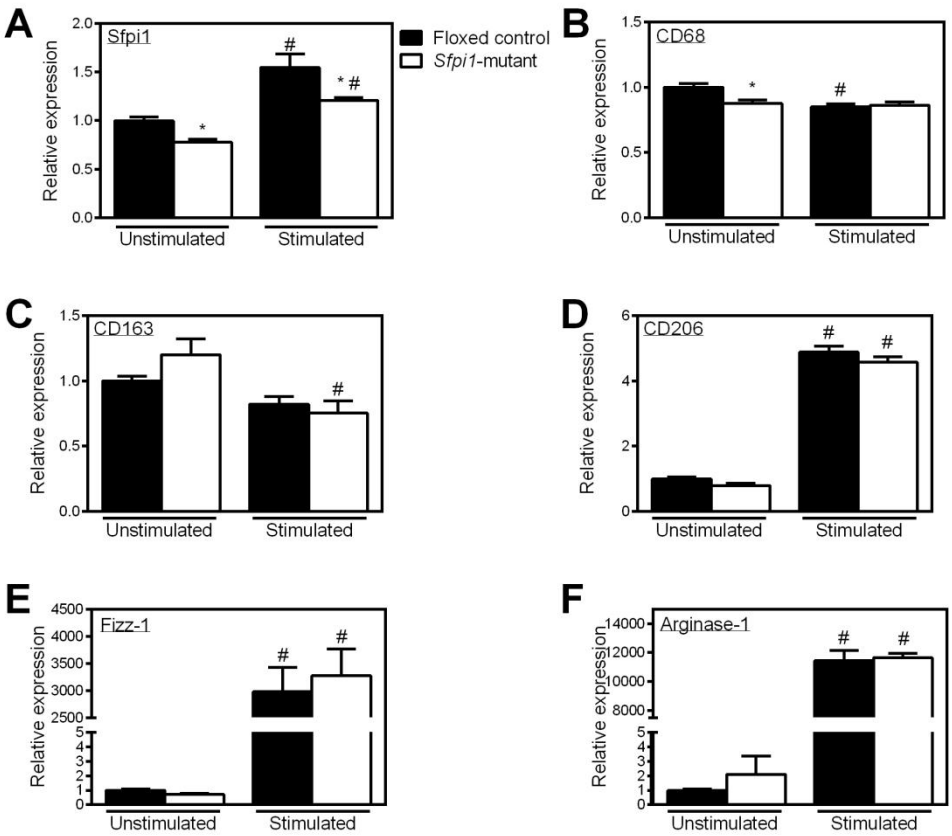
A
Sfpi1
Relative expression
Floxed control
Sfpi1-mutant
Unstimulated
Stimulated
B
CD68
C
CD163
D
CD206
E
Fizz-1
F
Arginase-1

Figure 16.

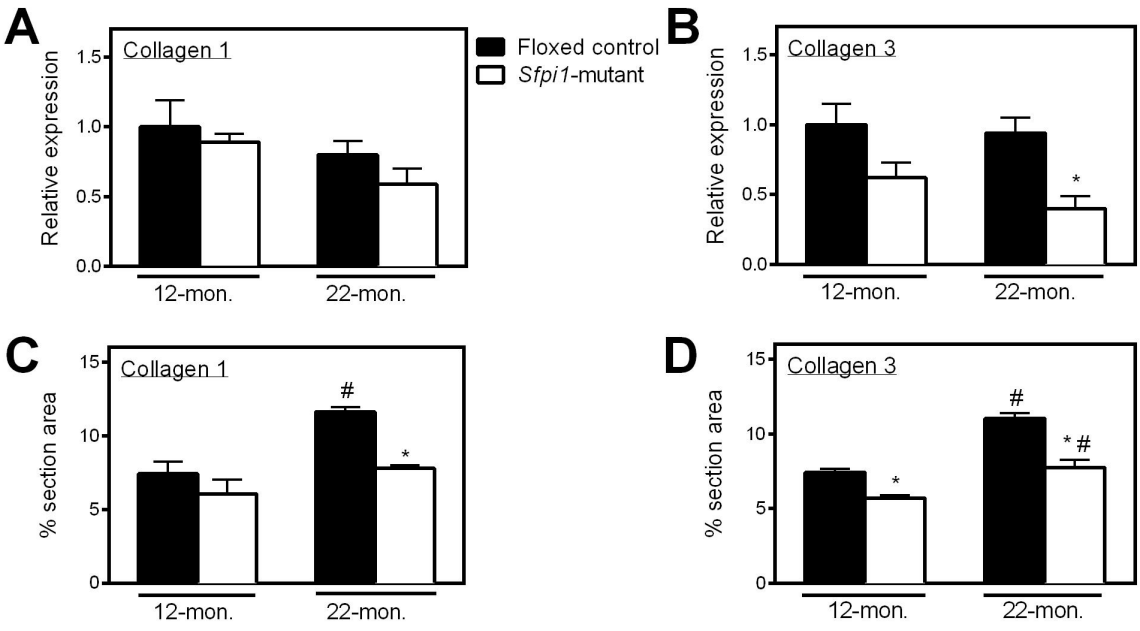
A
Collagen 1
Relative expression
1.5
1.0
0.5
0.0
12-mon.
22-mon.
Floxed control
Sfpi1-mutant
B
Collagen 3
Relative expression
1.5
1.0
0.5
0.0
*
12-mon.
22-mon.
C
Collagen 1
% section area
15
10
5
0
#
*
12-mon.
22-mon.
D
Collagen 3
% section area
15
10
5
0
#
*
*#
12-mon.
22-mon.

Figure 17.

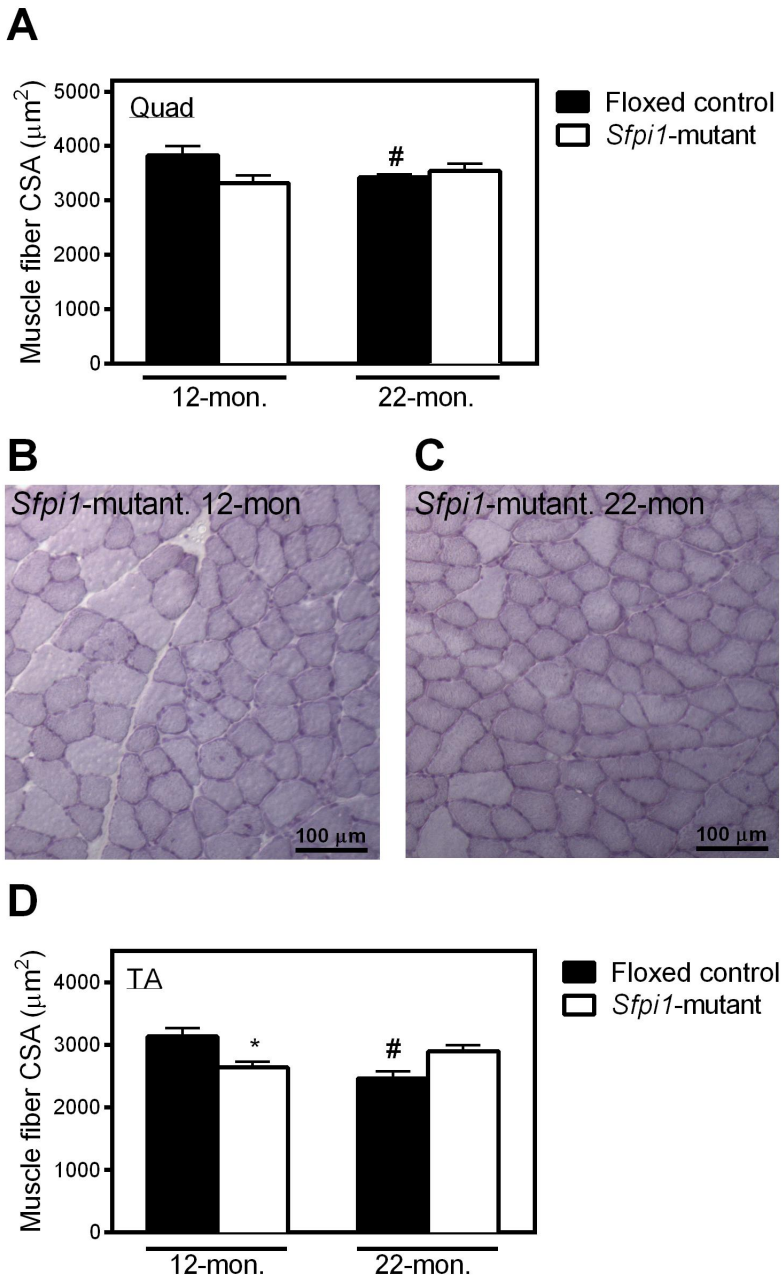
A
Quad
Muscle fiber CSA (μm²)
5000
4000
3000
2000
1000
0
#
12-mon.
22-mon.
Floxed control
Sfpi1-mutant
B
Sfpi1-mutant. 12-mon
100 μm
C
Sfpi1-mutant. 22-mon
100 μm
D
TA
Muscle fiber CSA (μm²)
4000
3000
2000
1000
0
*
#
12-mon.
22-mon.
Floxed control
Sfpi1-mutant

Figure 18.

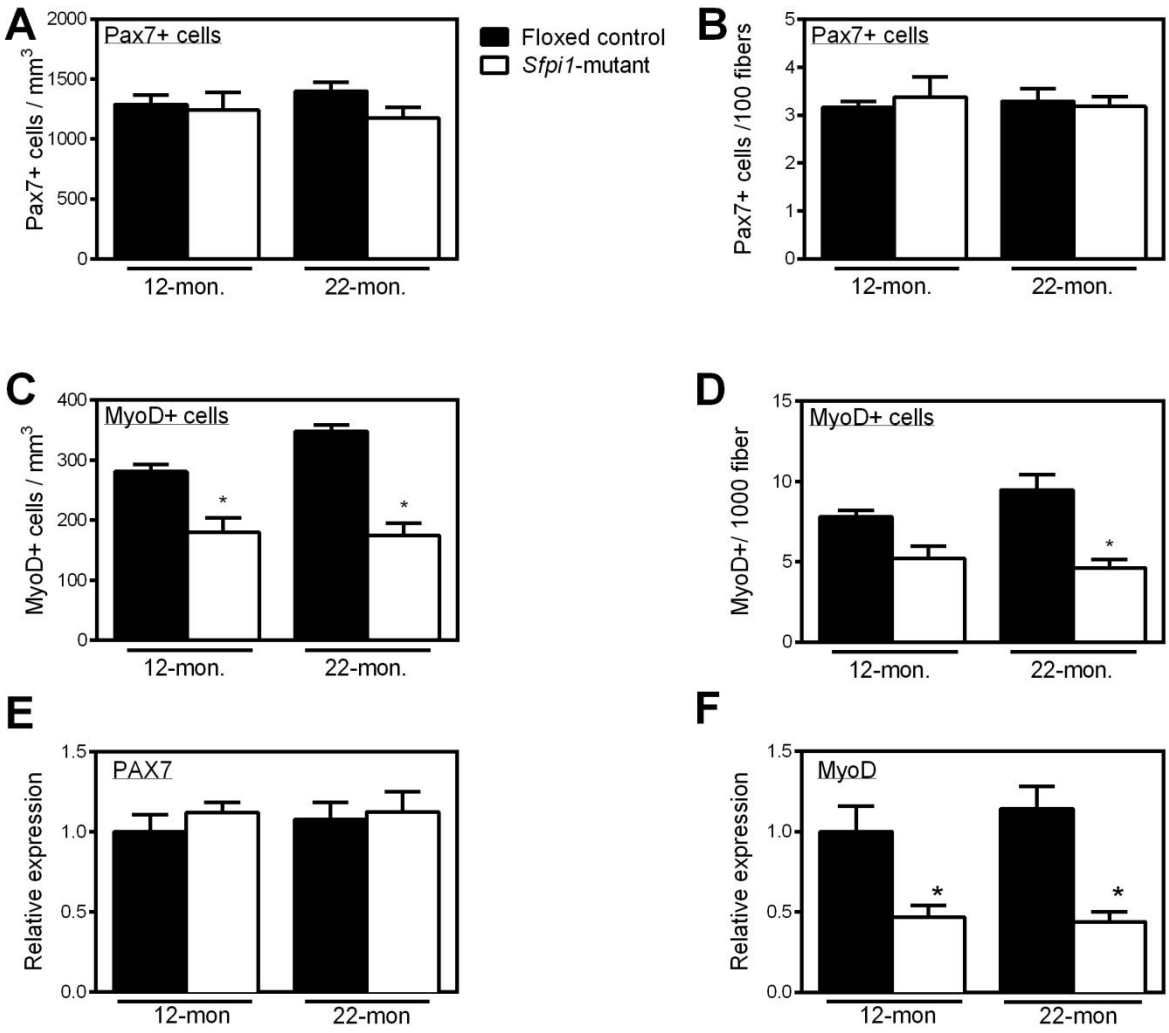
A
Pax7+ cells
Pax7+ cells / mm3
2000
1500
1000
500
0
12-mon.
22-mon.
Floxed control
Sfpi1-mutant
B
Pax7+ cells
Pax7+ cells /100 fibers
5
4
3
2
1
0
12-mon.
22-mon.
C
MyoD+ cells
MyoD+ cells / mm3
400
300
200
100
0
*
*
12-mon.
22-mon.
D
MyoD+ cells
MyoD+/ 1000 fiber
15
10
5
0
*
12-mon.
22-mon.
E
PAX7
Relative expression
1.5
1.0
0.5
0.0
12-mon
22-mon
F
MyoD
Relative expression
1.5
1.0
0.5
0.0
*
*
12-mon
22-mon

Figure Legends

Figure 13. Myeloid-cell-specific mutation of *Sfpi1* reduced M2 macrophage numbers in muscle without affecting M1 macrophage numbers. A. Myeloid-cell-specific mutation of *Sfpi1* reduced the number of PU.1+ cells in 22-month-old quadriceps muscles. Number of PU.1+ positive cells per unit muscle volume were counted on quadriceps muscle cross-sections from 22-month-old *Sfpi1*-mutant and floxed control mice. B. Number of CD68+ macrophages were not different in *Sfpi1*-mutant and floxed control mice at 12- and 22-months. C. Expression levels of *CD68* were not different in *Sfpi1*-mutant and floxed control mice at 12- and 22-months. D. Representative image of a quadriceps muscle cross-section from a 22-month-old floxed control mouse stained for CD163. E. Representative image of a quadriceps muscle cross-section from a 22-month-old *Sfpi1*-mutant mouse stained for CD163. Bars = 50 μm. F. Numbers of CD163+ macrophages were reduced in 12- and 22-month-old *Sfpi1*-mutant mice compared to age-matched floxed control mice. CD163+ cells in the same genotype was not significantly different between 12- and 22-months old. G. *CD163* expression showed an insignificant trend of decrease in *Sfpi1*-mutant mice compared to age-matched floxed control mice at 12- and 22-months old. H. Numbers of CD206+ macrophages were reduced in 12- and 22-month-old *Sfpi1*-mutant mice compared to age-matched floxed control mice. CD206+ cells in the same genotype was not significantly different between 12- and 22-months old. I. *CD206* expression showed an insignificant trend for a decrease in *Sfpi1*-mutant mice compared to age-matched floxed control mice at 12- and 22-months old. J. *Fizz-1* expression is significantly decreased in *Sfpi1*-mutant mice compared to

age-matched floxed control mice at 12 and 22-months old. K. *Arginase-1* expression showed an insignificant trend for a decrease in *Sfpi1*-mutant mice compared to age-matched floxed control mice at 12-months old. *Arginase-1* expression is significantly decreased in 22-month-old *Sfpi1*-mutant mice compared to age-matched floxed control mice. For all panels, * indicates significant difference from age-matched, floxed control group. N = 4-5 per data set.

Figure 14. Hematopoietic function and the frequencies and cellularities of subpopulations of hematopoiesis cells in floxed control and *Sfpi1*-mutant mice. A. The proportion of myeloid cells in peripheral blood leukocytes increased in floxed control mice between 12- and 22- months. The proportion of myeloid cells in peripheral blood leukocytes were not different in age-matched floxed control and *Sfpi1*-mutant mice at 12- and 22-months old. * indicates significant difference from age-matched, floxed control group. N = 4 - 7 per data set. B. The colony forming ability of bone marrow cells were not different between 22-month-old floxed control and *Sfpi1*-mutant mice. C. The frequencies of lymphoid-biased hematopoietic stem cells (Ly-HSC) and myeloid-biased hematopoietic stem cells (My-HSC) were not different between 22-month-old floxed control and *Sfpi1*-mutant mice. D. The cellularities of Ly-HSC and My-HSC were not different between 22-month-old floxed control and *Sfpi1*-mutant mice. E. The frequencies of common myeloid progenitor (CMP), granulocyte monocyte progenitor (GMP) and megakaryocyte erythrocyte progenitor (MEP) were not different between 22-month-old floxed control and *Sfpi1*-mutant mice. F. The cellularities of CMP, GMP and MEP were not different between 22-month-old floxed control and *Sfpi1*-mutant mice. G. The frequencies of granulocyte

and monocyte were not different between 22-month-old floxed control and *Sfpi1*-mutant mice. H. The cellularity of granulocytes was significantly lower in 22-month-old *Sfpi1*-mutant mice compared to age-matched floxed control mice. The cellularity of monocytes was not different between 22-month-old floxed control and *Sfpi1*-mutant mice. I. The frequency of common lymphoid progenitor (CLP) was not different between 22-month-old floxed control and *Sfpi1*-mutant mice. J. The cellularity of CLP was significantly lower in 22-month-old *Sfpi1*-mutant mice compared to age-matched floxed control mice. K. The frequency of naive / mature B cells and immature B cells were not different between 22-month-old floxed control and *Sfpi1*-mutant mice. L. The cellularity of naive / mature B cells was significantly lower in 22-month-old *Sfpi1*-mutant mice compared to age-matched floxed control mice. The cellularity of immature B cells was not different between 22-month-old floxed control and *Sfpi1*-mutant mice. For panels B-L, * indicates significant difference between genotype. N = 4-6 per data set.

Figure 15. Expression levels of *Sfpi1* and macrophage phenotypic markers in BMDMs of 12-month-old floxed control and *Sfpi1*-mutant mice without stimulation and with M2 polarization (stimulated). A. *Sfpi1* expression increased in both floxed control and *Sfpi1*-mutant BMDMs with M2 polarization. *Sfpi1* expression is lower in *Sfpi1*-mutant BMDMs compared to floxed control BMDMs with the same treatments. B. *CD68* expression in floxed control BMDMs decreased with M2 polarization. *CD68* expression in *Sfpi1*-mutant BMDMs was not affected by M2 polarization. *CD68* expression in unstimulated *Sfpi1*-mutant BMDMs was lower compared to expression in unstimulated floxed control BMDMs. C. *CD163* expressions were decreased by M2 polarization

between floxed control BMDMs but not in floxed control BMDMs. *CD163* expression was not significantly different in floxed control and *Sfpi1*-mutant BMDMs with the same treatment. D. *CD206* expression was increased by M2 polarization in both floxed control and floxed control BMDMs. *CD206* expression was not different between floxed control and *Sfpi1*-mutant BMDMs with the same treatment. E. *Fizz-1* expression was increased by M2 polarization in both floxed control and floxed control BMDMs. *Fizz-1* expression was not different between floxed control and *Sfpi1*-mutant BMDMs with the same treatment. F. *Arginase-1* expression was increased by M2 polarization in both floxed control and floxed control BMDMs. *Arginase-1* expression was not different between floxed control and *Sfpi1*-mutant BMDMs with the same treatment. For all panels, * indicates significant difference between genotypes with the same treatment. # indicates significant differences between treatments with the same genotype. N = 4-5 per data set.

Figure 16. Myeloid cell specific mutation of *Sfpi1* reduced the accumulation of connective tissues in aging muscles. A. Collagen type I (*Collagen 1*) expression was not different between 12- and 22-months in floxed control and *Sfpi1*-mutant mice. Collagen 1 expression was not different between floxed control and *Sfpi1*-mutant mice of the same age. B. Collagen type III (*Collagen 3*) expression was not different between 12- and 22-months in floxed control and *Sfpi1*-mutant mice. *Collagen 3* expression in *Sfpi1*-mutant mice showed an insignificant trend for a decrease compared to floxed control mice at 12 months. *Collagen 3* expression in 22-month-old *Sfpi1*-mutant mice was significantly lower compared to age-matched floxed control

mice. C. The proportion of section area consisting of collagen 1 increased in floxed control, but not *Sfpi1*-mutant mice between 12- and 22-months. The proportion of section area consisting of collagen 1 was significantly lower in *Sfpi1*-mutant mice compared to floxed control mice at 22-months. D. The proportion of section area consisting of collagen 3 increased in floxed control and *Sfpi1*-mutant mice between 12- and 22-months. The proportion of section area consisting of collagen 3 was significantly lower in *Sfpi1*-mutant mice compared to age-matched floxed control mice at both 12- and 22-months. For all panels, * indicates significant difference in age-matched groups between genotypes. # indicates significant differences between ages of same genotype. N = 5 per data set.

Figure 17. Myeloid-cell-specific mutation of *Sfpi1* prevents sarcopenia. A. Muscle fiber cross-sectional area (CSA) of quadriceps (Quad) decreased in floxed control mice between 12 and 22-months, but did not change in *Sfpi1*-mutant mice between 12 and 22 months. # indicates significant differences between ages of same genotype. N = 5 per data set. B. Representative image of a hematoxylin-stained cross section of a quadriceps muscle from a 12-month-old *Sfpi1*-mutant mouse C. Representative image of a hematoxylin-stained cross section of a quadriceps muscle from a 22-month-old *Sfpi1*-mutant mouse. Bars = 100 μm. D. CSA of tibialis anterior (TA) decreased in floxed control mice between 12- and 22-months, but did not change in *Sfpi1*-mutant mice between 12 and 22 months. CSA of TA were smaller in *Sfpi1*-mutant mice compared to floxed control mice at 12 months. For all panels, * indicates significant difference in age-matched groups between genotypes. # indicates significant differences between ages of

same genotype. N = 5 per data set.

Figure 18. Myeloid-cell-specific mutation of *Sfpi1* reduced *MyoD* expression and reduced MyoD+ cell numbers in 12- and 22-month-old muscles. A. The numbers of Pax7+ cells per unit muscle volume did not differ between 12 and 22 months in floxed control and *Sfpi1*-mutant muscles. *Sfpi1* mutation did not change Pax7+ cells per unit muscle volume at either 12- or 22-months. B. The numbers of Pax7+ cells per 100 muscle fibers did not differ between 12- and 22-months in floxed control and *Sfpi1*-mutant muscles. *Sfpi1* mutation did not change Pax7+ cells per 100 muscle fibers at either 12- or 22-months old. C. The numbers of MyoD+ cells per unit muscle volume did not differ between 12- and 22-months in floxed control and *Sfpi1*-mutant muscles. The numbers of MyoD+ cells per unit muscle volume were significantly lower in *Sfpi1*-mutant muscles compared to floxed control muscles at both 12- and 22-months. D. The numbers of MyoD+ cells per 1000 muscle fibers did not differ between 12- and 22-months in floxed control and *Sfpi1*-mutant muscles. The numbers of MyoD+ cells per 1000 muscle fiber were significantly lower in *Sfpi1*-mutant muscles compared to floxed control muscles at 22 months. E. *Pax7* expression did not differ between 12- and 22-months in floxed control and *Sfpi1*-mutant muscles. *Sfpi1* mutation did not change *Pax7* expression at either 12- or 22-month. F. *MyoD* expression did not differ between 12- and 22-months in floxed control and *Sfpi1*-mutant muscles. *MyoD* expression in *Sfpi1*-mutant muscles was significantly lower compared to age-matched floxed control muscles at both 12- and 22-months. For all panels, * indicates significant difference in age-matched groups between genotypes. N = 5 per data set.

Tables

Table 2

Antigen	Company and REF. #	Concentration
PU.1	eBioscience #14-9819	1:50
CD68	Biorad #mca1957	1:100
CD163	Santa Cruz #SC33560	1:50
CD206	Serotec #MC2235	1:150
Collagen type I	Southern Biotech #1310-01	1:50
Collagen type III	Southern Biotech #1330-01	1:50
Pax7	Prepared as stated in previous chapters	1:200
MyoD	Santa Cruz #SC760	1:50

Table 2. Antibodies and their concentration used for immunohistochemistry.

Table 3

Reagent	Company	Final Concentration
Minimum Essential Medium, Alpha	Corning Cellgro	-
Methycellulose	STEMCELL	1%
Heat Inactivated FSC	Gibco	30%
Penicillin / Streptomycin	Gibco	1%
L-Glutamine	Gibco	1%
2-Mercaptoethanol	Sigma	5×10^{-3} %
Sodium Pyruvate	Gibco	1%
MEM Vitamin Solution	Gibco	1%
Non-essential Amino Acid	Gibco	1%
GM-CSF	Biosource	20 ng/ml
IL-3	Invitrogen	10 ng/ml
IL-6	Gibco	10 ng/ml
Stem Cell Factor	Gibco	10 ng/ml

Table 3. Reagents and their concentrations used for colony forming assay.

Table 4

Cell Population	Antibody		Company and clone	Secondary staining	Company
CMP/ GMP/ MEP	CD16/32 (blocking)		eBioscience 93		
	Lin-FITC	CD3	eBioscience 145-2C11		
		CD8	eBioscience 53-6.7		
		TCRab	eBioscience H57-597		
		TCRgd	eBioscience UC7-13D5		
		NK1.1	eBioscience PK136		
		Gr-1	eBioscience RB6-8C5		
		IgM	Southern Biotech		
		Ter-119	eBioscience TER119		
		B220	eBioscience RA3-6B2		
	CD16/32 PE		eBioscience 93		
	CD117 APC		eBioscience ACK2		
	Sca-1 Percp Cy5.5		eBioscience D7		
	CD34 Biotin		eBioscience RAM34	Strept-avidin Pac Blue	eBioscience
Granulocyte and monocyte	CD 16/32		eBioscience 93		
	Gr-1 PE		eBioscience RB6-8C5		
	CD11b FITC		eBioscience M1/70		
HSC/ CLP	CD 16/32		eBioscience 93		
	Lin-FITC		Same as above		
	CD150 PE		Biolegend C15-12F12		
	Sca-1 Percp Cy5.5		eBioscience D7		
	CD117 APC		eBioscience ACK2		
	CD127 PE Cy7		eBioscience A7R34		
	CD135 Biotin		eBioscience A2F10	Strept-avidin Pac Blue	eBioscience
B Cells	CD 16/32		eBioscience 93		
	CD19 PE		eBioscience		
	IgM FITC		Southern Biotech		

Tables 4. Antibodies used for FACS.

References

Alvarez B, Quinn LS, Busquets Sl, Quiles MT, López-Soriano FJ, Argilés JM (2002). Tumor necrosis factor-α exerts interleukin-6-dependent and-independent effects on cultured skeletal muscle cells. *Biochimica et Biophysica Acta (BBA)-Molecular Cell Research*. **1542**, 66-72.

Bernet JD, Doles JD, Hall JK, Tanaka KK, Carter TA, Olwin BB (2014). p38 MAPK signaling underlies a cell-autonomous loss of stem cell self-renewal in skeletal muscle of aged mice. *Nature Medicine*. **20**, 265-271.

Brack AS, Bildsoe H, Hughes SM (2005). Evidence that satellite cell decrement contributes to preferential decline in nuclear number from large fibres during murine age-related muscle atrophy. *Journal of Cell Science*. **118**, 4813-4821.

Brack AS, Rando TA (2007). Intrinsic changes and extrinsic influences of myogenic stem cell function during aging. *Stem Cell Reviews*. **3**, 226-237.

Carlson B, Faulkner J (1989). Muscle transplantation between young and old rats: age of host determines recovery. *American Journal of Physiology-Cell Physiology*. **256**, C1262-C1266.

Chakkalakal JV, Jones KM, Basson MA, Brack AS (2012). The aged niche disrupts muscle stem cell quiescence. *Nature*. **490**, 355-360.

Charge SB, Rudnicki MA (2004). Cellular and molecular regulation of muscle regeneration. *Physiological Reviews*. **84**, 209-238.

Chen S-E, Jin B, Li Y-P (2007). TNF-α regulates myogenesis and muscle regeneration by activating p38 MAPK. *American Journal of Physiology-Cell Physiology*. **292**, C1660-C1671.

Cheng M, Nguyen M-H, Fantuzzi G, Koh TJ (2008). Endogenous interferon-γ is required for efficient skeletal muscle regeneration. *American Journal of Physiology-Cell Physiology*. **294**, C1183-C1191.

Ciciliot S, Rossi AC, Dyar KA, Blaauw B, Schiaffino S (2013). Muscle type and fiber type specificity in muscle wasting. *The International Journal of Biochemistry & Cell Biology*. **45**, 2191-2199.

Coletti D, Moresi V, Adamo S, Molinaro M, Sassoon D (2005). Tumor necrosis factor‐α gene transfer induces cachexia and inhibits muscle regeneration. *Genesis*. **43**, 120-128.

Conboy IM, Conboy MJ, Smythe GM, Rando TA (2003). Notch-mediated restoration of regenerative potential to aged muscle. *Science*. **302**, 1575-1577.

Conboy IM, Conboy MJ, Wagers AJ, Girma ER, Weissman IL, Rando TA (2005). Rejuvenation of aged progenitor cells by exposure to a young systemic environment. *Nature*. **433**, 760-764.

Cosgrove BD, Gilbert PM, Porpiglia E, Mourkioti F, Lee SP, Corbel SY, Llewellyn ME, Delp SL, Blau HM (2014). Rejuvenation of the muscle stem cell population restores strength to injured aged muscles. *Nature Medicine*. **20**, 255-264.

Deb C, Li B, Baylink DJ, Xing W, Zhang W, Chen M, Wergedal JE, Mohan S, Qin X (2012).

Transgenic overexpression of pregnancy-associated plasma protein-A in skeletal muscle of mice increases myofiber size and central nucleation in sedentary muscle and promotes muscle regeneration in the injured muscle. *Growth Hormone & IGF Research*. **22**, 173-179.

Deschenes M, Gaertner J, O'Reilly S (2013). The effects of sarcopenia on muscles with different recruitment patterns and myofiber profiles. *Current Aging Science*. **6**, 266-272.

Frost RA, Lang CH, Gelato MC (1997). Transient exposure of human myoblasts to tumor necrosis factor-α inhibits serum and insulin-like growth factor-I stimulated protein synthesis. *Endocrinology*. **138**, 4153-4159.

Fry CS, Lee JD, Mula J, Kirby TJ, Jackson JR, Liu F, Yang L, Mendias CL, Dupont-Versteegden EE, McCarthy JJ (2015). Inducible depletion of satellite cells in adult, sedentary mice impairs muscle regenerative capacity without affecting sarcopenia. *Nature Medicine*. **21**, 76-80.

Greiwe JS, Cheng B, Rubin DC, Yarasheski KE, Semenkovich CF (2001). Resistance exercise decreases skeletal muscle tumor necrosis factor α in frail elderly humans. *The FASEB Journal*. **15**, 475-482.

Guttridge DC, Mayo MW, Madrid LV, Wang C-Y, Baldwin Jr AS (2000). NF-κB-induced loss of MyoD messenger RNA: possible role in muscle decay and cachexia. *Science*. **289**, 2363-2366.

Hawke TJ (2005). Muscle stem cells and exercise training. *Exercise and Sport Sciences reviews*.

33, 63-68.

Jo E, Lee S-R, Park B-S, Kim J-S (2012). Potential mechanisms underlying the role of chronic inflammation in age-related muscle wasting. *Aging Clinical and Experimental Research*. **24**, 412-422.

Karlsen A, Couppé C, Andersen JL, Mikkelsen UR, Nielsen RH, Magnusson SP, Kjaer M, Mackey AL (2015). Matters of fiber size and myonuclear domain: Does size matter more than age? *Muscle & Nerve*. **52**, 1040-1046.

Langen RC, Schols AM, Kelders MC, Wouters EF, Janssen-Heininger YM (2001). Inflammatory cytokines inhibit myogenic differentiation through activation of nuclear factor-κB. *The FASEB Journal.* **15**, 1169-1180.

Langen RC, Van Der Velden JL, Schols AM, Kelders MC, Wouters EF, Janssen-Heininger YM (2004). Tumor necrosis factor-alpha inhibits myogenic differentiation through MyoD protein destabilization. *The FASEB Journal*. **18**, 227-237.

Lees SJ, Zwetsloot KA, Booth FW (2009). Muscle precursor cells isolated from aged rats exhibit an increased tumor necrosis factor-α response. *Aging Cell*. **8**, 26-35.

Léger B, Derave W, De Bock K, Hespel P, Russell AP (2008). Human sarcopenia reveals an increase in SOCS-3 and myostatin and a reduced efficiency of Akt phosphorylation. *Rejuvenation Research*. **11**, 163-175B.

Li Y-P (2003). TNF-α is a mitogen in skeletal muscle. *American Journal of Physiology-Cell Physiology*. **285**, C370-C376.

Li Y-P, Schwartz RJ, Waddell ID, Holloway BR, Reid MB (1998). Skeletal muscle myocytes undergo protein loss and reactive oxygen-mediated NF-κB activation in response to tumor necrosis factor α. *The FASEB Journal*. **12**, 871-880.

Lieskovska J, Guo D, Derman E (2003). Growth impairment in IL-6-overexpressing transgenic mice is associated with induction of SOCS3 mRNA. *Growth Hormone & IGF Research*. **13**, 26-35.

Lin S-Y, Chen W-Y, Lee F-Y, Huang C-J, Sheu WH-H (2005). Activation of ubiquitin-proteasome pathway is involved in skeletal muscle wasting in a rat model with biliary cirrhosis: potential role of TNF-α. *American Journal of Physiology-Endocrinology and Metabolism*. **288**, E493-E501.

Marty E, Liu Y, Samuel A, Or O, Lane J (2017). A review of sarcopenia: Enhancing awareness of an increasingly prevalent disease. *Bone*. **105**, 276-286

Melton 3rd L, Khosla S, Crowson CS, O'connor MK, O'Fallon WM, Riggs BL (2000). Epidemiology of sarcopenia. *Journal of the American Geriatrics Society*. **48**, 625-630.

Metter EJ, Conwit R, Tobin J, Fozard JL (1997). Age-associated loss of power and strength in the upper extremities in women and men. *The Journals of Gerontology. Series A, Biological Sciences and Medical Sciences.* **52**, B267-276.

Otis JS, Niccoli S, Hawdon N, Sarvas JL, Frye MA, Chicco AJ, Lees SJ (2014). Pro-inflammatory mediation of myoblast proliferation. *PLoS One*. **9**, e92363.

Palacios D, Mozzetta C, Consalvi S, Caretti G, Saccone V, Proserpio V, Marquez VE, Valente S,

Mai A, Forcales SV (2010). TNF/p38α/polycomb signaling to Pax7 locus in satellite cells links inflammation to the epigenetic control of muscle regeneration. *Cell Stem Cell*. **7**, 455-469.

Patel HJ, Patel BM (2017). TNF-α and cancer cachexia: molecular insights and clinical implications. *Life Sciences*. **170**, 56-63.

Petrella JK, Kim J-s, Cross JM, Kosek DJ, Bamman MM (2006). Efficacy of myonuclear addition may explain differential myofiber growth among resistance-trained young and older men and women. *American Journal of Physiology-Endocrinology and Metabolism*. **291**, E937-E946.

Plonquet A, Eliezer-Vanerot M-C, Poron F, Belec L, Barlovatz-Meimon G, Gherardi RK (1999). Differential expression of the IL-1 system components during in vitro myogenesis: Implication of IL-1b in induction of myogenic cell apoptosis. *Cell Death and Differentiation*. **6**, 1012-1021.

Reid MB, Li Y-P (2001). Tumor necrosis factor-α and muscle wasting: a cellular perspective. *Respiratory Research*. **2**, 269.

Relaix F, Zammit PS (2012). Satellite cells are essential for skeletal muscle regeneration: the cell on the edge returns centre stage. *Development*. **139**, 2845-2856.

Roberts P, McGeachie JK, Grounds MD (1997). The host environment determines strain-specific differences in the timing of skeletal muscle regeneration: cross-transplantation studies between SJL/J and BALB/c mice. *The Journal of Anatomy*. **191**, 585-594.

Sambasivan R, Yao R, Kissenpfennig A, Van Wittenberghe L, Paldi A, Gayraud-Morel B, Guenou H, Malissen B, Tajbakhsh S, Galy A (2011). Pax7-expressing satellite cells are indispensable for adult skeletal muscle regeneration. *Development*. **138**, 3647-3656.

Schwartz LM, Brown C, McLaughlin K, Smith W, Bigelow C (2016). The myonuclear domain is not maintained in skeletal muscle during either atrophy or programmed cell death. *American Journal of Physiology-Cell Physiology*. **311**, C607-C615.

Song J, Saeman MR, De Libero J, Wolf SE (2015). Skeletal muscle loss is associated with TNFα mediated insufficient skeletal myogenic activation after burn. *Shock*. **44**, 479-486.

Sousa-Victor P, Gutarra S, García-Prat L, Rodriguez-Ubreva J, Ortet L, Ruiz-Bonilla V, Jardí M, Ballestar E, González S, Serrano AL (2014). Geriatric muscle stem cells switch reversible quiescence into senescence. *Nature*. **506**, 316-321.

Van der Meer S, Jaspers R, Degens H (2011). Is the myonuclear domain size fixed? *Journal of Musculoskeletal & Neuronal Interactions*. **11**, 286-297

Verdijk LB, Koopman R, Schaart G, Meijer K, Savelberg HH, van Loon LJ (2007). Satellite cell content is specifically reduced in type II skeletal muscle fibers in the elderly. *American Journal of Physiology-Endocrinology and Metabolism*. **292**, E151-E157.

Visser M, Pahor M, Taaffe DR, Goodpaster BH, Simonsick EM, Newman AB, Nevitt M, Harris TB (2002). Relationship of interleukin-6 and tumor necrosis factor-α with muscle mass and muscle strength in elderly men and women: the Health ABC Study. *The Journals of Gerontology Series A: Biological Sciences and Medical Sciences*. **57**, M326-M332.

Walston JD (2012). Sarcopenia in older adults. *Current Opinion in Rheumatology*. **24**, 623.

Wang Y, Wehling-Henricks M, Samengo G, Tidball JG (2015). Increases of M2a macrophages and fibrosis in aging muscle are influenced by bone marrow aging and negatively regulated by muscle‐derived nitric oxide. *Aging Cell*. **14**, 678-688.

Wehling-Henricks M, Li Z, Lindsey C, Wang Y, Welc SS, Ramos JN, Khanlou N, Kuro-o M, Tidball JG (2016). Klotho gene silencing promotes pathology in the mdx mouse model of Duchenne muscular dystrophy. *Human Molecular Genetics*. **25**, 2465-2482.

Wilson D, Jackson T, Sapey E, Lord JM (2017). Frailty and sarcopenia: the potential role of an aged immune system. *Ageing Research Reviews*. **36**, 1-10

Chapter 5. Macrophage-derived tumor necrosis factor-alpha promotes sarcopenia and regulates muscle cell fusion with aging muscle fibers

5.1 Abstract

Sarcopenia is age-related muscle wasting that currently lacks effective therapeutic interventions. We found that systemic ablation of tumor necrosis factor-α (*TNFα*) prevented sarcopenia and prevented the age-related change in muscle fiber phenotype. Furthermore, *TNFα* ablation reduced the number of satellite cells, in aging muscle and promoted muscle cells fusion *in vivo* and *in vitro*. Because CD68+ macrophages are important sources of TNFα and the number of CD68+ macrophages increases in aging muscle, we tested whether macrophage-derived TNFα affects myogenesis. Media conditioned by *TNFα*-null macrophages increased muscle cell fusion *in vitro*, compared to media conditioned by wild-type macrophages. In addition, transplantation of bone marrow cells from wild-type mice into *TNFα*-null recipients increased satellite cell numbers and reduced numbers of centrally-nucleated myofibers, indicating that macrophage-secreted TNFα reduces muscle cell fusion. Transplantation of bone marrow cells from wild-type mice into *TNFα*-null recipients also increased sarcopenia, although transplantation did not restore the age-related change in fiber type phenotype. Collectively, we show that macrophage-derived TNFα contributes to muscle aging by regulating sarcopenia and muscle cell fusion with aging muscle fibers. Our findings also show that TNFα intrinsic to muscle and TNFα secreted by immune cells work together to regulate muscle aging.

5.2 Introduction

Aging skeletal muscle undergoes a gradual decline in muscle mass, termed sarcopenia. Epidemiological studies in elderly people showed that total skeletal muscle mass declines 30–50% from the 4th to the 8th decade of life, and that muscle functional capacity declines at the rate of up to a 3% annually after age 60 (Metter *et al.* 1997; Melton *et al.* 2000; Walston 2012). Sarcopenia is usually associated with a decrease in muscle strength, function, and regenerative capacity. These age-related changes in skeletal muscle together lead to increased risk of falling, loss of physical independence, and increased morbidity and mortality rates (Marty *et al.* 2017). The cause of sarcopenia is multifactorial, including both intrinsic changes in the muscle compartment and extrinsic influence of other systems (Walston 2012). Although awareness of the importance of sarcopenia has risen in recent years with the rapid increase in the elderly population, the mechanisms that drive sarcopenia are still largely unknown and effective therapies and treatment options are very limited.

Inflammaging, the increase in chronic low-grade systemic inflammation with age, is associated with sarcopenia and frailty (Jo *et al.* 2012; Wilson *et al.* 2017). Our previous study showed that the number of macrophages in muscle increases significantly during aging (Wang *et al.* 2015). Macrophages are the primary source of various inflammatory cytokines, including tumor necrosis factor alpha (TNFα), which have the potential to modify muscle mass and function. TNFα is a proinflammatory cytokine that increases in the serum of men during aging

(Léger *et al.* 2008) and its increase correlates with the loss of muscle mass and muscle strength (Greiwe *et al.* 2001; Visser *et al.* 2002). Moreover, in other models of muscle atrophy, including cachexia and injury-induced muscle atrophy, exogenous administration of TNFα to mice causes a decrease in muscle mass and regenerative capacity (Coletti *et al.* 2005; Song *et al.* 2015). Those data suggested that macrophage-secreted TNFα might play an important role in muscle aging.

TNFα may contribute to sarcopenia by regulating the number or regenerative capacity of satellite cells. Satellite cells are specialized myogenic stem cells located beneath the basement membranes of muscle fibers that are required for muscle regeneration and growth (Sambasivan *et al.* 2011). In response to injury, satellite cells exit their quiescent state, proliferate, differentiate and fuse with existing myofibers to become new myonuclei and replace and/or repair the injured cells (Relaix & Zammit 2012). Previous studies have shown that TNFα can inhibit satellite cell differentiation and myogenesis. For example, TNFα reduces myogenic differentiation through transcriptional activation of NF-κB and by decreasing protein stability of MyoD, a transcription factor that plays a key role in regulating myoblast transition from proliferation to differentiation (Guttridge *et al.* 2000; Langen *et al.* 2004). In line with those findings, *in vitro* observations of C2C12 myoblasts or primary satellite cells indicated that TNFα has bimodal effects on myogenesis, promoting myoblast proliferation at early stages of myogenesis while repressing myoblast differentiation (Langen *et al.* 2001; Chen *et al.* 2007; Palacios *et al.* 2010).

Coinciding with the increasing serum concentration of TNFα, the myogenic capacity of satellite cells declines significantly during aging (Conboy *et al.* 2003; Brack & Rando 2007; Sousa-Victor *et al.* 2014), suggesting that TNFα may contribute to sarcopenia by influencing the regenerative capacity of aging satellite cells. Intriguingly, whether the age-related impairment of satellite cell function is caused by changes intrinsic to satellite cells or by extrinsic factors is disputed. For example, previous studies utilizing muscle transplantation showed impaired regeneration of young muscles transplanted into old animals and an improved regeneration of old muscles when incorporated into young animals (Carlson & Faulkner 1989; Roberts *et al.* 1997). Those observations indicated a significant role for the tissue environment extrinsic to muscle cells in regulating their regenerations. Similarly, more recent studies using heterochronic parabiosis experiments showed that exposure of aged satellite cells to a youthful environment could significantly enhance the regenerative capacity of the skeletal muscle from old animals (Conboy *et al.* 2005; Brack & Rando 2007). However, other research groups demonstrated that transplantation of old satellite cells into a young environment failed to restore the phenotype or myogenic capacity of satellite cells (Bernet *et al.* 2014; Cosgrove *et al.* 2014). Despite the discrepancies that may be caused by different experimental approaches, these data together suggest that intrinsic and extrinsic factors work in concert and each may contribute partly to muscle aging. Interestingly, TNFα is expressed in both myofibers and tissue-resident macrophages in aging muscle, suggesting that TNFα might serve as one of the nodes integrating the intrinsic and extrinsic factors leading to sarcopenia.

In the present study, we utilized a mouse model with systemic genetic ablation of *TNFα* (*TNFα*-null mice) to investigate the role of TNFα in regulating satellite cell function and sarcopenia. We found that ablating *TNFα* resulted in hyper-fusion of muscle cells and increased muscle mass and muscle fiber size in aging muscle. Furthermore, our *in vitro* experiments showed that TNFα intrinsic to satellite cells and that TNFα secreted by macrophages both influenced myogenesis. We then specifically tested the importance of macrophage secreted TNFα by performing bone marrow transplantation of wild-type bone marrow cells into *TNFα*-null mice and found that macrophage-secreted TNFα contributed to sarcopenia and reduced muscle cell fusion, but was insufficient to prevent age-related changes in muscle fiber phenotype.

5.3 Results

Genetic ablation of TNFα prevents sarcopenia and muscle fiber type composition switch in aging muscle

Previous researchers have reported that increased *TNFα* expression was associated with lower muscle mass and strength, as well as higher mortality in elderly persons (Greiwe *et al.* 2001; Visser *et al.* 2002). We performed qPCR analysis of quadriceps muscles from adult (12-month-old) and old (24-month-old) wild-type mice and showed that aging is associated with significantly greater expression of TNFα (Figure 19A). Those findings led us to test whether genetic ablation of *TNFα* would affect age-related changes in muscle. *TNFα*-null mice have no detectable expression of *TNFα* at either 12- or 24-months of age (Figure 19A). Our analysis showed a significant decrease in wet muscle mass of quadriceps, soleus and gastrocnemius muscles in aged wild-type mice compared to adult wild-type mice. However, no change in muscle mass was seen during aging in *TNFα*-null mice (Figures 19B - D). Similarly, the decrease in quadriceps mass to body mass ratio observed during aging in wild-type mice was also ablated in *TNFα*-null animals (Figure 19E). Because reductions in muscle mass could reflect changes in the tissue other than changes in muscle fibers themselves, we also assayed for changes in the cross-sectional area (CSA) of muscle fibers. Using this more specific assay, we were able to show significant sarcopenia occurred by 20-months of age (Figure 19F). Although quadriceps muscle fiber CSA decreased significantly between 10- and 20-months of

age in wild-type mice, no reduction of fiber size occurred in *TNFα* mutant mice during that period (Figure 19F). In addition, muscle fibers in 20-month-old, *TNFα*-null mice were significantly larger than age-matched wild-type mice (Figure 19F).

Previous investigations have shown that Type II or fast-twitch fibers are more susceptible to muscle wasting during aging (Verdijk *et al.* 2007; Ciciliot *et al.* 2013). Preferential atrophy and loss of fast-twitch fibers caused an increased ratio of slow-twitch fibers to total fiber in aging muscle (Deschenes *et al.* 2013). We performed slow myosin heavy chain (sMHC) staining on cross sections of soleus muscle and found that the percentage of sMHC+ fibers / total fibers increased significantly in wild-type mice from 10-months to 20-months of age. This age-related change of fiber composition ratio was prevented by *TNFα* ablation (Figures 19G, H). Together, these data suggest that TNFα contributes to muscle wasting and preferential loss of fast-twitch fibers during aging.

Genetic ablation of TNFα promotes satellite cell activation in aging muscle

Satellite cell senescence during aging has been reported to contribute to sarcopenia. Previous studies have shown that TNFα affects myogenesis and muscle regeneration by regulating satellite cell function in injured and dystrophic muscles (Chen *et al.* 2007; Palacios *et al.* 2010). We tested whether TNFα affects satellite cell activation in aging muscle. At 10-months of age, the number of satellite cells per unit volume, measured by immunohistochemistry of Pax7, was similar in wild-type and *TNFα*-null mice. However, at 20-months of age, *TNFα*-null

mice had significantly fewer Pax7+ cells, while Pax7+ cell number in wild-type mice remained at a similar level compared to 10-month-old mice (Figure 20A). Our qPCR analysis results showed that at 20-months of age, quadriceps muscle isolated from *TNFα*-null mice had lower expression of *Pax7* and *myogenin* and increased expression of *MyoD*, compared to muscle from wild-type mice at the same age (Figure 20B).

TNFα deficient mice have more myonuclei in aging muscle and regenerative muscle

Activated satellite cells proliferate, differentiate and then fuse with existing muscle fibers to contribute to myogenesis following acute or chronic muscle injury, creating centrally nucleated fibers which provide an index of muscle regeneration. The number of centrally-nucleated fibers was very low in healthy non-injured quadriceps muscle of both adult and old wild-type mice (Figures 21A, B). However, more than 25% of the muscle fibers in old, *TNFα*-null mice quadriceps muscles contained central nuclei (Figures 21C, D). Furthermore, many of the central-nucleated fibers showed more than one central nucleus in a single plane of section, indicating an abnormal, hyper-nucleated status (Figure 21C). The percentage of fibers with 1, 2, 3 or 4 and more central nuclei were all significantly increased in old *TNFα*-null mice compared to old wild-type mice (Figure 21E). Because the observed increase in central nuclei in old *TNFα*-null muscles could be caused by increased muscle cell fusion and by translocation of myonuclei from their normal location near the fiber surface to a central location, we also measured total number of myonuclei in muscle cross-sections, including both central and

peripheral nuclei in the counts (Figures 21F, G). Total number of myonuclei per muscle fiber in cross sections increased in *TNFα*-null mice, which validated an increase in fusion caused by the *TNFα* mutation (Figure 21G). These results suggested that *TNFα* deficiency can promote an increase in muscle cell fusion with muscle fibers, leading to increased centrally-nucleated fibers as well as the number of central nuclei per fiber.

We then performed acute injury to healthy adult *TNFα* null mice to test whether the increase of central nucleation was restricted to aging muscle. Quadriceps muscles of 12-month-old wild-type and *TNFα*-null mice was injured by $BaCl_2$ injection. Muscle fiber central nucleation was quantified at 21-days after injury. Our results showed that injured muscles from *TNFα*-null mice had significantly more centrally-nucleated fibers compared to muscle from wild-type mice (Figures 21H, I). Collectively, these findings suggest that TNFα contributes to the decrease of the myogenic capacity of satellite cells during aging, while genetic ablation of *TNFα* can prevent sarcopenia by increasing satellite cell activation and fusion.

Primary myoblasts isolated from TNFα-null mice are more fusogenic than wild-type myoblasts

We then tested whether muscle-derived TNFα inhibited satellite cell fusion by analyzing *in vitro* primary cell cultures. Myoblasts isolated from adult wild-type and *TNFα*-null mice (Figure 22A) were cultured and induced to differentiation by serum restriction. Myoblasts isolated from *TNFα*-null mice started fusing with each other and formed myotubes more rapidly compared to myoblasts from wild-type mice. We then quantified the number of nuclei in each myotube at day

6 after induction of differentiation and found that myotubes formed by muscle stem cells from *TNFα*-null mice had more myonuclei (Figure 22B). These data support our *in vivo* observation that *TNFα* deficiency promotes muscle cell fusion and increases myonuclei numbers. However, our qPCR analysis of primary muscle cells showed no significant differences in *Pax7, MyoD* or m*yogenin* expression between wild-type and *TNFα*-null mice (Figure 22C). Together, these findings suggest that *TNFα* deficiency in satellite cells directly contributes to their increased fusion capacity, without significantly affecting their expression of key transcription factors that influence muscle differentiation.

TNFα secreted by macrophages affects the fusion capacity of muscle cells

Macrophages are an important source of inflammatory cytokines, including TNFα. Our previous investigations showed that the number of macrophages increases significantly in aging muscle, consistent with a systemic increase in pro-inflammatory cytokines during aging (Wang *et al.* 2015). We assayed for TNFα expression in old muscle by immunofluorescence and found that CD68+ macrophages in the muscle of healthy old mice express TNFα (Figures 23A-C). Intriguingly, we also observed that TNFα accumulated in the basal lamina surrounding muscle fibers. Moreover, necrotic fibers that were infiltrated by CD68+ macrophages also showed high expression of TNFα (Figures 23D-F). Unsurprisingly, TNFα was not detectable in TNFα-null muscles (data not shown). These results indicate that CD68+ macrophages may provide a source of TNFα can that can influence muscle health. There was no difference in either *CD68*

mRNA expression or the number of CD68+ macrophages in old wild-type and *TNFα*-null mice (Figures 23G-H). We also tested whether *TNFα* ablation affected the expression in old muscle of other inflammatory cytokines that can affect myogenesis (Plonquet *et al.* 1999; Lieskovska *et al.* 2003; Cheng *et al.* 2008). Our qPCR results showed that the expressions of *IFNγ, IL-6*, and *IL-1β* did not differ significantly in 24-month-old, *TNFα*-null muscles compared to age-matched wild-type muscles (Figure 23I). These findings indicate that macrophages in *TNFα*-null mice had normal expression of other pro-inflammatory cytokines that can influence myogenesis, despite the deficiency of *TNFα.* They also show that the changes in muscle fiber size and satellite cell numbers during aging that were caused by *TNFα* ablation were not attributable to changes in macrophage numbers or levels of other inflammatory cytokines. We next tested whether *TNFα* deficiency in macrophages can contribute to increased activation and fusion of muscle cells. Conditioned media were collected from bone marrow-derived macrophage (BMDM) cultures from adult wild-type and *TNFα*-null mice. Five days after induction of differentiation, C2C12 cells were treated with the conditioned media for 24 hours. Muscle cell fusion was then quantified by counting the number of nuclei per myofiber. C2C12 cells receiving conditioned media from BMDM isolated from *TNFα*-null mice had more nuclei per fiber than cultures receiving media conditioned by wild-type BMDMs (Figure 23J). These results indicate that macrophage-derived TNFα significantly influences muscle cell fusion.

Transplantation of wild-type bone marrow cells into TNFα-null mice reduced myonuclei numbers and increased sarcopenia

Because macrophages from *TNFα*-null mice increased myoblast activation and fusion, we tested whether TNFα secreted by macrophages is important in muscle aging by cross-genotype bone marrow transplantation (Figure 24A). Results of qPCR analysis and immunofluorescence proved that *TNFα*-null mice that received wild-type BMCs had significantly elevated expression of TNFα in skeletal muscle (Figures 24B, C). Transplantation of wild-type BMCs into *TNFα*-null mice did not affect mRNA expression of pro- and anti-inflammatory cytokines or macrophage-related genes (Figure 24D).

Twenty-month old TNFα-null mice that received transplantation of wild-type BMCs showed a partial restoration of sarcopenia; although *TNFα* ablation caused 49% larger CSA of quadriceps muscle fibers in 20-month-old mice compared to wild-type mice, transplantation of TNFα expressing BMCs into *TNFα*-null recipients produced fiber CSAs that were only 33% larger than controls (Figure 24E). However, the decrease of sMHC+ fiber percentage in soleus muscle induced by *TNFα* deficiency is not prevented by transplantation of wild-type bone marrow (Figure 24F). In addition, transplantation of wild-type bone marrow into old *TNFα*-null mice reduced the number of centrally-nucleated fibers compared to old, non-transplanted, *TNFα*-null mice (Figure 24G). Intriguingly, we also found that transplantation of wild-type BMCs into old *TNFα*-null mice prevented the reduction of satellite cell numbers observed in

non-transplanted, old *TNFα*-null mice compared to old wild-type mice (Figure 24H). In summary, these results suggested that BMCs from wild-type mice maintained satellite cell numbers and reduced muscle cell fusion while increasing sarcopenia.

5.4 Discussion

In the present study, we demonstrated that TNFα is an important factor driving sarcopenia and regulating satellite cell numbers. Our finding that the systemic ablation of *TNFα* resulted in a significant increase in numbers of central nuclei in aging muscle fibers is particularly intriguing. As adult skeletal muscle is a fully-differentiated tissue with little turnover of nuclei, central nucleation of muscle fibers is usually reported only in injured or diseased muscles, in which central nucleation is widely accepted as a marker of regeneration (Charge & Rudnicki 2004). The observation that over 30% of myofibers in the non-injured quadriceps muscle of TNFα-null mice contained centrally-localized nuclei (Figure 21D) suggested that TNFα-null satellite cells undergo spontaneous activation and fusion to existing myofibers without exogenous stimuli such as muscle injury. A similar phenotype has been reported in pregnancy-associated plasma protein-A (PAPP-A) transgenic mice in which muscle fiber size and central nucleation is elevated in non-injured muscle compared to wild-type mice at 12 months of age (Deb *et al.* 2012). However, the increase of muscle cell fusion and muscle fiber central nucleation in aging muscles without injury has not been reported or investigated.

Many previous studies have investigated the involvement of TNFα in cachexia and muscle wasting caused by other disease models (Guttridge *et al.* 2000; Lin *et al.* 2005; Patel & Patel 2017). The most well-established mechanism through which TNFα affects muscle wasting is through its catabolic role in regulating muscle protein content. TNFα treatment of differentiated

myotubes causes reductions in protein content and stimulate total ubiquitin conjugation though NFκB signaling activation (Li *et al.* 1998). TNFα also induces the ubiquitin-proteasome system in cachexia, which can be attenuated by blocking the activation of NFκB signaling (Reid & Li 2001; Patel & Patel 2017). TNFα can also decrease muscle protein content by inhibiting protein synthesis through the induction of IL-6 and/or inhibition of insulin-like growth factor-I signaling (Frost *et al.* 1997; Alvarez *et al.* 2002). Increased TNFα levels can induce apoptosis in disease models and during muscle aging through the increase of cell death inducing receptor, Fas (CD95), and the interaction of the TNFα-receptor complex and the Fas-associated protein with death domain (FADD) (Li *et al.* 1998; Lees *et al.* 2009). Although TNFα can affect sarcopenia by regulating protein balance and muscle cell apoptosis, our current investigation reveals a novel mechanism through which TNFα regulates satellite cell function and muscle cell fusion during aging. Our data show that genetic ablation of TNFα increased the number of muscle fiber nuclei and helped sustain fiber size during aging.

One, debated, regulatory mechanism through which the high frequency of muscle cell fusion to muscle fibers can contribute to muscle hypertrophy is known as the "myonuclear domain" hypothesis (Van der Meer *et al.* 2011). This theory indicates that a single myonucleus controls the translational and transcriptional regulation of protein synthesis for a limited cell volume or cytosolic space known as the myonuclear domain. Hence, any increases beyond the existing domain threshold would necessitate the incorporation of new myonuclei from satellite cell proliferation and differentiation (Hawke 2005 ; Petrella *et al.* 2006). Although

more recent studies supported the idea that age-related myofiber atrophy was due more to the decrease of myonuclear domain size instead of the loss of myonuclei numbers (Van der Meer *et al.* 2011; Karlsen *et al.* 2015; Schwartz *et al.* 2016), it is still widely believed that increased myonuclei fusion facilitates muscle hypertrophy, especially when the myonuclear domain size exceeds a certain threshold (Van der Meer *et al.* 2011; Jo *et al.* 2012). Our findings in the current study support the possibility that ablation of TNFα contributes to increased myofiber size in aging muscle by causing an increased frequency of muscle cell fusion with aging muscle fibers.

We were also interested to observe a 45% decrease in the number of Pax7+ satellite cells in 20-month-old TNFα-null mice compared to age-matched wild-type mice (Figure 21B), which is consistent with the interpretation that more satellite cells had broken quiescence to differentiate and fuse with existing myofibers. Although the age-related decline in satellite cell number has been proven to contribute to the loss of regenerative capacity of injured, aging muscle (Brack *et al.* 2005; Chakkalakal *et al.* 2012), whether satellite cell loss contributes to the reduced homeostatic maintenance and progressive reduction in muscle mass in uninjured, aging muscle is questionable. For example, ablating Pax7+ satellite cells did not induce sarcopenia in sedentary mice (Fry *et al.* 2015). The observation in our present study showed that the reduction in satellite cell numbers in TNFα-null mice is accompanied by a reduction in sarcopenia supports the view that depletions of satellite cells are not sufficient to drive sarcopenia in non-injured aging muscle.

Although the mechanisms through which TNFα ablation contribute to loss of satellite cell numbers and maintenance of muscle fiber size during aging is unknown, we hypothesize that the bimodal role of TNFα in regulating myogenesis may underlie these effects. Previous studies indicated that TNFα promotes myoblast proliferation at early stages of myogenesis while repressing myoblast differentiation (Guttridge *et al.* 2000; Langen *et al.* 2001; Li 2003; Chen *et al.* 2007). Administration of recombinant TNFα to rat primary myoblast cultures over a 24-hour period increased total DNA content and the number of primary myoblasts incorporating BrdU (Li 2003). In addition, recombinant TNFα also increased myoblast proliferation in C2C12 cultures (Alvarez *et al.* 2002; Otis *et al.* 2014). However, administration of recombinant TNFα to C2C12 cultures for 72-hours beginning immediately after induction of differentiation inhibited the formation of myotubes, decreased the total protein content per dish and decreased the expression of myogenin and fast-twitch isotype of myosin heavy chain (Langen *et al.* 2001). These TNFα-induced effects that increased proliferation and inhibited differentiation of muscle cells can be affected by both the concentration of TNFα and the duration of treatment. For example, C2C12 cultures treated with TNFα for 48-hours by incubation in differentiating media showed that TNFα stimulated myogenesis at 0.05 ng/ml while inhibited it at 0.5 and 5 ng/ml (Chen *et al.* 2007).

Previous investigations have suggested multiple molecular pathways through which TNFα can affect muscle cell proliferation and differentiation. For example, TNFα-induced myogenesis is dependent on activation of p38 signaling, and deficiency in TNFα-mediated p38 activation

causes impaired myogenesis and regeneration in adult muscle (Chen *et al.* 2007). TNFα can also interfere with the expression of muscle proteins in differentiating myoblasts by activating the binding of NF-κB to its targeted DNA sequence and stimulate degradation of the NF-κB inhibitory protein I-κBα (Li *et al.* 1998; Langen *et al.* 2001). Forced activation of NF-κB blocks myogenesis, whereas Introduction of a mutant form of I-κBα restored myogenic differentiation in myoblasts treated with TNFα (Langen *et al.* 2001). TNFα-induced NF-κB signaling also downregulates the expression of MyoD at a post-transcriptional level (Guttridge *et al.* 2000). Interestingly, aging of the muscle cells may affect their response to TNFα stimulation (Lees *et al.* 2009). Myogenic precursor cells isolated from 32-month-old rats exhibited greater NF-κB activation in response to 24 hours of TNFα treatment, compared to myogenic precursor cells isolated from 3-month-old rats (Lees *et al.* 2009). Our observation in the present study that genetic ablation of TNFα increases the number of muscle fiber nuclei and decreases Pax7+ satellite cell numbers in aging muscle is consistent with the previous studies showing that TNFα promotes muscle cell proliferation while suppresses their differentiation. Thus, TNFα ablation could have negative effect on myoblast proliferation throughout life, and may also promote muscle cell fusion with muscle fibers, leading to further depletion of satellite cell population (Figure 25).

Another intriguing finding in the present study is that we showed that TNFα secreted by both satellite cells and macrophages plays important roles in regulating myogenesis. An increased fusion index and ability to form myotubes *in vitro* was seen in both primary myoblast isolated from TNFα-null mice (Figure 22B) and C2C12 myoblast cells cultured with conditioned media

from BMDMs isolated from TNFα-null mice (Figure 23J). These data suggest that TNFα can regulate satellite cell function through both autocrine and paracrine regulation. Moreover, we showed that TNFα-null mice that received bone marrow transplantation of wild-type BMCs exhibited smaller muscle fiber size at 20-months of age compared to TNFα-null mice without bone marrow transplantation (Figure 24E). Transplantation of wild-type BMCs into TNFα-null mice also restored the number of satellite cells in aging muscle and inhibited the hyper-fusion of muscle cells seen in non-transplanted TNFα-null mice (Figures 24G, H). These results indicated that macrophage-secreted TNFα contributes to muscle aging by regulating satellite cell function. However, transplantation of wild-type BMCs into TNFα-null mice was insufficient to restore the age-related changes in fiber type (Figure 24F), suggesting that TNFα derived from other cell types, like aging muscle cells, also contributes to muscle aging.

Our study indicates a novel strategy for reducing age-related changes in muscle, especially sarcopenia, through manipulating the immune system. Experimental or therapeutic m0dulation of TNFα levels, which play an important role in regulating satellite cell fusion in aging muscle, may provide a particularly useful target for reducing age-related changes in muscle. Future investigations are needed to fully elaborate the mechanism through which TNFα contributes to muscle aging and the translational potential of preventing sarcopenia through TNFα related therapies.

5.5 Materials and Methods

Mice

All experimental protocols involving the use of mice were conducted according to the National Institutes of Health Guide for the Care and Use of Laboratory Animals and were approved by the University of California, Los Angeles Institutional Animal Care and Use Committee. Wild-type mice (C57 BL/6) and *TNFα*-null mice were obtained from Jackson Laboratories (Bar Harbor, ME, USA) or from the National Institute on Aging mouse colony.

Dissection and muscle mass measurement

WT and *TNFα*-null mice were euthanized by inhalation of isoflurane. Body weights were measured immediately after euthanization to an accuracy of 0.1 g. The hind-limb muscles were dissected, and wet weight was determined to an accuracy of 1 mg. Muscles were then either frozen in liquid nitrogen or embedded in Optimal cutting temperature compound (OCT) and rapidly frozen in isopentane cooled in liquid nitrogen.

Cross-sectional area measurement

Frozen cross-sections were cut from the mid-belly of quadriceps femoris muscle at a thickness of 10 μm. Section was then stained with hematoxylin (Vector) for 10 min. The muscle fiber cross-sectional area was measured for 500 fibers randomly sampled from complete

cross-sections using a digital imaging system (Bioquant).

Muscle fiber central nuclei counting

Hematoxylin staining was performed on quadriceps muscle sections. Nuclei were stained blue by hematoxylin. The number of central nuclei was counted for each fiber for a total of 500 fibers that were randomly sampled throughout the entire cross-section.

Myonuclei counting

Frozen cross-sections were cut from the mid-belly of quadriceps or soleus muscle at a thickness of 10 μm. The frozen sections were air-dried for 30 minutes and fixed in ice-cold acetone for 10 minutes. Sections were then blocked in 3% bovine serum albumin (BSA) and 2% gelatin in 50 mM Tris buffer (pH 7.2) for 30 minutes and then immunolabeled with rabbit-anti-desmin antibody for 3 hours at room temperature. Sections were washed with phosphate buffered saline solution (PBS) and then stained with Dylight 400-anti-rabbit IgG (1/200; Vector) for 30 minutes, followed by PBS wash and staining with propidium iodide (1:10) for 10 minutes. Myonuclei were characterized as propidium iodide positive nuclei beneath within the anti-desmin-stained muscle fiber. The number of myonuclei were counted for each fiber for a total of 500 fibers that were randomly sampled throughout the entire cross-section.

sMHC and CD68 immunohistochemistry and counting

Frozen cross-sections were cut from the mid-belly of quadriceps or soleus muscle at a thickness of 10 μm. The frozen sections were air-dried for 30 minutes and fixed in ice-cold acetone for 10 minutes, and endogenous peroxidase activity was quenched with 0.3% H_2O_2. Sections were then blocked in 3% BSA and 2% gelatin in 50 mM Tris buffer (pH 7.2) for 1 hour and then immunolabeled with rabbit anti-slow myosin heavy chain (Abcam) or rat anti-CD68 (Serotec), for 3 hours at room temperature. Sections were washed with PBS and then probed with biotin-conjugated secondary antibodies (1/200; Vector) for 30 minutes. Sections were subsequently washed with PBS and then incubated for 30 minutes with avidin D-conjugated horseradish peroxidase (1/1000; Vector). Staining was visualized with the peroxidase substrate 3-amino-9-ethylcarbazole (AEC kit; Vector), yielding a red reaction product. For fiber type composition assay, images were taken from sMHC stained sections and merged to cover the complete cross-sections on which numbers of total fiber and sMHC+ fiber are counted. For macrophage number counting, CD68 positive cells were counted under the microscope. The volume of muscle tissue was determined by measuring the total volume of each section using a stereological, point-counting technique to determine section area and then multiplying that value by the section thickness (10 μm). The numbers of immunolabeled cells in each section were counted and expressed as the number of cells/unit volume of each section.

Pax7 antibody preparation and immunohistochemistry

Pax7 hybridoma cells were purchased from Developmental Studies Hybridoma Bank (Iowa City Iowa). Cells were cultured in complete medium consisting of Dulbecco's Modified Eagle Medium (DMEM) with 1% penicillin- streptomycin (Gibco) and 20% heat-inactivated fetal bovine serum (FBS). Conditioned medium was collected from the cultures and used for purification of antibodies to Pax7, as described previously (Wang *et al.* 2015). The Pax7 antibody was then used for immunohistochemistry staining of cross-sections from quadriceps muscles rapidly frozen in liquid nitrogen-cooled isopentane. Sections were then fixed in 2% paraformaldehyde for 10 minutes and then immersed in antigen retrieval buffer (10 mM sodium citrate, 0.05% Tween 20, pH 6.0) at 95 - 100^{o} C for 40 minutes. Endogenous peroxidase activity in the sectioned tissue was quenched by immersion in 0.3% H_2O_2. Sections were then treated with blocking buffer from a mouse-on-mouse immunohistochemistry kit (M.O.M kit; Vector) for 1 hour and immunolabeled with mouse anti-Pax7 antibody overnight at 4^{o} C. Sections were subsequently washed with PBS and then incubated with biotin-conjugated anti-mouse IgG for 30 minutes, followed by incubation for 30 minutes with ABC reagents from the M.O.M kit. Staining was visualized with the AEC kit (Vector). The number of satellite cells/sectioned muscle fiber was determined by counting the number of Pax7+ cells in mid-belly cross-sections of muscles and the total number of fibers per cross-section.

RNA isolation and quantitative PCR

Muscles were homogenized in Trizol (Invitrogen) and RNA extracted, isolated and DNase-treated using RNeasy spin columns according to the manufacturer's protocol (Qiagen). RNA was then electrophoresed on 1.2% agarose gels and RNA quality assessed by determining 28S and 18S ribosomal RNA integrity. Total RNA was reverse transcribed with Super Script Reverse Transcriptase II using oligo dTs to prime extension (Invitrogen) to produce cDNA. The cDNA was used to measure the expression of selected transcripts using SYBR green qPCR master mix according to the manufacturer's protocol (Bio-Rad). Real-time PCR was performed on an iCycler thermocycler system equipped with iQ5 optical system software (Bio-Rad). Reference genes were chose based following previously described methods (Wang *et al.* 2015). Based on that analysis, RSP4X and SRP14 were used as reference genes for QPCR experiments with quadriceps muscles. PPIA and TPT1 were used as reference genes for QPCR experiments using myoblasts or bone marrow derived macrophages. The normalization factor for each sample was calculated by geometric averaging of the Ct values of both reference genes using the geNorm software. Primers used for QPCR are listed in Supplemental Table 1.

Double-labeling for TNFα and CD68

Frozen, acetone-fixed sections of quadriceps muscles were treated with blocking buffer from M.O.M kit for 1 hour and then immunolabeled with a combination of mouse anti-TNFα (Santa Cruz) and rat anti-CD68 (Biorad) overnight at 4°C. Sections were washed with PBS and then

incubated with a combination of Dylight 488 anti-rat IgG and Dylight 594 anti-mouse IgG (1/100; Vector) for 30 minutes in the dark. Sections were then washed with PBS and cover-slipped with Prolong Gold anti-fade reagent with DAPI (Invitrogen).

Primary myoblast isolation and fusion assay

Primary myoblasts were isolated following a previously described protocol (Wehling-Henricks *et al.* 2016). Hindlimb and forelimb muscles from 12-month-old mice were removed and rinsed in Dulbecco's phosphate buffered saline (DPBS). Muscles were minced and digested in 2 ml enzyme buffer (2.4 U/ml dispase, type II (Invitrogen), 1% collagenase, type II (Invitrogen), 2.5 mM $CaCl_2$) per mg muscle for 45 minutes at 37˚C with gentle trituration each 15 minutes. The digestate was passed through 70 µm mesh filters and cells were pelleted at 350 x g for 5 minutes. Cells were resuspended in growth medium (Hams F10 (Sigma), 20% FBS (Omega), 2.5 ng/ml bFGF (Sigma), 200 U/ml penicillin and 200 µg/ml streptomycin (Life Technologies)) and pre-plated for 1 hour to remove fibroblasts. Enriched myoblasts were plated on culture dishes coated with 0.01% collagen, type I (Life Technologies) and 2% gelatin and maintained at 37˚C in 5% CO_2 with medium changes every 3 days. Myoblasts were passed once before seeding for fusion assay.

Myoblasts were seeded at 1 x 10^6 cells/well on 6-well plate with sterile glass coverslips coated as stated above in growth medium. On day 3 of culture, cells were cultured in Hams F10 media without FBS overnight and then cultured in differentiation medium (Hams F10 (Sigma), 2%

horse serum (Omega), 2.5 ng/ml basic fibroblast growth factor (bFGF; Sigma), 200 U/ml penicillin and 200 µg/ml streptomycin (Life Technologies)) for 6 days, with medium changes every alternate day. Coverslips were then collected and stained with rabbit-anti-desmin (Sigma) with hematoxylin counterstain, using immunohistochemistry protocols described above. For fusion index quantification, the number of myonuclei per myofiber was counted for 500 myofibers randomly sampled throughout the section.

A separate set of cells was seeded on coated coverslips for the imaging of myofibers. Instead of differentiation medium, these cells were returned to growth medium after overnight serum starvation. Immunofluorescence staining was performed on these coverslips using rabbit-anti-desmin and Dylight 488 anti-rabbit IgG. Images were taken with Bioquant software using the BH2 microscope.

C2C12 fusion assay with conditioned media from bone marrow-derived macrophages

Bone marrow cells (BMCs) were isolated following previously described protocol (Wang *et al.* 2015). BMCs were aseptically flushed from femurs and tibias with DPBS (Sigma) and treated with ACK lysing buffer (Gibco, Waltham, MA) to clear red blood cells. Following a DPBS wash and filtration through a 70-µm filter, BMCs were seeded at 5 x 10^6 per 6-cm dish in RPMI-1640 (Sigma) with 20% heat-inactivated fetal bovine serum (FBS; Omega Scientific, Tarzana, CA), penicillin (100 U/ml; Gibco), streptomycin (100 µg/ml; Gibco) and 10 ng/ml macrophage colony stimulating factor (MCSF; R&D, Minneapolis, MN) at 37˚C with 5% CO_2 for 6 days. BMDMs were

then stimulated for 24-hours with activation media consisting of DMEM with 0.25% heat-inactivated FBS, penicillin, streptomycin and 10 ng/ml MCSF. Conditioned media were collected following activation and spun at 500xg for 5 minutes to remove floating cells and then frozen at -20 ºC.

C2C12 cells were obtained from American Type Culture Collection (ATCC). C2C12 cells were seeded at 6 x 10^5 cells/well on 6-well plate with sterile glass coverslips coated as stated above in DMEM with 10% FBS. Sixteen hours after seeding, seeding medium was removed from culture and cells were washed with DPBS before adding 2 ml/well of BMDM conditioned media. Two days after culture in conditioned media, cells were starved with DMEM only overnight followed by culture in BMDM conditioned media for 5 days, with media changes every 36 hours. Coverslips were then collected and proceed to desmin staining and fusion index quantification as stated above.

Bone marrow transplantation and chimerism assay

BMCs from 2-month-old or 18-month-old wild-type mice were collected as stated above. Recipient *TNFα*-null mice were subjected to myeloablative irradiation prior to bone marrow transplantation. 1 x 10^7 BMCs were transplanted through tail vein injection following the protocol described previously (Wang *et al.* 2015). Survival of irradiated and transplanted mice is greater than 70% at 20 months of age. Eight months following bone marrow transplantation, muscles and blood were collected from recipient mice. Engraftment of transplanted cells was assessed

by fluorescent *in situ* hybridization for X and Y chromosome markers (Kreatech, Leica Labs, Buffalo Grove, IL, USA) in leukocytes isolated from blood collected from each mouse. Isolated leukocytes were adhered to microscope slides, and XY immunolabeled cells and XX immunolabeled cells on each slide were counted. Chimerism was expressed as the number of XX cells/total cell number for each mouse. The percentage of donor derived-cells was greater than 80% for all the animals used in the current investigation.

Data are presented as mean ± sem. One-way analysis of variance was used to test whether differences between 3 or more groups were significant at $p < 0.05$. Significant differences between groups were identified using Tukey's Post Hoc test. Comparisons of two groups of values were analyzed using the unpaired, two-tailed t test.

Figures

Figure 19.

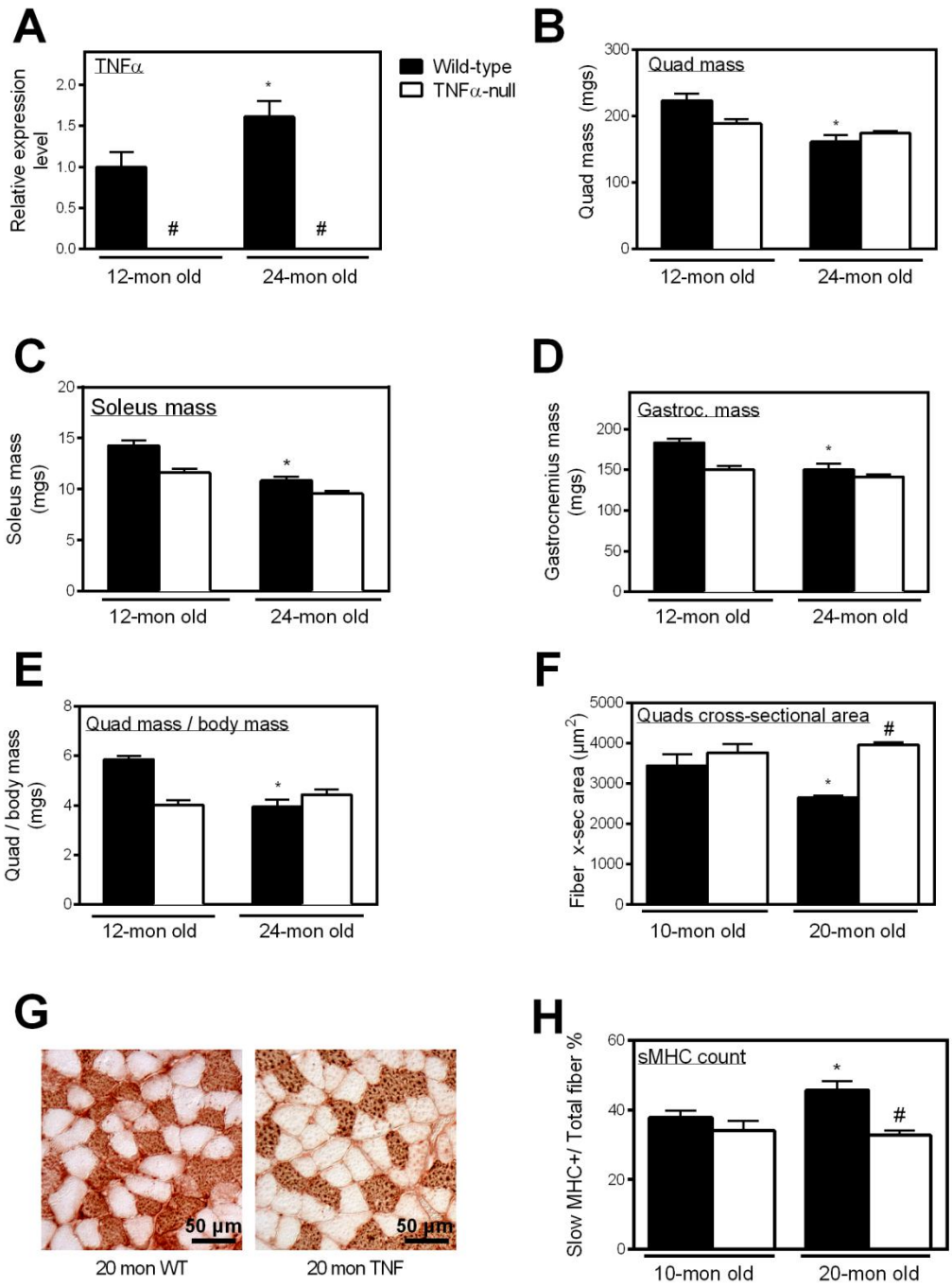

Figure 20.

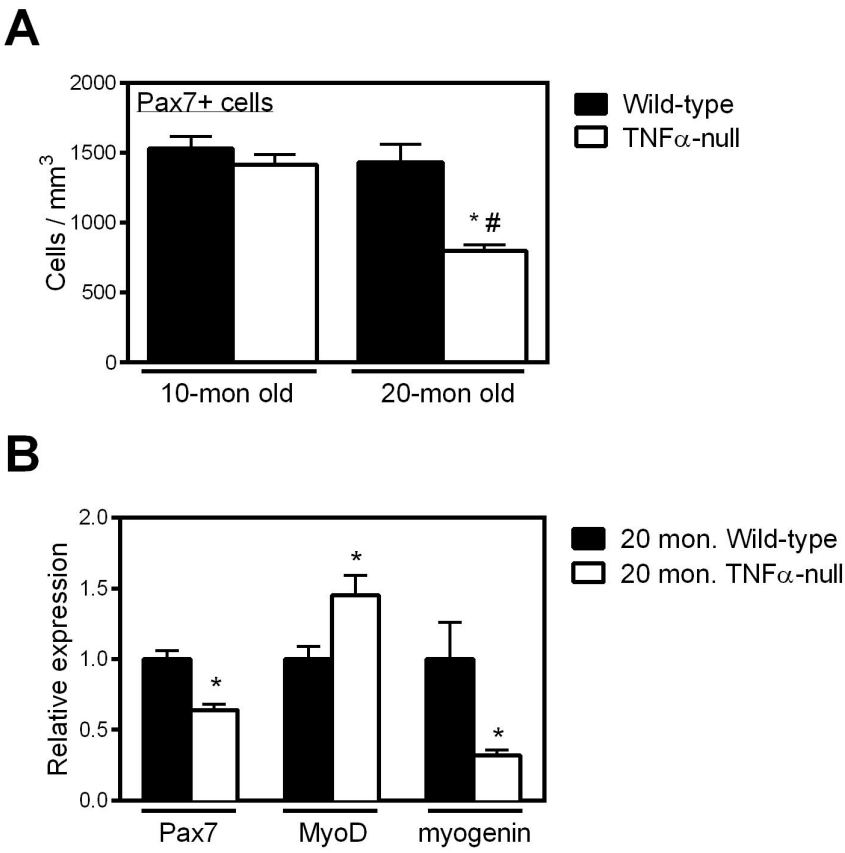
A
Pax7+ cells
Cells / mm3
2000
1500
1000
500
0
*#
10-mon old
20-mon old
Wild-type
TNFα-null
B
Relative expression
2.0
1.5
1.0
0.5
0.0
*
*
*
Pax7
MyoD
myogenin
20 mon. Wild-type
20 mon. TNFα-null

Figure 21.

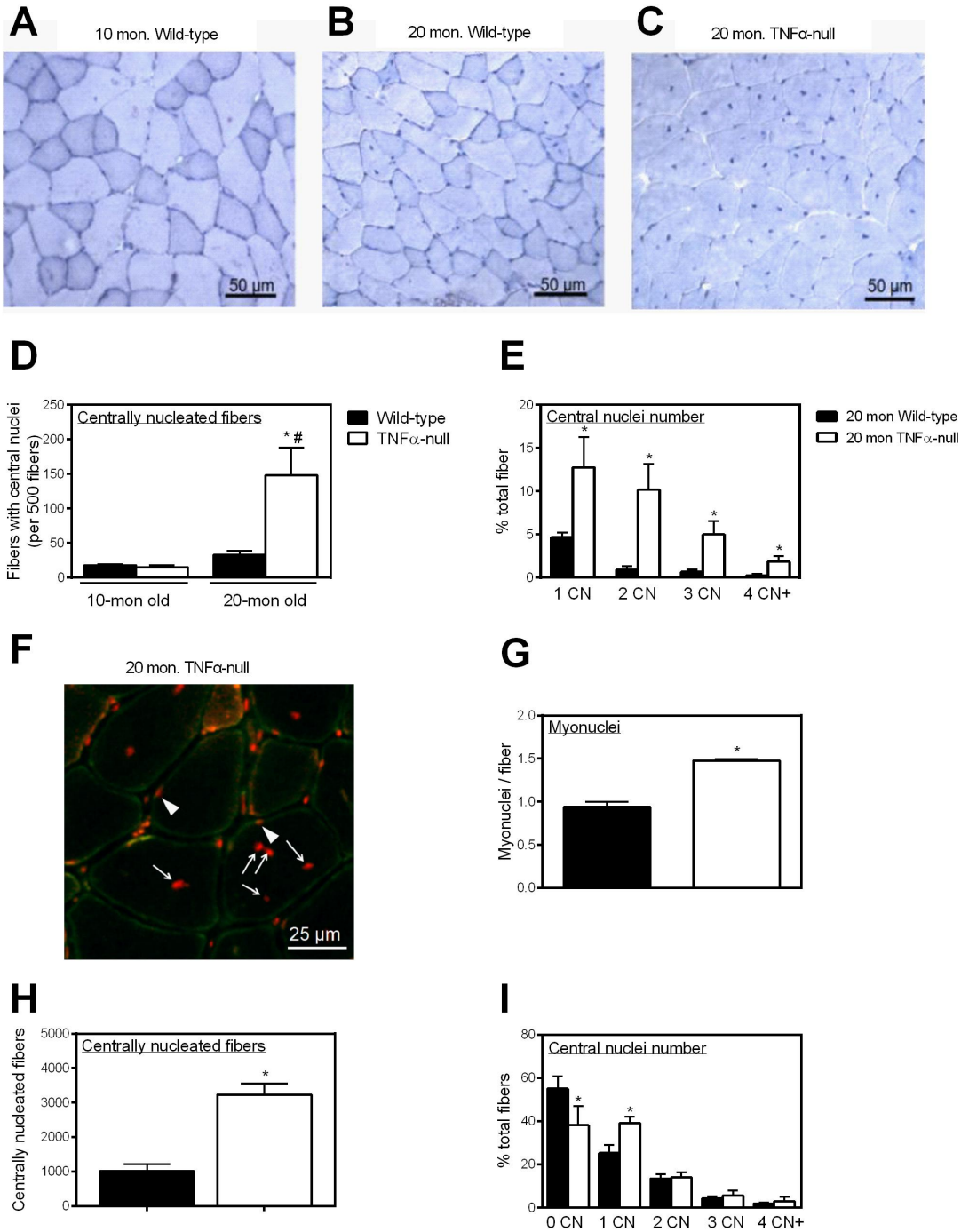
A
10 mon. Wild-type
50 µm
B
20 mon. Wild-type
50 µm
C
20 mon. TNFα-null
50 µm
D
Centrally nucleated fibers
Fibers with central nuclei (per 500 fibers)
250
200
150
100
50
0
*#
Wild-type
TNFα-null
10-mon old
20-mon old
E
Central nuclei number
% total fiber
20
15
10
5
0
*
20 mon Wild-type
20 mon TNFα-null
1 CN
2 CN
3 CN
4 CN+
F
20 mon. TNFα-null
25 µm
G
Myonuclei
Myonuclei / fiber
2.0
1.5
1.0
0.5
0.0
*
H
Centrally nucleated fibers
Centrally nucleated fibers
5000
4000
3000
2000
1000
0
*
I
Central nuclei number
% total fibers
80
60
40
20
0
*
0 CN
1 CN
2 CN
3 CN
4 CN+

Figure 22.

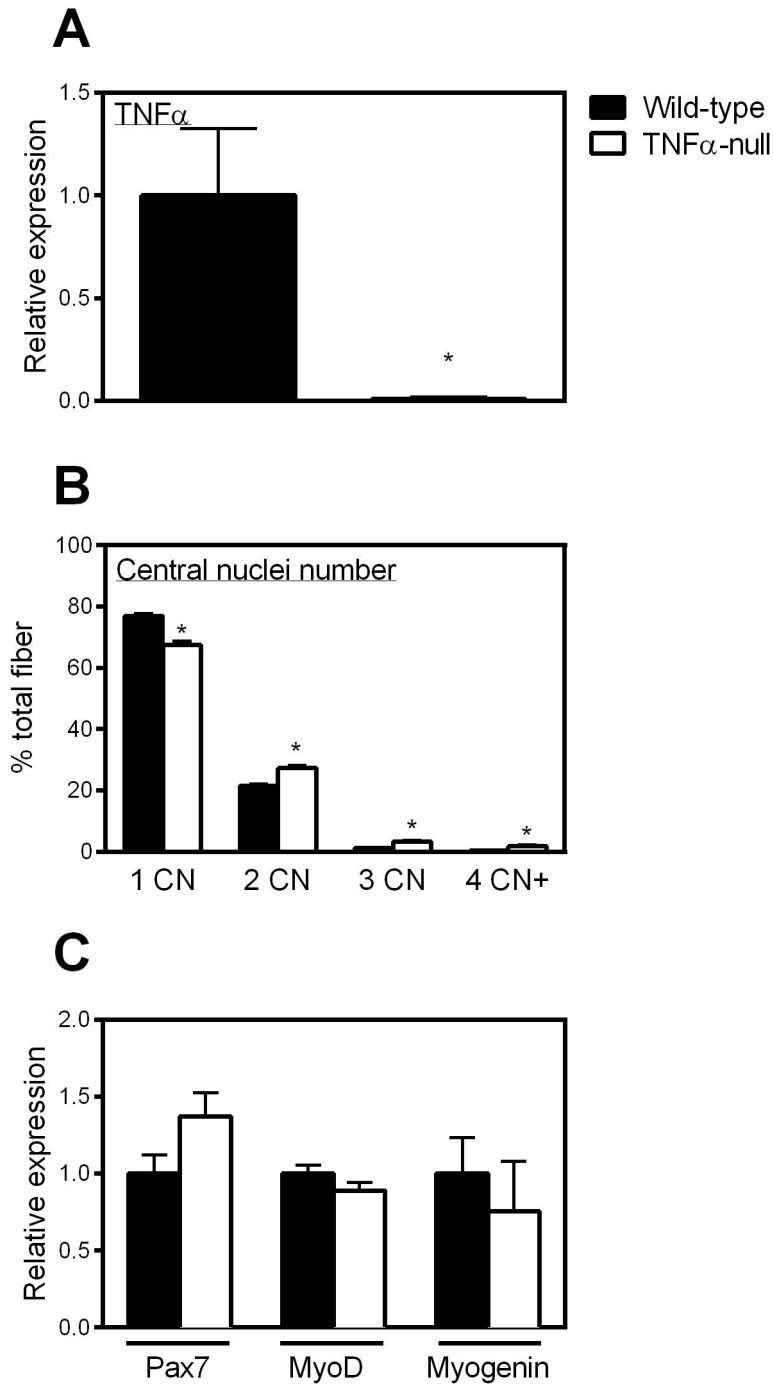
A
TNFα
Relative expression
1.5
1.0
0.5
0.0
*
Wild-type
TNFα-null
B
Central nuclei number
% total fiber
100
80
60
40
20
0
*
*
*
*
1 CN
2 CN
3 CN
4 CN+
C
Relative expression
2.0
1.5
1.0
0.5
0.0
Pax7
MyoD
Myogenin

Figure 23.

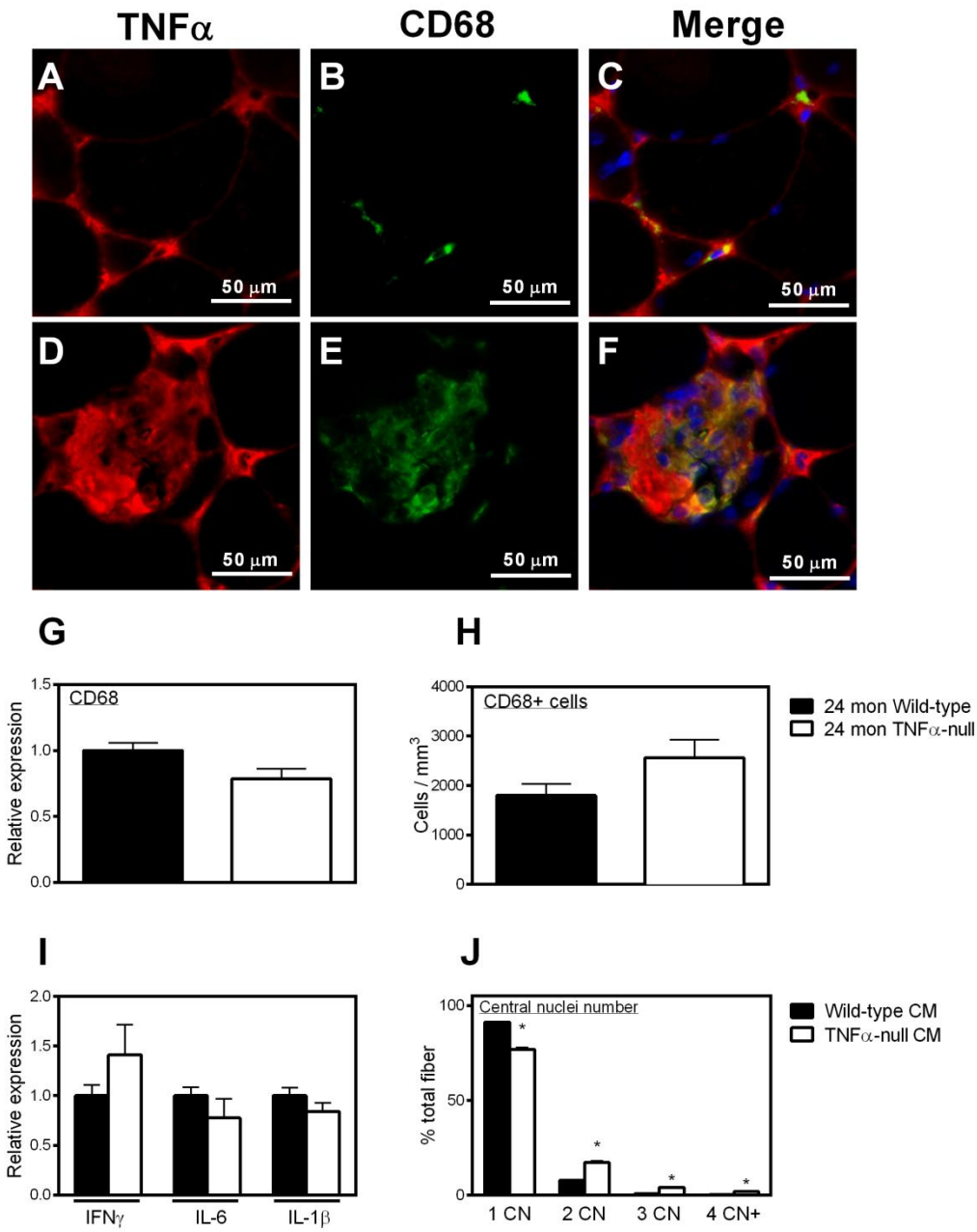
TNFα
CD68
Merge
A
B
C
D
E
F
50 μm
G
CD68
Relative expression
1.5
1.0
0.5
0.0
H
CD68+ cells
Cells / mm3
4000
3000
2000
1000
0
24 mon Wild-type
24 mon TNFα-null
I
Relative expression
2.0
1.5
1.0
0.5
0.0
IFNγ
IL-6
IL-1β
J
Central nuclei number
% total fiber
100
50
0
1 CN
2 CN
3 CN
4 CN+
Wild-type CM
TNFα-null CM

Figure 24.

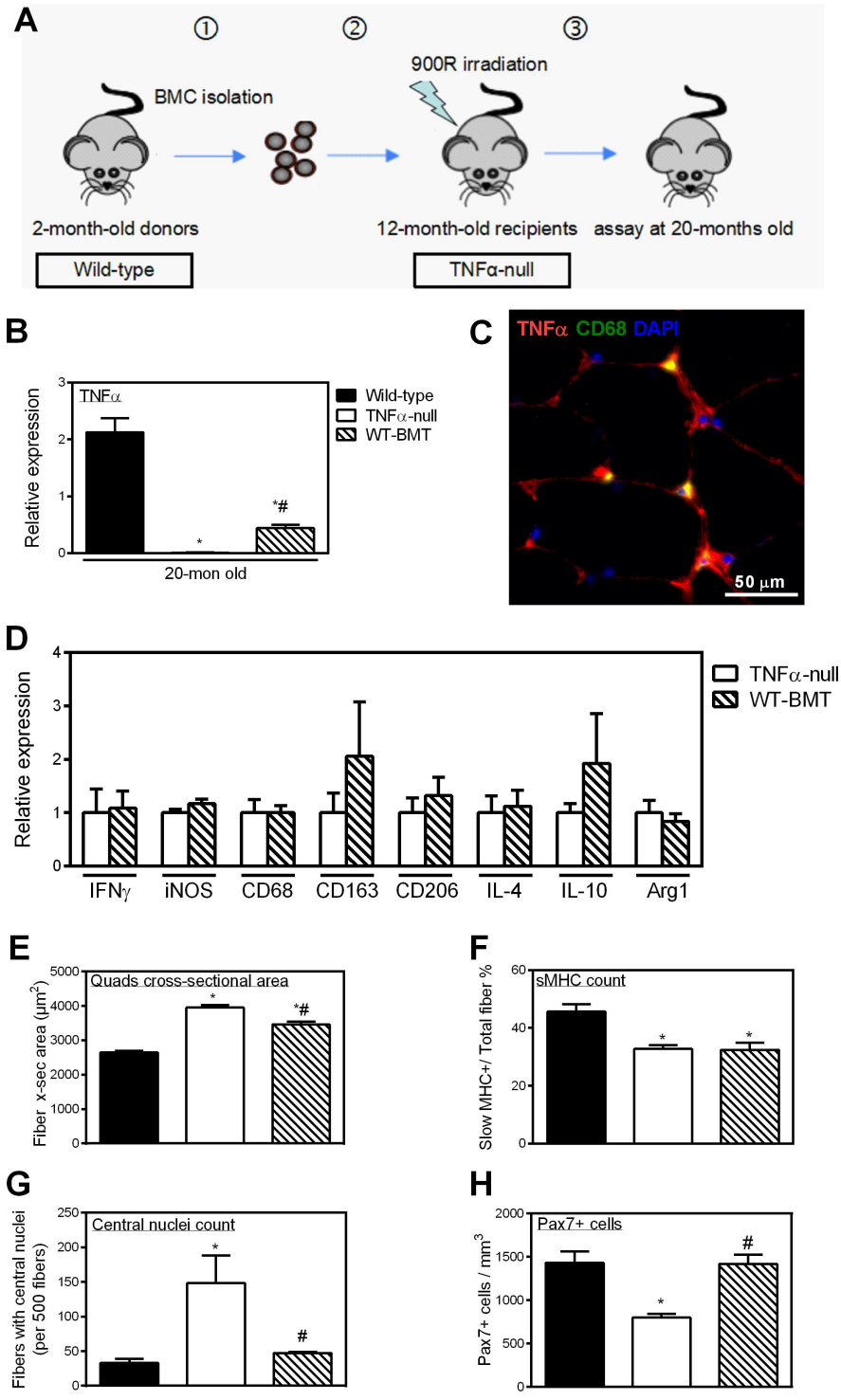
A
①
②
③
900R irradiation
BMC isolation
2-month-old donors
12-month-old recipients
assay at 20-months old
Wild-type
TNFα-null
B
TNFα
Relative expression
Wild-type
TNFα-null
WT-BMT
20-mon old
C
TNFα CD68 DAPI
50 μm
D
Relative expression
TNFα-null
WT-BMT
IFNγ
iNOS
CD68
CD163
CD206
IL-4
IL-10
Arg1
E
Quads cross-sectional area
Fiber x-sec area (μm²)
F
sMHC count
Slow MHC+/ Total fiber %
G
Central nuclei count
Fibers with central nuclei (per 500 fibers)
H
Pax7+ cells
Pax7+ cells / mm³

Figure 25.

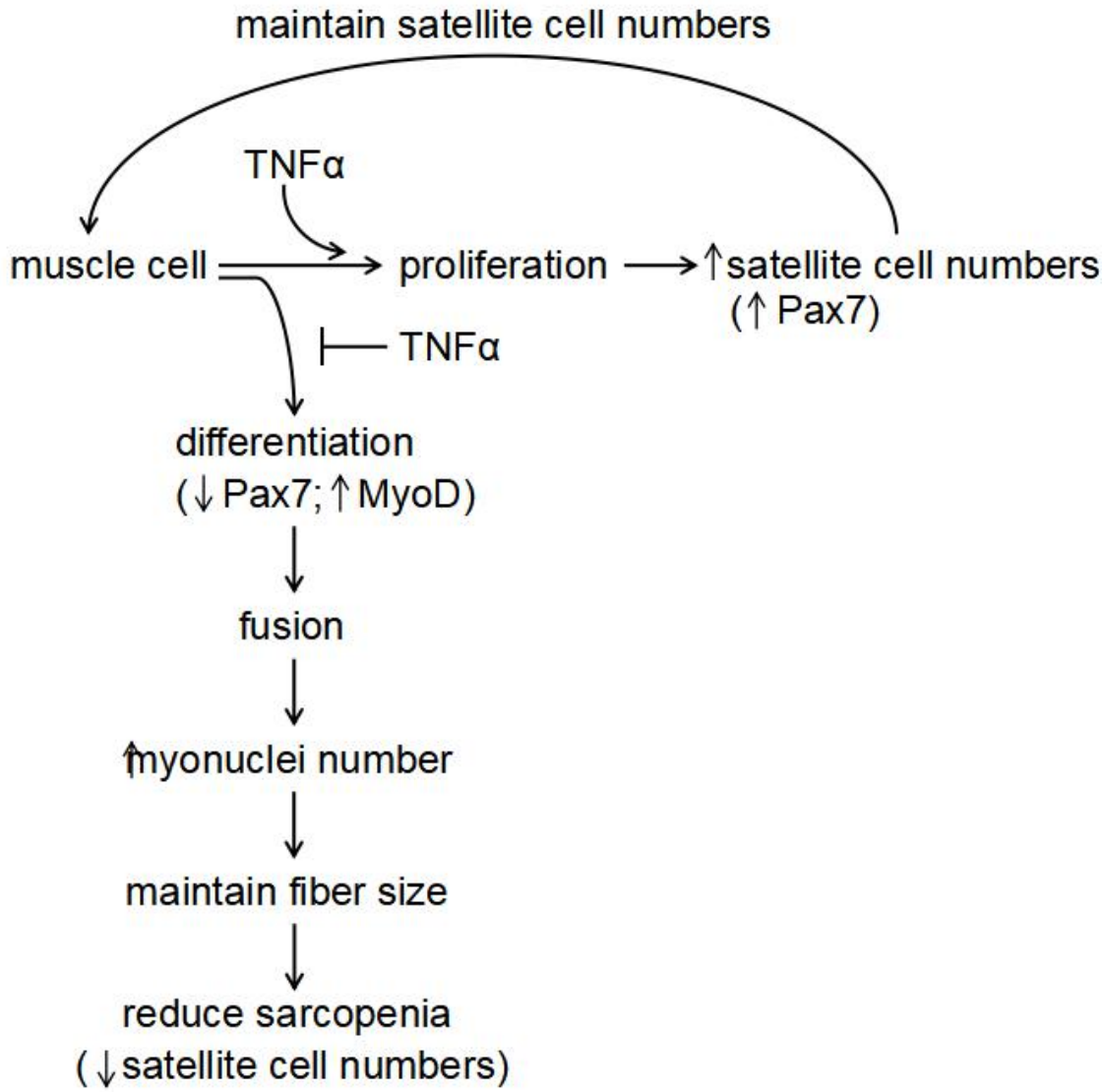
maintain satellite cell numbers
TNFα
muscle cell
proliferation
↑satellite cell numbers
(↑ Pax7)
TNFα
differentiation
(↓Pax7; ↑MyoD)
fusion
↑myonuclei number
maintain fiber size
reduce sarcopenia
(↓satellite cell numbers)

Figure legends

Figure 19. Genetic ablation of *TNFα* prevents sarcopenia and age-related change in muscle fiber type composition. A. QPCR analysis of *TNFα* expression in 12- and 24-month-old, wild-type quadriceps muscles showed a significant increase of *TNFα* with aging. Values normalized to 12-month-old wild-type mice. *TNFα* expression was not detectable in 12- or 24-month-old *TNFα*-null mice. N = 5 per data set. B - D. *TNFα* deficiency prevented the age-related decrease in muscle mass of: (B) quadriceps muscles; (C) soleus muscles; (D) gastrocnemius muscles. (E) Quadriceps muscle mass normalized to body mass significantly reduced from 12-month-old to 24-month-old in wild-type mice, but not in *TNFα*-null mice. F. *TNFα* knockout prevented the decrease in fiber cross-sectional area of the quadriceps muscles seen in wild-type mice from 10- to 20-month-old. G. Representative cross sections of soleus muscles of 20-month-old, wild-type and *TNFα*-null mice labeled with antibody to slow myosin heavy chain (sMHC). Bar = 50 μm. (H) The percentage of sMHC+ fibers/ total fibers in soleus muscles decreased from 12-month-old to 24-month-old in wild-type mice, but not in *TNFα*-null mice. For all panels, * indicates significant difference from young, genotype-matched muscles at $P < 0.05$. # indicates significant difference from age-matched, wild-type muscles at $P < 0.05$. N = 5 per data set.

Figure 20. *TNFα* knockout promotes satellite cell activation in aging muscle *in vivo*. A. Stereological counts for Pax7+ cells showed that aging did not affect satellite cell numbers in wild-type mice between 10- and 20-months. *TNFα* deficiency caused a significant decrease in

satellite cell numbers at 20-months of age but not at 10-months. * indicates significant difference from 10-month-old, genotype-matched muscles at $P < 0.05$. # indicates significant difference from age-matched, wild-type muscles at $P < 0.05$. N = 5 per data set. B. QPCR analysis of 20-month-old muscles in wild-type and *TNFα*-null mice showed that *TNFα* deficiency caused a decrease in *Pax7* and *myogenin* and an increase in *MyoD*. Values normalized to 20-month-old wild-type mice. * indicates significant difference at $P < 0.05$. N = 5 per data set.

Figure 21. TNFα deficient mice have more central nuclei in aging muscle and regenerative muscle. A - C. Representative images of cross sections of quadriceps muscles from 10-month-old, wild-type mice (A), 20-month-old, wild-type mice (B) or 20-month-old, TNFα-null mice (C) after hematoxylin staining, showing an increased number of centrally-nucleated fibers and fibers with multiple central nuclei in old *TNFα*-null mice. Bars = 50 μm. D. Old, *TNFα*-null muscles have significantly more centrally-nucleated fibers. * indicates significant difference from 10-month-old, genotype-matched muscles at $P < 0.05$. # indicates significant difference from age-matched, wild-type muscles at $P < 0.05$. N = 5 per data set. E. Quantification of central nuclei numbers in each fiber showed that old *TNFα*-null mice have a higher percentage of fibers in each category. Bars in the column labeled “1 CN” indicate the proportion of muscle fibers with 1 central nuclei in total fibers measured. Bars in the column labeled “2 CN” indicate the proportion of muscle fibers with 2 central nuclei in total fibers measured, and so forth. * indicates significant difference from wild-type muscle fibers with the same number of central nuclei at $P < 0.05$. N = 5 per data set. F. Immunofluorescence labeling for desmin (green) with propidium

iodide staining (red). Arrow head: Myonuclei on the peripheral of a muscles fiber; Arrow: Myonuclei inside a muscles fiber (central nuclei). G. Quantification of total myonuclei in each fiber showed that old *TNFα*-null mice have more myonuclei per fiber compared to age-matched wild-type mice. * indicates significant difference at $p < 0.05$. H. *TNFα* ablation increased the number of centrally nucleated fiber at 21 days after acute injury. N = 5 per data set. * indicates significant difference at $p < 0.05$. I. Total fiber numbers within the injury site was counted in wild-type and *TNFα*-null muscles at 21 days after injury. Muscle fibers with 0, 1, 2, 3, and 4 or more central nuclei were quantified and expressed as proportion in total injure site fibers. * indicates significant difference from wild-type muscle fibers with the same number of central nuclei at $P < 0.05$. N = 5 per data set.

Figure 22. TNFα knockout promoted myoblast fusion *in vitro.* A. QPCR analysis proved that primary myoblasts isolated from *TNFα*-null mice have no detectable *TNFα* expression. * indicates significant difference from wild-type myoblasts at $P < 0.05$. N = 6 per data set. B. Quantification of myotube nuclei numbers showed that *TNFα*-null myotubes have more nuclei compared to wild-type. * indicates significant difference from wild-type myotubes with the same number of nuclei at $P < 0.05$. Results are from 3 independent experiments. N = 6 per data set. C. QPCR analysis of primary myoblasts isolated from wild-type and TNFα-null mice showed no difference in *Pax7, MyoD* and *myogenin* expression. Values normalized to myoblast isolated from wild-type mice. N = 5 per data set.

Figure 23. TNFα secreted by macrophages affects the fusion capacity of muscle cells *in vitro*. A - F. Immunofluorescence, double-labeling for TNFα and CD68. Cross sections of 20-month-old wild-type quadriceps muscle labeled with anti-TNFα (red; panel A, D) and anti-CD68 (green; panel B, E) and the merged images (yellow; panel C, F) showed that CD68+ cells expressed TNFα. G. QPCR analysis showed no difference in *CD68* mRNA expression between 24-month-old wild-type and TNFα-null quadriceps muscles. N = 5 per data set. H. Stereological counts for CD68+ cells showed that *TNFα* ablation did not affect macrophage numbers in aging muscle. N = 5 per data set. I. QPCR analysis showed that *TNFα* ablation did not affect the expression of inflammatory cytokines IFNγ, IL-6 and IL-1β. J. Quantification of nuclei numbers per myotube showed that C2C12 cells receiving conditioned media from *TNFα*-null BMDM had increased number of nuclei. Wild-type CM: media conditioned by wild-type BMDMs. *TNFα*-null CM: media conditioned by *TNFα*-null BMDMs. * indicates significant difference from wild-type myofibers with the same number of nuclei at $P < 0.05$. N = 6 per data set.

Figure 24. Effects of transplantation of wild-type bone marrow cells into *TNFα*-null mice on myonuclei numbers and muscle aging. A. Schematic of experimental design for bone marrow transplantation experiments. B. QPCR analysis of *TNFα* expression in quadriceps muscle from 20-month-old wild-type mice, *TNFα*-null mice and *TNFα*-null mice receiving BMC transplantation. Transplantation of wild-type BMCs induced *TNFα* expression in *TNFα*-null mice. Values normalized to 20-month-old wild-type mice. C. Cross sections of quadriceps muscle of 20-month-old *TNFα*-null mice that received transplantation of wild-type BMCs when the

recipients were 12-months of age. Section was labeled with anti-TNFα (red) and anti-CD68 (green) antibody showed that transplantation recipients had detectable expression of TNFα at the muscle fiber surface (red) and within macrophages (yellow). D. QPCR analysis of pro-inflammatory cytokine *IFNγ*, anti-inflammatory cytokines *IL-4* and *IL-10*, M1 macrophage-related genes *iNOS* and *CD68*, M2 macrophage-related genes *CD163, CD206* and *Arg1*. These data showed that transplantation of wild-type BMCs into *TNFα*-null did not affect expressions of cytokines and macrophage-related genes compared to non-transplanted, *TNFα*-null mice. E. Increased muscle fiber CSA in 20-month-old *TNFα*-null compared to age-matched, wild-type mice was significantly reduced by transplantation of wild-type BMCs. F. 20-month-old *TNFα*-null mice had lower percentage of sMHC+ muscle fibers in soleus muscles compared to 20-month-old wild-type mice and the decrease is not rescued by transplantation of BMCs from wild-type mice. G. Centrally-nucleated fibers increased in number significantly in 20-month-old *TNFα*-null mice compared to wild-type mice, but the increase did not occur in 20-month-old *TNFα*-null mice that had received transplantation of wild-type BMCs when the recipients were 12-months of age. H. Anti-Pax7 immunohistochemistry showed that satellite cell number decreased significantly in 20-month-old *TNFα*-null mice compared to wild-type mice. The increase is ablated by transplantation of wild-type BMCs. For all panels, * indicates significant difference from 20-month-old wild-type muscles at $P < 0.05$. # indicates significant difference from 20-month-old *TNFα*-null muscles at $P < 0.05$. N = 5 per data set.

Figure 25. Summary diagram that illustrates potential mechanisms through which *TNFα* can

influence sarcopenia and satellite cell numbers in aging muscle. *TNFα* increases muscle cell proliferation and inhibits its differentiation. Genetic ablation of *TNFα* shifts the muscle cells towards more prevalent differentiation and fusion with muscle fibers. The increase of myonuclei numbers caused by *TNFα* ablation contributes to maintaining muscle fiber size during aging and reducing sarcopenia. The decrease of satellite cell proliferation and increase of muscle cell fusion also decreased satellite cell numbers in aging muscle of *TNFα*-null mice.

References

Alvarez B, Quinn LS, Busquets Sl, Quiles MT, López-Soriano FJ, Argilés JM (2002). Tumor necrosis factor-α exerts interleukin-6-dependent and-independent effects on cultured skeletal muscle cells. *Biochimica et Biophysica Acta (BBA)-Molecular Cell Research*. **1542**, 66-72.

Bernet JD, Doles JD, Hall JK, Tanaka KK, Carter TA, Olwin BB (2014). p38 MAPK signaling underlies a cell-autonomous loss of stem cell self-renewal in skeletal muscle of aged mice. *Nature Medicine*. **20**, 265-271.

Brack AS, Bildsoe H, Hughes SM (2005). Evidence that satellite cell decrement contributes to preferential decline in nuclear number from large fibres during murine age-related muscle atrophy. *Journal of Cell Science*. **118**, 4813-4821.

Brack AS, Rando TA (2007). Intrinsic changes and extrinsic influences of myogenic stem cell function during aging. *Stem Cell Reviews*. **3**, 226-237.

Carlson B, Faulkner J (1989). Muscle transplantation between young and old rats: age of host determines recovery. *American Journal of Physiology-Cell Physiology*. **256**, C1262-C1266.

Chakkalakal JV, Jones KM, Basson MA, Brack AS (2012). The aged niche disrupts muscle stem cell quiescence. *Nature*. **490**, 355-360.

Charge SB, Rudnicki MA (2004). Cellular and molecular regulation of muscle regeneration. *Physiological Reviews*. **84**, 209-238.

Chen S-E, Jin B, Li Y-P (2007). TNF-α regulates myogenesis and muscle regeneration by activating p38 MAPK. *American Journal of Physiology-Cell Physiology*. **292**, C1660-C1671.

Cheng M, Nguyen M-H, Fantuzzi G, Koh TJ (2008). Endogenous interferon-γ is required for efficient skeletal muscle regeneration. *American Journal of Physiology-Cell Physiology*. **294**, C1183-C1191.

Ciciliot S, Rossi AC, Dyar KA, Blaauw B, Schiaffino S (2013). Muscle type and fiber type specificity in muscle wasting. *The International Journal of Biochemistry & Cell Biology*. **45**, 2191-2199.

Coletti D, Moresi V, Adamo S, Molinaro M, Sassoon D (2005). Tumor necrosis factor‐α gene transfer induces cachexia and inhibits muscle regeneration. *Genesis*. **43**, 120-128.

Conboy IM, Conboy MJ, Smythe GM, Rando TA (2003). Notch-mediated restoration of regenerative potential to aged muscle. *Science*. **302**, 1575-1577.

Conboy IM, Conboy MJ, Wagers AJ, Girma ER, Weissman IL, Rando TA (2005). Rejuvenation of aged progenitor cells by exposure to a young systemic environment. *Nature*. **433**, 760-764.

Cosgrove BD, Gilbert PM, Porpiglia E, Mourkioti F, Lee SP, Corbel SY, Llewellyn ME, Delp SL, Blau HM (2014). Rejuvenation of the muscle stem cell population restores strength to injured aged muscles. *Nature Medicine*. **20**, 255-264.

Deb C, Li B, Baylink DJ, Xing W, Zhang W, Chen M, Wergedal JE, Mohan S, Qin X (2012).

Transgenic overexpression of pregnancy-associated plasma protein-A in skeletal muscle of mice increases myofiber size and central nucleation in sedentary muscle and promotes muscle regeneration in the injured muscle. *Growth Hormone & IGF Research*. **22**, 173-179.

Deschenes M, Gaertner J, O'Reilly S (2013). The effects of sarcopenia on muscles with different recruitment patterns and myofiber profiles. *Current Aging Science*. **6**, 266-272.

Frost RA, Lang CH, Gelato MC (1997). Transient exposure of human myoblasts to tumor necrosis factor-α inhibits serum and insulin-like growth factor-I stimulated protein synthesis. *Endocrinology*. **138**, 4153-4159.

Fry CS, Lee JD, Mula J, Kirby TJ, Jackson JR, Liu F, Yang L, Mendias CL, Dupont-Versteegden EE, McCarthy JJ (2015). Inducible depletion of satellite cells in adult, sedentary mice impairs muscle regenerative capacity without affecting sarcopenia. *Nature Medicine*. **21**, 76-80.

Greiwe JS, Cheng B, Rubin DC, Yarasheski KE, Semenkovich CF (2001). Resistance exercise decreases skeletal muscle tumor necrosis factor α in frail elderly humans. *The FASEB Journal*. **15**, 475-482.

Guttridge DC, Mayo MW, Madrid LV, Wang C-Y, Baldwin Jr AS (2000). NF-κB-induced loss of MyoD messenger RNA: possible role in muscle decay and cachexia. *Science*. **289**, 2363-2366.

Hawke TJ (2005). Muscle stem cells and exercise training. *Exercise and Sport Sciences*

Reviews. **33**, 63-68.

Jo E, Lee S-R, Park B-S, Kim J-S (2012). Potential mechanisms underlying the role of chronic inflammation in age-related muscle wasting. *Aging Clinical and Experimental Research*. **24**, 412-422.

Karlsen A, Couppé C, Andersen JL, Mikkelsen UR, Nielsen RH, Magnusson SP, Kjaer M, Mackey AL (2015). Matters of fiber size and myonuclear domain: Does size matter more than age? *Muscle & Nerve*. **52**, 1040-1046.

Langen RC, Schols AM, Kelders MC, Wouters EF, Janssen-Heininger YM (2001). Inflammatory cytokines inhibit myogenic differentiation through activation of nuclear factor-κB. *The FASEB Journal.* **15**, 1169-1180.

Langen RC, Van Der Velden JL, Schols AM, Kelders MC, Wouters EF, Janssen-Heininger YM (2004). Tumor necrosis factor-alpha inhibits myogenic differentiation through MyoD protein destabilization. *The FASEB Journal*. **18**, 227-237.

Lees SJ, Zwetsloot KA, Booth FW (2009). Muscle precursor cells isolated from aged rats exhibit an increased tumor necrosis factor-α response. *Aging Cell*. **8**, 26-35.

Léger B, Derave W, De Bock K, Hespel P, Russell AP (2008). Human sarcopenia reveals an increase in SOCS-3 and myostatin and a reduced efficiency of Akt phosphorylation. *Rejuvenation Research*. **11**, 163-175B.

Li Y-P (2003). TNF-α is a mitogen in skeletal muscle. *American Journal of Physiology-Cell Physiology*. **285**, C370-C376.

Li Y-P, Schwartz RJ, Waddell ID, Holloway BR, Reid MB (1998). Skeletal muscle myocytes undergo protein loss and reactive oxygen-mediated NF-κB activation in response to tumor necrosis factor α. *The FASEB Journal*. **12**, 871-880.

Lieskovska J, Guo D, Derman E (2003). Growth impairment in IL-6-overexpressing transgenic mice is associated with induction of SOCS3 mRNA. *Growth Hormone & IGF research*. **13**, 26-35.

Lin S-Y, Chen W-Y, Lee F-Y, Huang C-J, Sheu WH-H (2005). Activation of ubiquitin-proteasome pathway is involved in skeletal muscle wasting in a rat model with biliary cirrhosis: potential role of TNF-α. *American Journal of Physiology-Endocrinology and Metabolism*. **288**, E493-E501.

Marty E, Liu Y, Samuel A, Or O, Lane J (2017). A review of sarcopenia: Enhancing awareness of an increasingly prevalent disease. *Bone*. **105**, 276-286

Melton 3rd L, Khosla S, Crowson CS, O'connor MK, O'Fallon WM, Riggs BL (2000). Epidemiology of sarcopenia. *Journal of the American Geriatrics Society.* **48**, 625-630.

Metter EJ, Conwit R, Tobin J, Fozard JL (1997). Age-associated loss of power and strength in the upper extremities in women and men. *The journals of gerontology. Series A, Biological sciences and medical sciences.* **52**, B267-276.

Otis JS, Niccoli S, Hawdon N, Sarvas JL, Frye MA, Chicco AJ, Lees SJ (2014). Pro-inflammatory mediation of myoblast proliferation. *PLoS One*. **9**, e92363.

Palacios D, Mozzetta C, Consalvi S, Caretti G, Saccone V, Proserpio V, Marquez VE, Valente S,

Mai A, Forcales SV (2010). TNF/p38α/polycomb signaling to Pax7 locus in satellite cells links inflammation to the epigenetic control of muscle regeneration. *Cell Stem Cell*. **7**, 455-469.

Patel HJ, Patel BM (2017). TNF-α and cancer cachexia: molecular insights and clinical implications. *Life Sciences*. **170**, 56-63.

Petrella JK, Kim J-s, Cross JM, Kosek DJ, Bamman MM (2006). Efficacy of myonuclear addition may explain differential myofiber growth among resistance-trained young and older men and women. *American Journal of Physiology-Endocrinology and Metabolism*. **291**, E937-E946.

Plonquet A, Eliezer-Vanerot M-C, Poron F, Belec L, Barlovatz-Meimon G, Gherardi RK (1999). Differential expression of the IL-1 system components during in vitro myogenesis: Implication of IL-1b in induction of myogenic cell apoptosis. *Cell Death and Differentiation*. **6**, 1012-1021.

Reid MB, Li Y-P (2001). Tumor necrosis factor-α and muscle wasting: a cellular perspective. *Respiratory Research*. **2**, 269.

Relaix F, Zammit PS (2012). Satellite cells are essential for skeletal muscle regeneration: the cell on the edge returns centre stage. *Development*. **139**, 2845-2856.

Roberts P, McGeachie JK, Grounds MD (1997). The host environment determines strain-specific differences in the timing of skeletal muscle regeneration: cross-transplantation studies between SJL/J and BALB/c mice. *The Journal of Anatomy*. **191**, 585-594.

Sambasivan R, Yao R, Kissenpfennig A, Van Wittenberghe L, Paldi A, Gayraud-Morel B, Guenou H, Malissen B, Tajbakhsh S, Galy A (2011). Pax7-expressing satellite cells are indispensable for adult skeletal muscle regeneration. *Development*. **138**, 3647-3656.

Schwartz LM, Brown C, McLaughlin K, Smith W, Bigelow C (2016). The myonuclear domain is not maintained in skeletal muscle during either atrophy or programmed cell death. *American Journal of Physiology-Cell Physiology*. **311**, C607-C615.

Song J, Saeman MR, De Libero J, Wolf SE (2015). Skeletal Muscle Loss is Associated with TNF Mediated Insufficient Skeletal Myogenic Activation After Burn. *Shock* **44**, 479-486.

Sousa-Victor P, Gutarra S, García-Prat L, Rodriguez-Ubreva J, Ortet L, Ruiz-Bonilla V, Jardí M, Ballestar E, González S, Serrano AL (2014). Geriatric muscle stem cells switch reversible quiescence into senescence. *Nature*. **506**, 316-321.

Van der Meer S, Jaspers R, Degens H (2011). Is the myonuclear domain size fixed? *Journal of Musculoskeletal & Neuronal Interactions*. **11**, 286-297.

Verdijk LB, Koopman R, Schaart G, Meijer K, Savelberg HH, van Loon LJ (2007). Satellite cell content is specifically reduced in type II skeletal muscle fibers in the elderly. *American Journal of Physiology-Endocrinology and Metabolism*. **292**, E151-E157.

Visser M, Pahor M, Taaffe DR, Goodpaster BH, Simonsick EM, Newman AB, Nevitt M, Harris TB (2002). Relationship of interleukin-6 and tumor necrosis factor-α with muscle mass and muscle strength in elderly men and women: the Health ABC Study. *The Journals of Gerontology Series A: Biological Sciences and Medical Sciences*. **57**, M326-M332.

Walston JD (2012). Sarcopenia in older adults. *Current Opinion in Rheumatology*. **24**, 623.

Wang Y, Wehling‐Henricks M, Samengo G, Tidball JG (2015). Increases of M2a macrophages and fibrosis in aging muscle are influenced by bone marrow aging and negatively regulated by muscle‐derived nitric oxide. *Aging Cell*. **14**, 678-688.

Wehling-Henricks M, Li Z, Lindsey C, Wang Y, Welc SS, Ramos JN, Khanlou N, Kuro-o M, Tidball JG (2016). Klotho gene silencing promotes pathology in the mdx mouse model of Duchenne muscular dystrophy. *Human Molecular Genetics*. **25**, 2465-2482.

Wilson D, Jackson T, Sapey E, Lord JM (2017). Frailty and sarcopenia: the potential role of an aged immune system. *Ageing Research Reviews*. **36**, 1-10

Chapter 6. Conclusion

Our investigation provides new insights into the mechanisms that underlie age-related changes in skeletal muscle and highlight the importance of regulatory interactions between immune cells, satellite cells and muscle fibers. Our most fundamental new finding is that myeloid cells contribute to sarcopenia and age-related muscle fibrosis. In addition, we found that aging is associated with increased numbers of both M1 and M2 macrophages in muscle and that reductions of macrophage numbers in *nNOS* transgenic mice were associated with decreased connective tissue accumulation in aging muscle. However, we found that age-related changes in muscle are not only affected by the number of intramuscular myeloid cells; the age of the bone marrow from which the myeloid cells are derived has important influences on how they influence muscle aging. Transplantation of young BMCs into old recipients prevented sarcopenia and reduced the accumulation of connective tissue during aging. Furthermore, transplantation of old BMCs into young recipients reduced satellite cell numbers and promoted satellite cell switching to a fibrogenic phenotype.

Although our findings obtained in the *nNOS* transgenic model and the heterochronic BMT model support our interpretation that myeloid cells are important effector cells influencing sarcopenia, fibrosis and satellite cell functions, neither model was specific for myeloid cells. However, in our third model we designed a mouse line with a myeloid-cell-specific mutation of *Sfpi1* which enabled us to specifically reduce the number of M2 macrophages in muscle. We

learned that mice with mutation of *Sfpi1* in myeloid cells did not experience sarcopenia and showed decreased muscle fibrosis during aging. That finding provides strong support for our interpretation that many of the treatment effects achieved in the *nNOS* transgenic and heterochronic BMT models resulted from perturbations of macrophage number or function.

Myeloid cells express numerous cytokines and factors that have the potential to influence muscle aging, but we focused on TNFα because of extensive, previous findings showing that it plays important regulatory roles in myogenesis (Langen *et al.* 2001; Reid *et al.* 2001; Chen *et al.* 2007) and it also is associated with muscle wasting in disease and aging (Greiwe *et al.* 2001; Visser *et al.* 2002; Schaap *et al.* 2009). Our initial observations of the effects of a systemic *TNFα* knockout showed that loss of *TNFα* expression prevented sarcopenia. We also made the unexpected observation that *TNFα* ablation caused extensive muscle cell fusion into muscle fibers in old muscle, which may feasibly be a significant factor underlying the reduction in sarcopenia in the mutant mice. Although these findings were based on analysis of systemic *TNFα* mutants, our further investigations showed that TNFα produced by myeloid cells was important in influencing sarcopenia and muscle cell fusion. Transplantation of wild-type BMCs into *TNFα* knockout mice induced sarcopenia and reduced muscle cell fusion, indicating that TNFα secreted by myeloid cells contributes significantly to the reduction of satellite cell myogenic capacity during aging and causes sarcopenia. However, our findings also showed that manipulation of cells in the immune compartment could affect sarcopenia without causing changes in *TNFα* expression; transplantation of young wild-type bone marrow cells into old

wild-type mice prevented sarcopenia although *TNFα* mRNA levels were unaffected. That observation indicates that other, unidentified factors derived from myeloid cells also play significant roles in regulation muscle mass loss during aging.

Our findings suggest new directions for therapeutic strategies to reduce sarcopenia and age-related muscle fibrosis. Although dietary protein supplements (Mitchell *et al.* 2012; Junior *et al.* 2017; Osuka *et al.* 2017) and various physical exercises (Yarasheski *et al.* 1999; Liu & Latham 2009; Junior *et al.* 2017; Osuka *et al.* 2017) can reduce muscle atrophy and increase muscle strength in the elderly, careful assessment and specific caution must be taken when using these treatment options (Taaffe 2006; Paddon-Jones & Rasmussen 2009). They are not always feasible for many elderly subjects with specific dietary requirements or limited physical ability due to illness or weakness. Pharmacologic treatment for muscle aging is currently very limited. Our findings in this project suggest the possibility of slowing or preventing muscle aging by reducing age-related changes in the immune system. Clinical interventions that target functions of the immune system are available at multiple levels that range from orally administered drugs to surgery and bone marrow transplantation, providing a wide choice of treatment options. For example, inhibiting the mammalian target of rapamycin (mTOR) signaling led to rejuvenation of aging hematopoietic stem cells (Chen *et al.* 2009). Rapamycin treatment in 22-month-old mice increased their life span, restored the self-renewal and regenerative capacity of their HSCs (Chen *et al.* 2009). Elevated activity of Cdc42 is significantly increased in aged HSCs and causes epigenetic modifications of histone H4 acetylation that may drive HSC aging

(Florian *et al.* 2012). Pharmacologic inhibition of Cdc42 activity by CASIN treatment restored the level and the spatial distribution of histone H4 acetylation in old HSCs and rejuvenated their lymphopoietic potential (Florian *et al.* 2012). Those investigations provide potential therapeutics tools to rejuvenate the immune system that may also reduce muscle aging.

Our observations also indicate that nitric oxide donor drugs and anti-inflammatory drugs may benefit muscle health in the elderly. This hypothesis is supported by a recent investigation showing that treatment with non-steroidal anti-inflammatory drugs (NSAIDs) in old rats significantly decreased muscle mass loss between 20 and 25 months of age that was accompanied by a reduction in IL6 and IL1β in plasma (Rieu *et al.* 2009). NSAID treatment with piroxicam increased Elderly Mobility Scale scores, grip strength and fatigue resistance in geriatric patients with acute infection-induced inflammation (Beyer *et al.* 2011). NSAID treatment also caused a greater increase in satellite cell numbers and faster muscle regeneration following injury compared with placebo treatment in young healthy men (Mackey *et al.* 2016). Together, these investigations suggest that NSAIDs may be used to prevent or treat sarcopenia.

In summary, our present investigation indicates that aging of the immune system, especially myeloid cells, contributes to muscle aging. Rejuvenating the immune system through bone marrow transplantation or other clinical interventions may be a feasible way to help sustain muscle health in old age.

Figures

Figure 26.

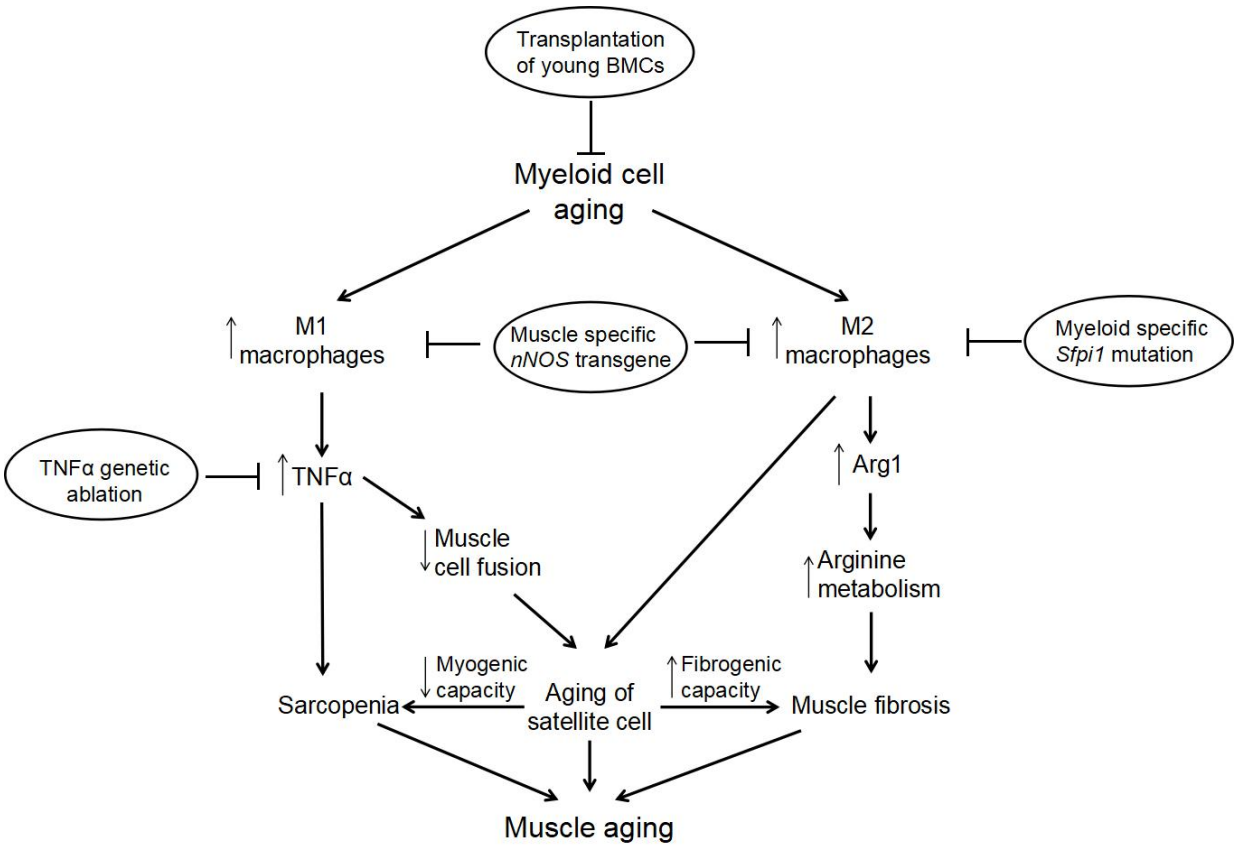

Figure legends

Figure 26. Schematic graph showing the proposed model of aging of myeloid cells regulating muscle aging. Circled items indicate experimental models used in the present study.

Tables

Table 5. QPCR primers used in this dissertation

Gene	Accession Number		Direction (5'->3')
Arg1	NM_007482	Fwd	CAATGAAGAGCTGGCTGGTGT
		Rev	GTGTGAGCATCCACCCAAATG
Axin2	NM_015732.4	Fwd	GACGCACTGACCGACGATTC
		Rev	CTGCGATGCATCTCTCTCTGG
CD163	NM_053094.2	Fwd	GCAAAAACTGGCAGTGGG
		Rev	GTCAAAATCACAGACGGAGC
CD206	NM_002438	Fwd	GGATTGTGGAGCAGATGGAAG
		Rev	CTTGAATGGAAATGCACAGAC
CD68	NM_001291058.1	Fwd	CAAAGCTTCTGCTGTGGAAAT
		Rev	GACTGGTCACGGTTGCAAG
Col I	NM_007742.3	Fwd	TGTGTGCGATGACGTGCAAT
		Rev	GGGTCCCTCGACTCCTACA
Col III	NM_009930.2	Fwd	ATCCCATTTGGAGAATGTTGTGC
		Rev	GGACATGATTCACAGATTCCAGG
Col V	NM_016919.2	Fwd	CGGGGTACTCCTGGTCCTAC
		Rev	GCATCCCTACTTCCCCCTTG
F4/80	NM_010130.4	Fwd	GATACAGCAATGCCAAGCAG
		Rev	CAGCACGAGGGAGACACTT
Fizz-1	NM_020509.3	Fwd	TCGTGGAGAATAAGGTCAAGG
		Rev	GGAGGCCCATCTGTTCATAG
FoxP3	NM_054039.2	Fwd	CTTTCACCTATGCCACCCTTATC
		Rev	TAGATTTCATTGAGTGTCCTCTGC

IFNγ	NM_008337.3	Fwd	GACAATCAGGCCATCAGCAAC
		Rev	CGGATGAGCTCATTGAATGCTT
IL1β	NM_008361.4	Fwd	GTAATGAAAGACGGCACACC
		Rev	CTCTGCAGACTCAAACTCC
IL4	NM_021283.2	Fwd	GGATGTGCCAAACGTCCTC
		Rev	GAGTTCTTCTTCAAGCATGGAG
IL5	NM_010558.1	Fwd	CAAGCAATGAGACGATGAGG
		Rev	CCACGGACAGTTTGATTCTTC
IL6	NM_031168.1	Fwd	GAACAACGATGATGCACTTGC
		Rev	CTTCATGTACTCCAGGTAGCTATGGT
IL10	NM_010548.2	Fwd	CAAGGAGCATTTGAATTCCC
		Rev	GGCCTTGTAGACACCTTGGTC
IL13	NM_008355.3	Fwd	GTCCTGGCTCTTGCTTGC
		Rev	CACTCCATACCATGCTGCC
iNOS	NM_010927.3	Fwd	CAGCACAGGAAATGTTTCAGC
		Rev	TAGCCAGCGTACCGGATGA
MyoD	NM_010866.2	Fwd	GAGCGCATCTCCACAGACAG
		Rev	AAATCGCATTGGGGTTTGAG
Myogenin	NM_031189.2	Fwd	CCAGTACATTGAGCGCTAC
		Rev	ACCGAACTCCAGTGCATTGC
Pax7	NM_011039.2	Fwd	CTCAGTGAGTTCGATTAGCCG
		Rev	AGACGGTTCCCTTTGTCGC
PPIA	NM_008907.1	Fwd	GCAAATGCTGGACCAAACAC
		Rev	TCACCTTCCCAAAGACCACAT
RNPS1	NM_001080127.1	Fwd	AGGCTCACCAGGAATGTGAC
		Rev	CTTGGCCATCAATTTGTCCT
Sfpi1	NM_011355.2	Fwd	GGAGGTGTCTGATGGAGAAGC
		Rev	CAGGAACTGGTACAGGCGAATC
SiglecF	NM_145581.2	Fwd	CAGCCCTGAAAGTAGCAGC
		Rev	GTGGCTGTTCTTTCTGGGTC

SRP14	NM_009273.4	Fwd	GAGAGCGAGCAGTTCCTGAC
		Rev	CGGTGCTGATCTTCCTTTTC
TGFβ	NM_011577.1	Fwd	CTCCACCTGCAAGACCAT
		Rev	CTTAGTTTGGACAGGATCTGG
TNFα	NM_013693.3	Fwd	CTTCTGTCTACTGAACTTCGGG
		Rev	CACTTGGTGGTTTGCTACGAC
TPT1	NM_009429.3	Fwd	GGAGGGCAAGATGGTCAGTAG
		Rev	CGGTGACTACTGTGCTTTCG
Vangl2	NM_033509.3	Fwd	CCAAGTCCGTCCTGGCCAAG
		Rev	GCTCATGCTCGGCTTCCTCG

References

Barberi L, Scicchitano BM, De Rossi M, Bigot A, Duguez S, Wielgosik A, Stewart C, McPhee J, Conte M, Narici M (2013). Age-dependent alteration in muscle regeneration: the critical role of tissue niche. *Biogerontology.* **14**, 273-292.

Beyer I, Bautmans I, Njemini R, Demanet C, Bergmann P, Mets T (2011). Effects on muscle performance of NSAID treatment with Piroxicam versus placebo in geriatric patients with acute infection-induced inflammation. a double blind randomized controlled trial. *BMC Musculoskeletal Disorders*. **12**, 292.

Brack AS, Rando TA (2007). Intrinsic changes and extrinsic influences of myogenic stem cell function during aging. *Stem Cell Reviews.* **3**, 226-237.

Carosio S, Berardinelli MG, Aucello M, Musarò A (2011). Impact of ageing on muscle cell regeneration. *Ageing Research Reviews.* **10**, 35-42.

Chen C, Liu Y, Liu Y, Zheng P (2009). mTOR regulation and therapeutic rejuvenation of aging hematopoietic stem cells. *Science Signaling*. **2**, ra75.

Chen S-E, Jin B, Li Y-P (2007). TNF-α regulates myogenesis and muscle regeneration by activating p38 MAPK. *American Journal of Physiology-Cell Physiology.* **292**, C1660-C1671.

Day K, Shefer G, Shearer A, Yablonka-Reuveni Z (2010). The depletion of skeletal muscle satellite cells with age is concomitant with reduced capacity of single progenitors to produce reserve progeny. *Developmental Biology.* **340**, 330-343.

Florian MC, Dörr K, Niebel A, Daria D, Schrezenmeier H, Rojewski M, Filippi MD, Hasenberg A, Gunzer M, Scharffetter-Kochanek K, Zheng Y, Geiger H (2012). Cdc42 activity regulates hematopoietic stem cell aging and rejuvenation. *Cell Stem Cell.* **10**, 520–530.

Fry CS, Lee JD, Mula J, Kirby TJ, Jackson JR, Liu F, Yang L, Mendias CL, Dupont-Versteegden EE, McCarthy JJ (2015). Inducible depletion of satellite cells in adult, sedentary mice impairs muscle regenerative capacity without affecting sarcopenia. *Nature Medicine.* **21**, 76-80.

Gibson MC, Schultz E (1983). Age-related differences in absolute numbers of skeletal muscle satellite cells. *Muscle & Nerve.* **6**, 574-580.

Greiwe JS, Cheng B, Rubin DC, Yarasheski KE, Semenkovich CF (2001) Resistance exercise decreases skeletal muscle tumor necrosis factor alpha in frail elderly humans. *The FASEB Journal.* **15**, 475-482.

Junior PS, Ribeiro AS, Nabuco HC, Fernandes RR, Tomeleri CM, Cunha PM, Venturini D, Barbosa DS, Schoenfeld BJ, Cyrino ES (2017). Effects of whey protein supplementation associated with resistance training on muscular strength, hypertrophy and muscle quality in pre-conditioned older women. *International Journal of Sport Nutrition and Exercise Metabolism*, 1-27.

Keefe AC, Lawson JA, Flygare SD, Fox ZD, Colasanto MP, Mathew SJ, Yandell M, Kardon G (2015). Muscle stem cells contribute to myofibers in sedentary adult mice. *Nature Communications.* **6**, 7087.

Langen RC, Schols AM, Kelders MC, Wouters EF, Janssen-Heininger YM (2001). Inflammatory cytokines inhibit myogenic differentiation through activation of nuclear factor-$_{K}$B. *The FASEB Journal.* **15**, 1169-1180.

Liu Cj, Latham NK (2009). Progressive resistance strength training for improving physical function in older adults. The Cochrane Library.

Mackey AL, Rasmussen LK, Kadi F, Schjerling P, Helmark IC, Ponsot E, Aagaard P, Durigan JLQ, Kjaer M (2016). Activation of satellite cells and the regeneration of human skeletal muscle are expedited by ingestion of nonsteroidal anti-inflammatory medication. *The FASEB Journal.* **30**, 2266-2281.

Mitchell WK, Williams J, Atherton P, Larvin M, Lund J, Narici M (2012). Sarcopenia, dynapenia, and the impact of advancing age on human skeletal muscle size and strength; a quantitative review. *Frontiers in Physiology.* **3.** 260

Osuka Y, Fujita S, Kitano N, Kosaki K, Seol J, Sawano Y, Shi H, Fujii Y, Maeda S, Okura T (2017). Effects of aerobic and resistance training combined with fortified milk on muscle mass, muscle strength, and physical performance in older adults: A randomized controlled trial. *The Journal of Nutrition, Health and Aging.* **21**, 1349-1357.

Paddon-Jones D, Rasmussen BB (2009). Dietary protein recommendations and the prevention of sarcopenia: protein, amino acid metabolism and therapy. *Current Opinion in Clinical Nutrition and Metabolic Care.* **12**, 86-90.

Reid MB, Li Y-P (2001). Tumor necrosis factor-α and muscle wasting: a cellular perspective.

Respiratory Research. **2**, 269-272.

Rieu I, Magne H, Savary-Auzeloux I, Averous J, Bos C, Peyron M, Combaret L, Dardevet D (2009). Reduction of low grade inflammation restores blunting of postprandial muscle anabolism and limits sarcopenia in old rats. *The Journal of Physiology.* **587**, 5483-5492.

Schaap LA, Pluijm SMF, Deeg DJH, Harris TB, Kritchevsky SB, Newman AB, Colbert LH, Pahor M, Rubin SM, Tylavsky FA, Visser M, Hlth ABCS (2009) Higher inflammatory marker levels in older persons: associations with 5-year change in muscle mass and muscle strength. *The Journals of Gerontology. Series A, Biological Sciences and Medical Sciences.* **64**, 1183-1189.

Shefer G, Van de Mark DP, Richardson JB, Yablonka-Reuveni Z (2006). Satellite-cell pool size does matter: defining the myogenic potency of aging skeletal muscle. *Developmental Biology.* **294**, 50-66.

Taaffe DR (2006). Sarcopenia: exercise as a treatment strategy. *Australian Family Physician*. **35**, 130-134.

Visser M, Pahor M, Taaffe DR, Goodpaster BH, Simonsick EM, Newman AB, Nevitt M, Harris TB (2002). Relationship of interleukin-6 and tumor necrosis factor-α with muscle mass and muscle strength in elderly men and women: the Health ABC Study. *The Journals of Gerontology Series A: Biological Sciences and Medical Sciences.* **57**, M326-M332.

Yarasheski KE, Pak-Loduca J, Hasten DL, Obert KA, Brown MB, Sinacore DR (1999). Resistance exercise training increases mixed muscle protein synthesis rate in frail

women and men ⩾ 76 yr old. *American Journal of Physiology - Endocrinology and Metabolism.* **277**, E118-E125.